INVESTIGATING THE ROLE OF FcRL4^{+} B CELLS AT THE SITE OF EPITHELIAL INFLAMMATION

by

YUXIN LIU

A thesis submitted to The University of Birmingham for the degree of
DOCTOR OF PHILOSOPHY

Institute of Inflammation and Ageing
College of Medical and Dental Sciences
The University of Birmingham
June 2022

UNIVERSITY OF
BIRMINGHAM

University of Birmingham Research Archive

e-theses repository

This unpublished thesis/dissertation is copyright of the author and/or third parties. The intellectual property rights of the author or third parties in respect of this work are as defined by The Copyright Designs and Patents Act 1988 or as modified by any successor legislation.

Any use made of information contained in this thesis/dissertation must be in accordance with that legislation and must be properly acknowledged. Further distribution or reproduction in any format is prohibited without the permission of the copyright holder.

ABSTRACT

The slow and progressive deterioration of the small bile ducts is a hallmark of primary biliary cholangitis (PBC). This damage is mediated by infiltrating lymphocytes which form aggregates surrounding the small bile ducts eventually leading to cholestasis and cirrhosis. A subset of memory B cells expressing the surface marker Fc receptor like 4 (FcRL4) have been implicated in the pathogenesis of rheumatoid arthritis and primary Sjogren's syndrome. Here, we addressed the hypothesis that the $FcRL4^+$ B cells are involved in the lymphoepithelial lesion that leads to the destruction of bile ducts in PBC patients and explored their role in the disease. In explant livers from patients undergoing liver transplantation, $FcRL4^+$ B cells were identified in PBC livers and were largely absent in other end-stage liver diseases. Within the PBC liver, these cells are highly proliferative and can be seen within immune infiltrates that surround and infiltrate the damaged biliary epithelium. $FcRL4^+$ B cells isolated from the PBC liver are enriched for $CD27^+IgD^-$ class-switched memory cells and $CD11c^+CD21^-$T-bet^+ age associated B cells (ABCs). FcRL4 is a receptor for IgA aggregates. $FcRL4^+$ B cells isolated from end-stage PBC liver have IgA captured on their surface. *In vitro*, FcRL4 expressing cells can bind IgA from patient derived bile. High levels of expression of co-stimulatory molecules CD80 and CD86 by $FcRL4^+$ suggest that they can act as antigen presenting cells. $FcRL4^+$ B cells preferentially express IgA BCR, suggesting a mucosal origin. Together with their ability to capture IgA immune complexes, these findings suggest that $FcRL4^+$ B cells may act as a link between mucosal immunity and immune mediated damage of the small bile ducts in PBC.

DEDICATION

To my Dad.

ACKNOWLEDGEMENTS

Firstly, I would like to thank my supervisors. To Professor Dagmar Scheel-Toellner for being a guiding beacon throughout my PhD, providing me with her endless support and enviable knowledge. To Dr Zania Stamataki for her ever available advice and expertise on liver immunology. Also, to Professor Gideon Hirschfield for his wisdom and for encouraging me to always look at the bigger picture. Finally, to Professor Karim Raza, for being a calming and encouraging presence, and for proof-reading my thesis.

I am indebted to the members of the Centre of Liver Research, specifically to Dr Gary Reynolds and Dr Evaggelia Liaskou, the Rheumatology Research Group, and the members of the DST group: Emily Powell, Dr James Cameron, and Dr Beth Clay. This project would not have been possible without the patients whom kindly and generously donated their livers for research. I would also like to acknowledge the Wellcome Trust for funding this project.

To my parents, whom always have been, and continue to be a source of inspiration. I will be forever grateful for your support in all aspects of my life.

To the Harveys, for adopting me as their Chinese academic.

Finally, to Ben, for being a constant source of encouragement, for convincing me that I am capable of more than I could ever have imagined, and for your ability to make me laugh even when I don't want to.

TABLE OF CONTENTS

1 INTRODUCTION 1

1.1 B CELL DEVELOPMENT AND ACTIVATION 1

1.1.1 B cell development 1

1.1.2 Immunoglobulin rearrangement and the mechanism of self-tolerance 2

1.1.3 B cell activation and differentiation 4

1.1.3.1 Follicular B cells 4

1.1.3.2 Germinal Centre 4

1.2 B CELL SUBSETS 8

1.2.1 Transitional Cells 8

1.2.2 Naïve B cells 9

1.2.2.1 B1 cells 9

1.2.3 Memory B cells 10

1.2.3.1 Human marginal zone B cells 12

1.2.4 Double negative B cells 12

1.2.5 Age-associated B cells 15

1.2.6 FcRL4 16

1.2.6.1 FcRL4 function 16

1.2.6.2 FcRL4^{+} B cells in disease 20

1.3 MUCOSAL IMMUNOLOGY 22

1.3.1 The intestinal mucosal immune system 22

1.3.1.1 The gut epithelial barrier 22

1.3.1.2 The lamina propria 23

1.3.2 IgA in the mucosa 24

1.3.2.1 Induction of IgA 24

1.3.2.2 Role of IgA 25

1.4 THE HUMAN LIVER 27

1.4.1 Introduction 27

1.4.2 Liver anatomy and function 27

1.4.3 Bile 30

1.4.4 Immune component of the liver 33

1.4.5 Liver immunotolerance 34
1.5 LIVER DISEASE 36
1.5.1 Non-alcoholic steatohepatitis 36
1.5.2 Polycystic liver disease 36
1.5.3 Primary sclerosing cholangitis 37
1.5.4 Primary biliary cholangitis 38
1.5.4.1 Introduction 38
1.5.4.2 Diagnosis 39
1.5.4.3 Disease pathogenesis 39
1.5.4.3.1 Autoantibodies 40
1.5.4.3.2 B cells 43
1.5.4.3.3 T cells 44
1.5.4.3.4 BECs 45
1.5.4.4 Disease aetiology 48
1.5.4.4.1 Genetics 48
1.5.4.4.2 Epigenetic modifications 48
1.5.4.4.3 Environmental factors 49
1.6 HYPOTHESIS AND AIMS 51
2 MATERIALS AND METHODS 52
2.1 PATIENTS AND PATIENTS' MATERIALS 52
2.2 ISOLATING LIVER INFILTRATING MONONUCLEAR CELLS (LIMCS) 52
2.3 STAINING LYMPHOCYTES FROM THE LIVER 53
2.3.1 Compensation 53
2.4 IGA ACID WASH AND IGA INCUBATION 56
2.5 FREEZING AND DEFROSTING CELLS 56
2.6 CELL CULTURE 56
2.6.1 Culturing of cell lines 56
2.6.2 Culturing biliary epithelial cells 57
2.7 CELL SORTS 57
2.8 CO-CULTURE OF FCRL4^{+} B CELLS AND BECS 57
2.9 REMOVING LIPIDS FROM BILE 58
2.10 BILE ASSAY 58

2.11 ANTIBODY STIMULATION 58
2.12 ELISA 59
2.13 IMMUNOHISTOCHEMISTRY 60
2.13.1 Preparation of sections for Immunohistochemistry Staining 60
2.13.2 Single colour staining 60
2.13.3 Double staining 61
2.13.4 Mounting 61
2.13.5 Immunohistochemistry analysis 63
2.13.5.1 Identification of FcRL4⁺ cells in end-stage livers 63
2.13.5.2 Quantification of Ki67 staining 63
2.13.5.3 Distance measurements between lymphocytes and the biliary epithelium 63
3 IDENTIFICATION OF FCRL4⁺ CELLS WITHIN END-STAGE LIVER DISEASE 65
3.1 INTRODUCTION 65
3.2 RESULTS 67
3.2.1 Identification of FcRL4⁺ cells in liver sections 67
3.2.2 Isolation of FcRL4⁺ cells from fresh liver tissue 69
3.2.3 Association of FcRL4⁺ B cell numbers with clinical parameters 74
3.3 DISCUSSION 76
4 PHENOTYPING FcRL4⁺ B CELLS IN END-STAGE LIVER DISEASE 78
4.1 INTRODUCTION 78
4.2 RESULTS 81
4.2.1 Ki-67 expression 81
4.2.2 IgA expression 84
4.2.3 Differentiation stage 87
4.2.4 CD11c, CD21, and T-bet expression 89
4.2.5 Ki67 expression of ABCs 92
4.2.6 CD80 and CD86 expression 94
4.3 DISCUSSION 97
5 FcRL4⁺ B CELL PARTICIPATION IN PBC PATHOGENESIS 100
5.1 INTRODUCTION 100
5.2 RESULTS 102

5.2.1 Proximity of FcRL4$^+$ to the biliary epithelium 102
5.2.2 FcRL4 binding to IgA 105
5.2.3 Co-culture of FcRL4$^+$ B cells and BECs 110
5.2.4 Antibody production by PBC derived FcRL4$^+$ B cells 114
5.3 DISCUSSION 119
6 DISCUSSION 124
6.1 SUMMARY 124
6.2 FCRL4$^+$ B CELLS 126
6.3 ROLE OF FCRL4$^+$ B CELLS IN PBC 127
6.4 FUTURE WORK AND LIMITATIONS 130
7 REFERENCES 136
8 APPENDIX 169

LIST OF FIGURES

Figure 1.1.1 B cell development in the bone marrow 2
Figure 1.1.2 The germinal centre 7
Figure 1.2.1 Overview of developmental and differentiation pathways of human B1 and B2 B cells 14
Figure 1.2.2 Protein structure of FcRL family of receptors and their signalling potential 18
Figure 1.2.3 Potential FcRL4 function in the mucosa 19
Figure 1.4.1 Anatomy of the liver 29
Figure 1.4.2 The biliary tree 31
Figure 1.4.3 Transcytosis of IgA across the epithelium with pIgR 32
Figure 1.5.1 PBC disease progression 40
Figure 1.5.2 Potential mechanisms of BEC damage 47
Figure 2.13.1 Method of measuring distance between lymphocytes and the biliary epithelium 64
Figure 3.2.1 $FcRL4^+$ cells can be identified in the PBC livers and are largely absent within other end-stage liver diseases 68
Figure 3.2.2 $FcRL4^+$ cells can be isolated from PBC livers 70
Figure 3.2.3 B cells are not enriched in end-stage PBC 72
Figure 3.2.4 Clinical significance of $FcRL4^+$ B cells 75
Figure 4.2.1 Proliferation of $FcRL4^+$ cells within PBC liver 83
Figure 4.2.2 $FcRL4^+$ B cells are enriched for IgA BCR 86
Figure 4.2.3 Most $FcRL4^+$ B cells in the PBC liver are class switched memory B cells 88
Figure 4.2.4 $FcRL4^+$ B cells in the PBC liver are enriched for $CD11c^+CD21^-$ ABCs 90
Figure 4.2.5 Ki67 by ABCs in end-stage liver disease 93
Figure 4.2.6 $FcRL4^+$ B cells have higher expression of CD80 and CD86 than $FcRL4^-$ B cells 96
Figure 5.2.1 In PBC $FcRL4^+$ B cells form aggregates around inserted in biliary epithelium 103
Figure 5.2.2 $FcRL4^+$ as a receptor for IgA aggregates 107
Figure 5.2.3 FcRL4 captures IgA from bile 109
Figure 5.2.4 Co-culture of BECs with $FcRL4^+$ B cells 113
Figure 5.2.5 Antibody production assay development 116
Figure 5.2.6 Antibody production by $FcRL4^+$ B cells 118

Figure 6.1.1 Potential pathogenic functions of FcRL4 expressing B cells in PBC 125

Supplementary Figure 7.1 Clinical significance of FcRL4^{+} B cells..... 169

Supplementary Figure 7.2 CD24 expression on FcRL4^{+} B cells 171

LIST OF TABLES

Table 2.3.1 Antibodies used for flow cytometry 55
Table 2.7.1 Antibodies used for cell sorting 57
Table 2.11.1 Stimulation cocktail for antibody stimulation assay 59
Table 2.13.1 Antibodies used for immunohistochemistry 62
Table 2.13.2 IHC incubation times 62

Supplementary Table 7.1 Clinical data from end-stage liver disease patients 172

ABBREVIATIONS

2-OADC	2-oxoacid dehydrogenase complex
ABC	Age-associated B cells
AID	Activation-induced cytidine deaminase
ALP	Alkaline phosphatase
AMA	Anti-mitochondrial antibody
ANA	Anti-nuclear antibody
APC	Antigen presenting cell
APRIL	A proliferation-inducing ligand
BAFF	B cell-activating factor
BCOADC-E2	Branched-chain 2-oxo-acid dehydrogenase complex E2
BCR	B cell receptor
BEC	Biliary epithelial cell
BSA	Bovine serum albumin
DC	Dendritic cell
DN	Double negative
E3BP	Dihydrolipoamide dehydrogenase-binding protein
ESLD	End-stage liver disease
FcRL	Fc receptor-like
FCS	Foetal calf serum
GALT	Gut-associated lymphoid tissue
GC	Germinal centre
HA-IgA	Heat-aggregated IgA
HIV	Human immunodeficiency virus
HSC	Haematopoietic stem cell
IBD	Inflammatory bowel disease
IFN	Interferon
LA	Lipoic acid
LPS	Lipopolysaccharide
LSEC	Liver sinusoidal endothelial cells

MALT	Mucosal-associated lymphoid tissue
MHC	Major histocompatibility complex
NAFLD	Non-alcoholic fatty liver disease
NASH	Non-alcoholic steatohepatitis
OGDC-E2	2-oxo-glutarate dehydrogenase complex E2
PAMP	Pathogen-associated molecular pattern
PBC	Primary biliary cholangitis
PBS	Phosphate buffered saline
PD-L1	Programmed death-ligand 1
PDC-E2	E2 subunit of pyruvate dehydrogenase complex
PLD	Polycystic liver disease
PSC	Primary sclerosing cholangitis
pSS	Primary Sjogren's syndrome
RA	Rheumatoid arthritis
RAG	Recombination-activating gene
SLE	Systemic lupus erythematosus
Tfh	T follicular helper
TGF-β	Transforming growth factor-β
TLR	Toll-like receptor
Tph	T peripheral helper
TRAIL	TNF-related apoptosis-inducing ligand
UDCA	Ursodeoxycholic acid

1 INTRODUCTION

1.1 B cell development and activation

1.1.1 B cell development

With the exception of B1 B cells, B lymphocytes originate primarily from the bone marrow. B cells develop from the pluripotent haematopoietic stem cell (HSC). The B cell lineage is determined by the expression of paired box protein 5 (Pax5)[1]. Within the bone marrow, B cells go through a sequential series of maturation steps before being released as immature B cells until they join the pool of recirculating naïve B cells which are migrate through follicles in lymphatic tissue and peripheral blood.

The main stages of early B cell development in the bone marrow can be divided into three stages: the pro-B, pre-B, and immature B cells (Figure 1.1.1). These stages are characterised by cell surface marker expression as well as rearrangements of the immunoglobulin heavy and light chain gene segments. Bone marrow stromal cells play a critical role in B cell development by providing critical adhesive integrins, growth factors, cytokines, and chemokines[1].

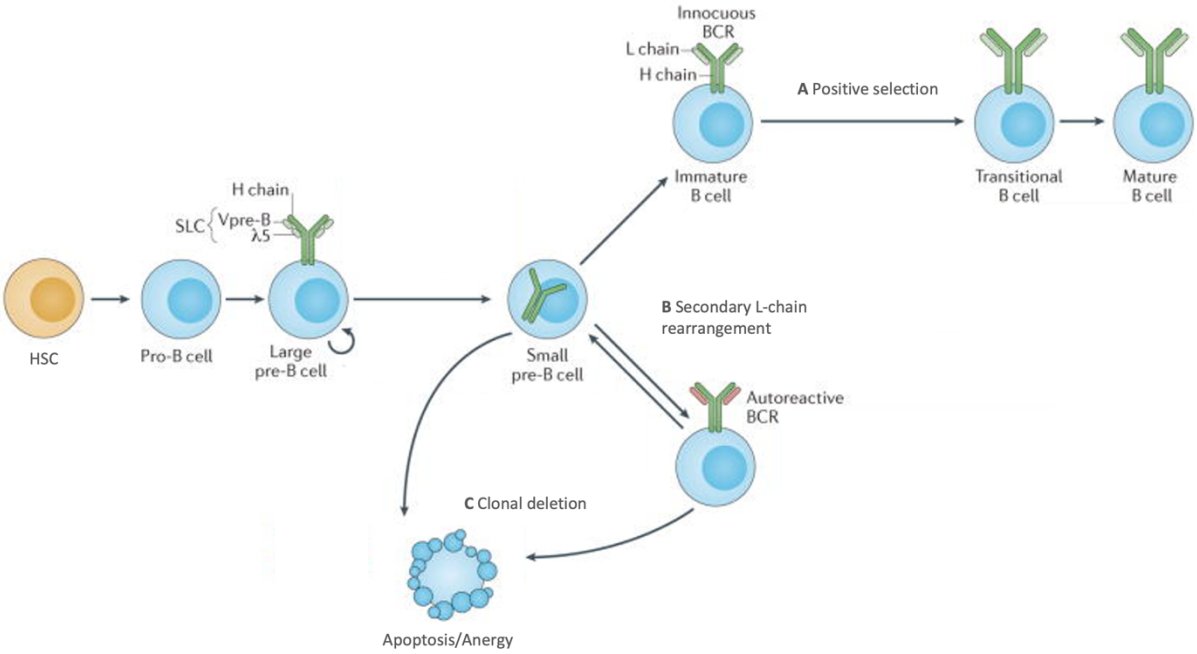


Figure 1.1.1 B cell development in the bone marrow. *B cells develop from the progenitor cell HSC. The pro-B cell initiates heavy chain rearrangement through the expression of RAG. Expression of the pre-BCR denotes development progression to the large pre-B cell. The pre-BCR is composed of the IgM heavy chain (μ-chain) and the surrogate light chain consisting of Vpre-B and λ5. Rearrangement of the light chain, also mediated by RAG occurs in the small pre-B cell. Light chain pairing to the heavy chain triggers tonic signalling of the BCR. (**A)** Non-autoreactive B cells received a positive survival signal and enter the transitional B cell pool. (**B)** Cells with autoreactive BCR or an insufficient or excessive tonic signal go through secondary light chain rearrangement. (**C)** If secondary light chain rearrangement is not successful, the clones are either deleted or rendered anergic.*
Adapted from[2]

1.1.2 Immunoglobulin rearrangement and the mechanism of self-tolerance

Immunoglobulin rearrangement during B cell development is required for the generation of a varied repertoire of BCR that can recognise a diverse range of antigens, which is important for host defence. The BCR is comprises two heavy chains and two light chains and can be expressed on the cell surface or secreted as an antibody. Rearrangement of the heavy and light chain genes is mediated by recombination-activating genes (*RAG1* and *RAG2*) collectively known as RAG.

The heavy chain gene segments are the first to be rearranged in the pre-B cell, which is required for the expression of the pre-BCR. The IgM heavy chain, known as the μ-heavy chain, forms the pre-BCR together with the surrogate light chain components V-preB and λ5, and the signal-transducing subunit Ig-α and Ig-β. Successful expression of the pre-BCR is required for further B cell development and progressing to light-chain rearrangement. The rearranged kappa or lambda light chains and the heavy chain form the IgM BCR on the now immature B cell[3]. Light chain rearrangement is the final stage of antigen-independent B cell development.

The random nature of immunoglobulin rearrangement will inevitably create BCRs that recognise self-antigens. Approximately 55-75% of immature B cells in humans are thought to be self-reactive[4], thus testing for autoreactivity is important to avoid the development of autoimmune disorders. In the bone marrow, developing B cells pass through checkpoints that remove autoreactive clones and establish self-tolerance[3]. A threshold of generated signals from the unligated BCR is used to select immature B cells for progression to transitional B cells. The current models suggest that clones with low-level (tonic) BCR signals are given a survival signal (positive selection), while clones with no BCR signals fail to survive (Figure 1.1.1). In the bone marrow microenvironment, antigens that could engage the BCR are likely to be self-antigens. Cells with BCR that react to self-antigen or have too strong a signal from their BCR are given a second chance to rearrange their light-chain immunoglobulin gene segments; should they fail, these clones will either be deleted through Fas and Bcl-2 signalling[5,6] or rendered anergic[2]. Re-expression of a BCR that meets the threshold for positive selection allows the cell to enter the transitional B cell pool and migrate from the bone marrow into the spleen.

In human B cell development, large numbers of self-reactive antibodies are generated[4]. Therefore, the selection mechanism in the bone marrow acts as an important checkpoint against autoantibodies[4]. The second selection mechanism occur within the periphery to further remove autoreactive clones[7]. Although there is a significant reduction of autoreactive B cells in this selection process, approximately 20% of antibodies produced by mature human B cells are self reactive[4]. Self-reactive B cells that escape are eliminated via Fas-Fas ligand and CD40-CD40L interactions[8,9].

1.1.3 B cell activation and differentiation

1.1.3.1 Follicular B cells

Protein antigens are predominantly recognised by follicular B cells. Activation of follicular B cells requires the presence of antigen-specific $CD4^+$ T cells. Upregulation of specific chemokine receptors leads to the migration of B cells to the T cell zone of the lymphoid tissue[10]. Upon antigen recognition by the BCR, the antigen is internalised and degraded into peptides before being presented on MHC II. This peptide-MHC II complex binds to antigen-specific $CD4^+$ T cells through the T-cell receptor. Cognate B-T interaction promotes the differentiation and proliferation of the B cell through CD40-CD40L binding as well as cytokines[11]. Activated follicular B cells differentiate into rapidly dividing blasts forming germinal centres (GC).

1.1.3.2 Germinal Centre

During the T cell-dependent antigen response, activated B and T cells form GCs in the secondary lymphoid tissues, including the spleen, lymph nodes, and tonsils. The GC is composed of a dark zone consisting almost entirely of proliferating B cells known as

centroblasts, and a light zone containing non-proliferating centrocytes within a network of follicular dendritic cells, T cells and macrophages (Figure 1.1.2).

B cells undergo immunoglobulin class switch recombination and somatic hypermutation to develop into high-affinity class-switched memory B cells and plasma cells[12]. Somatic hypermutation and class switch recombination both require the expression of the DNA-editing enzyme activation-induced cytidine deaminase (AID)[13–15]. AID converts cytosine into uracil in a single-stranded DNA, which produces a mismatch that requires removal[16,17]. In somatic hypermutation, which occurs in centroblasts within the dark zone, AID activity results in point mutations within the immunoglobulin gene segments encoding the variable antigen-binding regions[18,19]. This enables the generation of antibodies with varying antigen affinities, and through competition for antigen within the GC, high-affinity clones can be selected. Follicular dendritic cells in the light zone are responsible for presenting antigen captured on their surface to B cells. Follicular dendritic cells are critical for the organisation of the GC, as genetic ablation of these cells results in the loss of GCs[20]. B cells recognise and capture this antigen through their BCR before internalising and presentation on MHC-II to T follicular helper (Tfh) cells to elicit a second survival signal.

Successful selection and interaction with Tfh leads to the upregulation of the *Bcl2* family of pro-survival factors in the B cell[21]. B cells without strong affinity to antigen cannot compete for the scarce availability of antigen and T cell help. As a result, these low-affinity BCR clones do not receive a survival signal and are removed by apoptosis through death by neglect or potentially the activation of Fas and subsequent binding to Fas-L on follicular dendritic cells[22,23].

A subset of centrocytes within the light zone undergoes class switch recombination. In class switch recombination, AID mediates double-stranded DNA breaks in the constant region of the heavy chain, resulting in a change of isotypes such as IgG, IgE, or IgA. This allows the production of antibodies with different immunological functions without changing their antigen specificity[24–26].

B cells can either depart the GC as memory cells or plasmablasts or re-enter the dark zone after positive selection. A B cell can move multiple times between proliferation in the dark and selection in the light zone, and the frequency at which it does so determines its fate between memory and plasma cell development[27]. BCR with high affinity are selected into the plasma cell compartment[28], thus memory B cells have fewer SHM[23].

Chemokines produced by stromal cells are thought to be involved in B cell trafficking between the dark and light zones[29]. Centroblasts express CXCR4 and move towards the dark zone along the CXCL12 gradient. CXCR5 is expressed by centrocytes and is responsive to the CXCL13 expression in the light zone[29]. Within the GC microenvironment, the light/dark zone pattern is ill defined[30,31] and cell migration does not always follow the dark zone to light zone direction. In mouse splenic GCs for example, proliferating B cells can be seen within the light zone[31,32], which has previously been thought to contain only non-proliferating centrocytes. It is possible that the cycling of cells back and forth between the dark and light zones is aided by alternating overexpression and downregulation of CXCR4 and CXCR5 expression.

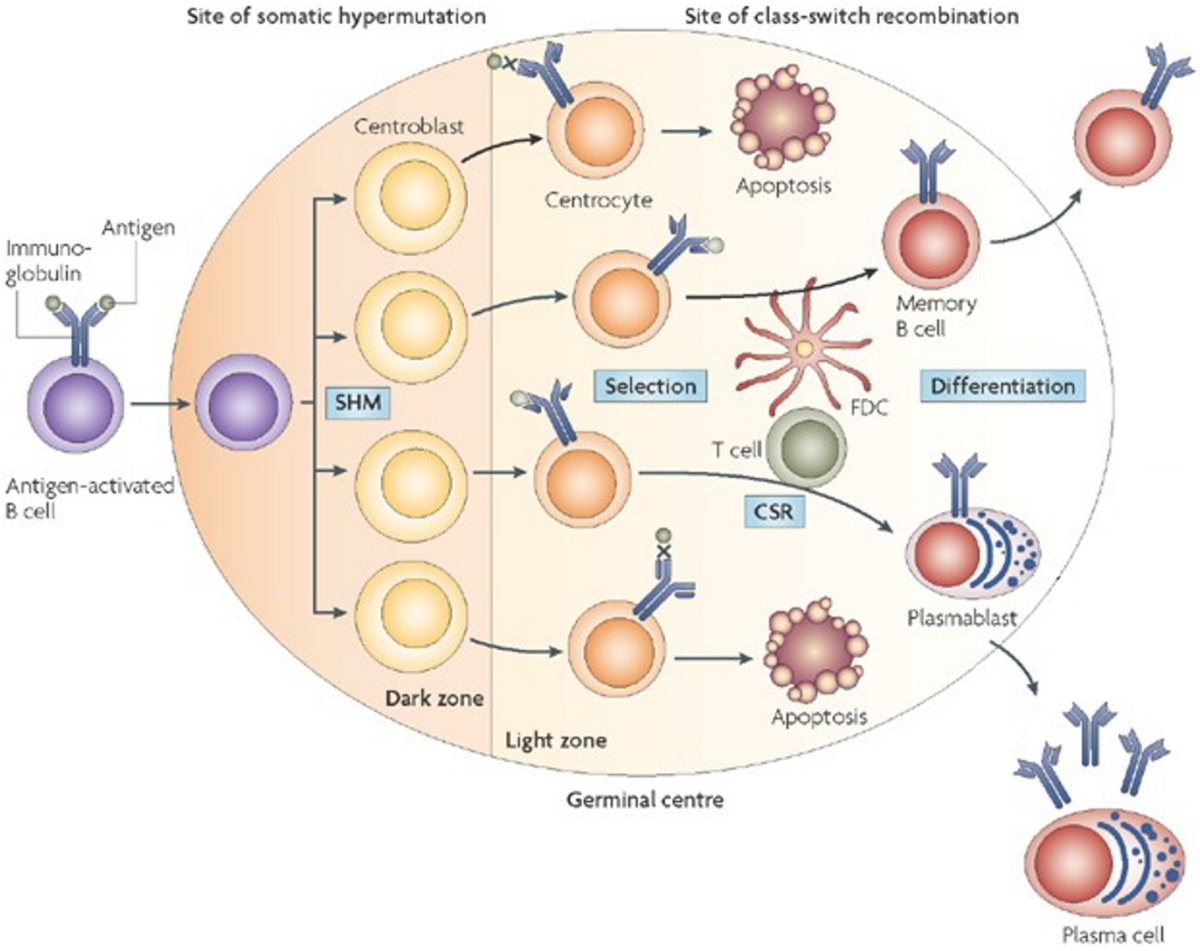


Figure 1.1.2 The germinal centre. *After T-cell dependent activation, B cells differentiate into centroblasts in the dark zone of the GC. Centroblasts are highly proliferative and undergo somatic hypermutation. AID mediates base-pair changes that result in modifications to the genes encoding the variable antigen-binding regions of the immunoglobulin. The cells then differentiate into centrocytes and migrate to the light zone. Within the light zone, the newly modified BCR competes for antigen binding. With the help of follicular dendritic cells and T cells, high-affinity BCR clones are selected. Clones that fail to bind antigen are removed from the pool through apoptosis. Some centrocytes will go through class switching to other immunoglobulin isotypes. Class switch recombination allows for the production of antibodies with different effector functions with the same antigen specificity. Finally, successfully selected centrocytes will differentiate into memory B cells or plasma cells. Adapted from*[20]

1.2 B cell subsets

1.2.1 Transitional Cells

In humans the current paradigm is that B cell development occurs through a linear pathway beginning with the development of pre-B cells into immature B cells which occurs in the BM, before migrating into the periphery where transitional cells develop into naïve cells[33].

Transitional cells describe the subset of B cells that migrate out of the BM prior to development into naïve cells in the periphery. These cells express IgD, CD10, and IgM, although their high expression of CD24 and CD38 has also been used to identify them in humans[34,35].

Transitional cells are divided into 3 subpopulations, T1, T2, and T3. T1 cells have been proven to be particularly susceptible to spontaneous apoptosis and are difficult to rescue[35], as a result, these cells provide another opportunity for negative selection[34]. T2 cells are more responsive to antigen stimulation resulting in positive selection[34]. These selection events are required to generate the B cell repertoire.

In mice, cells progress linearly from T1 to T2 to mature B cells, T3 B cells are not believed to give rise to mature B cells[36]. In humans, early stages of peripheral B cell development can be defined by the expression of ABCB1 transporter protein[37]. The human T3 transitional cell subset was identified within the blood of patients after undergoing rituximab treatment[38]. These cells lacked the ABCB1 transporter but were otherwise phenotypically similar to naïve B cells[38], suggesting that these cells represent the development stage between T2 cells and naïve B cells. Later, it was found that these T3 cells could be further subdivided into two

subclasses[39,40], indicating that the T3 population represents 2 pathways of differentiation instead of a linear development pathway[33].

1.2.2 Naïve B cells

B cells that have matured in the bone marrow and have been released into the blood but have yet to be exposed to antigens are termed naïve B cells. These cells have a short life span of only a few weeks[41] and typically have a low affinity to antigen. Human naïve B cells are phenotypically characterised by high levels of IgD and IgM as they are yet to undergo class switching.

1.2.3 B1 cells

In mice, B1 cells develop separately from marginal zone and follicular B cells and are predominantly found in the peritoneal and pleural cavities with only a small number found in the spleen[42]. These cells develop within the foetal liver and are the first B cell to develop[43,44]. B1 cells can spontaneously secrete antibodies against non-protein antigen and so provide immediate defence against microbial infection[45–47] which are known as "natural antibodies". Natural antibodies secreted by B1 cells are predominantly IgM[48], show little somatic hypermutation[49,50], and are often autoreactive[51]. These autoreactive antibodies function to aid disposal of apoptotic cell debris and are thought to be protective in autoimmunity[52], despite this, the B1 population is enriched in both murine and human autoimmune diseases[51,53]. B1 cells are also considered to be more effective as APCs compared to other B cells. They express high levels of costimulatory molecules[54] and a murine model of systemic lupus erythematosus (SLE) suggests a role of B1 cells in the activation and expansion of $CD4^+$ T cells[55]. B1 cells function as a potent APC that often

recognise self-antigens could indicate a role for these cells in the loss of tolerance during autoimmunity[55].

Although B1 cells are well characterised in mice, the existence of human B1 cells have been controversial. In mice the B1 lineage is defined by CD5 expression[56], however, CD5 expression in humans is not restricted to B1 cells as it is also expressed on B2 cells[57]. Additionally, both $CD5^+$ and $CD5^-$ B cells can produce IgM[58]. Subsequently, human B1 cells have been characterised as $CD20^+CD27^+CD43^+CD70^-$ based on their functional similarities to mouse B1 cells[59]. Like mouse B1 cells, these cells were able to spontaneously produce IgM, stimulate T cells, and expressed a skewed B cell receptor repertoire[59,60]. Recent extensive mapping of the human B1 population also demonstrated the increased capacity of self-renewal by these cells compared to mature B cells[60]. The number of human B1 cells declined with age[59,61] along with a reduction in both the capacity to produce IgM and clonal diversity[61], which could negatively impact the older population through the loss of these natural antibodies.

1.2.4 Memory B cells

An important hallmark of adaptive immunity is the generation of immune memory. Memory lymphocytes generated during an immune response to a specific antigen are long-lived and provide a rapid response upon re-infection with a similar antigen. This principle of immune memory is utilised in vaccinations to provide protection to previously deadly diseases.

Memory B cells have a long lifespan, potentially living for decades compared to the short life of a few weeks of naïve B cells[41,62,63]. Most human memory B cells have increased expression of CD27, which upon binding to its ligand CD70 on T cells promotes the

differentiation of activated memory B cells into antibody secreting plasma cells and proliferate rapidly[64,65]. A significant proportion of memory B cells have gone through class switching to downstream antibody isotypes from IgM to predominantly IgA and IgG[66,67]. A much stronger activation signal is observed from antigen-mediated crosslinking of cell surface IgG compared to IgM[68], leading to the rapid differentiation into plasma cells. Several subclass independent factors also play a part in this rapid response; memory B cells have a reduced expression of quiescence factors, increased expression of costimulatory molecules such as CD80 and CD86, as well as upregulation of pro-survival factors of the *Bcl2* family[69–71]. Long-lived plasma cells lack proliferative potential so newly differentiated plasma cells from memory B cells are vital for the production of high affinity antibodies[72].

Other than differentiation into plasma cells, reactivated memory B cells can also re-enter the GC[73,74]. In the GC they are able to undergo further somatic hypermutation and class switching to better adapt to the infection[72]. Overall, memory B cells improve immunity through adjustments to the antibody response in the event of re-infection.

Not only does the expression of higher affinity BCRs on memory B cells strengthen the effector functions of the secreted antibodies, but it also allows memory B cells to sense low doses of antigen. This also contributes to the memory B cells act as an antigen-presenting cell (APC)[75,76]. During the initiation of the immune response, the dendritic cells are the most important APC. However, during the later phases of chronic immune reactions for example in autoimmune disease, memory B cells could be important APCs. The therapeutic anti-CD20 monoclonal antibody rituximab has been shown to be successful in depleting B cells in peripheral blood. Rituximab treatment does not deplete all memory B cells[77,78], as patients can still generate robust responses to repeated influenza vaccines comparable to healthy

controls[79]. Relapse post rituximab treatment is thought to be caused by repopulation with $IgD^{-}CD27^{-}$ and $IgD^{-}CD27^{+}$ memory B cells[80].

The homing receptor CXCR3 is upregulated in activated B cells in response to IFN-γ[81,82]. CXCR3 is subsequently expressed on memory B cells derived from these B cells that were activated under inflammatory conditions such as in a flare of an autoimmune disease. A subpopulation of CXCR3 expressing memory B cells has been observed in blood[81,82]. While memory B cell homing is important to mount an effective response to re-infection, this suggests that memory B cells could migrate to inflamed tissues where they exacerbate the autoimmune response while being protected from therapeutic depletion.

1.2.4.1 Human marginal zone B cells

In mice, marginal zone B cells denote a population of B cells with largely unmodified immunoglobulin that does not require GC for activation[83]. In humans, the marginal zone B cells express CD27 and most carry modified immunoglobulins[84]. These cells phenotypically similar to $IgM^{+}IgD^{+}CD27^{+}$ memory B cells although it is unclear if they derive from GC B cells[85]. A precursor of marginal zone B cells has been described in the spleen of young children[86]. It is thought that two subsets of human marginal zone B cells exist, one in young children that have a distinct GC independent developmental pathway, and one in adults that predominantly post-GC IgM^{+} B cells[86].

1.2.5 Double negative B cells

The absence of the naïve cell marker IgD and the classical memory marker CD27 defines double negative (DN) B cells[87]. The origins of these cells are still unknown, but DN cells do display levels of somatic hypermutation suggesting that these cells have undergone antigen

drive maturation within the GC[88,89]. Because of this, it has been theorised that DN B cells either originate from $CD27^+$ memory cells[90], or that these cells represent a population of exhausted memory B cells[91]. However, the level of SHM in DN B cells is higher than that seen in naïve B cells, but is lower than in $CD27^+$ memory cells[92,93]. This led to the alternative theories that DN cells are a product of a defective GC reaction[89], or more recently through extrafollicular differentiation[94].

DN cells can be divided between tonsillar and circulating populations[89]. These two subsets are defined by FcRL4 expression, with the majority of tonsillar DNs expressing FcRL4[89,95]. Circulating DNs can be further divided into DN1 and DN2[96]. $CXCR5^+$ DN1 cells represent the majority of DNs in healthy individuals[96]. $CXCR5^-CD11c^+CD21^-$T-bet^+ DN2 cell population is expanded in SLE patients, correlating with disease activity[96]. These cells are able to differentiate into plasmablasts upon TLR7 stimulation[96]. DN B cells are also elevated in other autoimmune diseases including RA and MS[94,97,98].

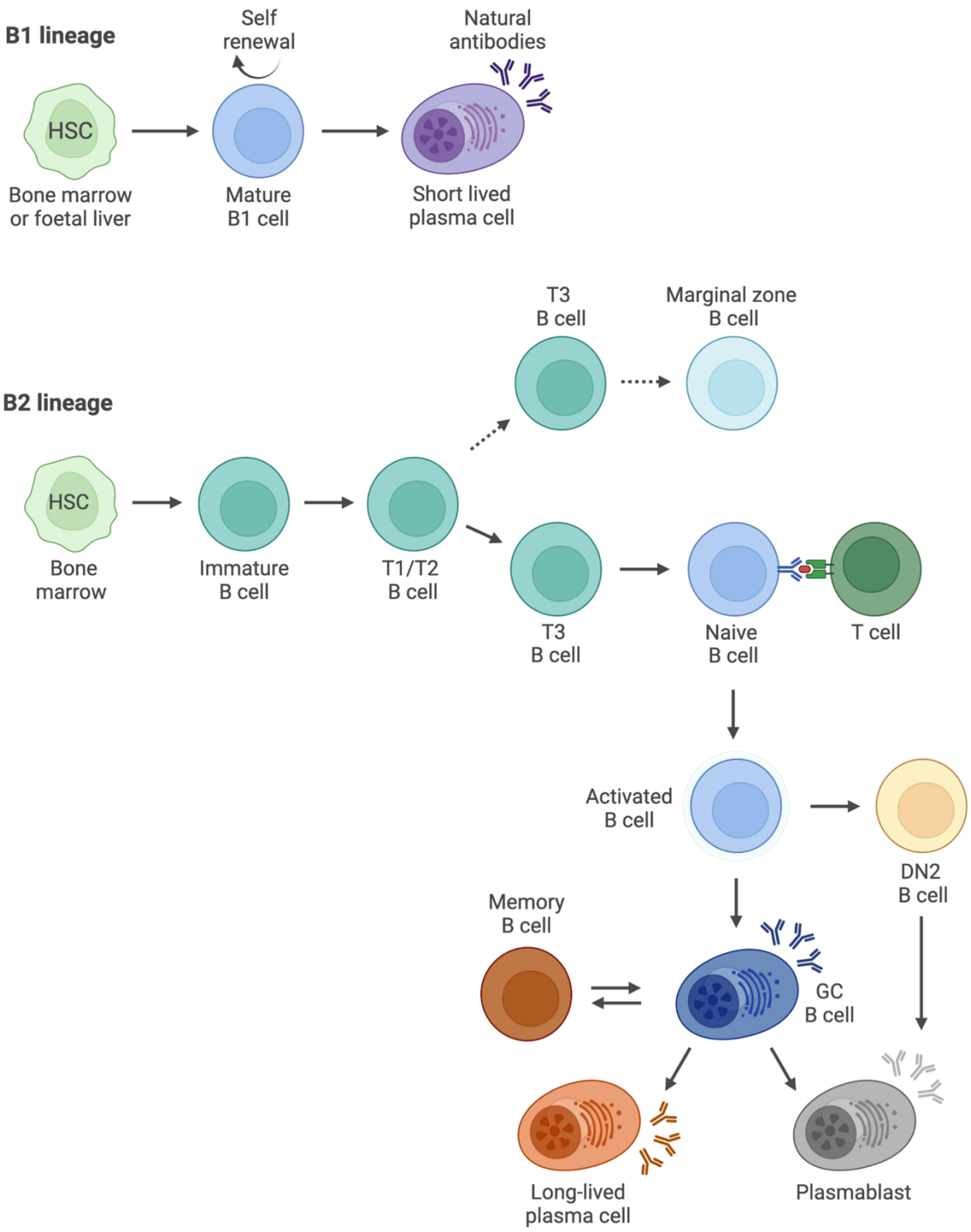


Figure 1.2.1 Overview of the developmental and differentiation pathways of human B1 and B2 B cells. *Solid lines represent association with clear support from the literature. Dashed lines used for theoretical associations. T1, transitional type 1 B cells; T2, transitional type 2 B cells; T3, transitional type 3 B cells; DN2, double-negative-1 B cells; GC, germinal centre. Adapted from*[93,99]*. Created using BioRender.*

1.2.6 Age-associated B cells

Age-associated B cells (ABCs) were first defined as B cells expressing high levels of CD11c but lacking in expression of CD21 and CD23[100,101]. Although there is heterogeneity within the ABC subset[102], these cells are also thought to consist of mostly memory B cells and express T-bet[103]. It remains unclear whether the ABC subset consists of unrelated pools of cells or the different stages of a single cell lineage[102].

T-bet is considered to be the regulator of ABC function[104]; however, T-bet does not appear to be a necessity in murine ABC production[105]. In mice and humans, T-bet expressing memory B cells can be subdivided into recirculating T-bet^{lo} and splenic resident T-bet^{hi} memory B cells[106]. Splenic T-bet^{hi} memory B cells have been speculated to act as broad immune surveillance and produce antibodies rapidly upon reinfection[106]. Indeed, when T-bet^{+} B cells are isolated from the blood, they can quickly differentiate into plasma cells[96]. The circulating T-bet^{lo} population could represent a short-lived cell population derived from the T-bet^{hi} memory B cells[106], which is supported by evidence showing the self-renewal capabilities of T-bet^{+} memory B cells in mice[106,107].

In mice, ABC numbers increase with age[108]. These cells are thought to be functionally exhausted, and so could contribute to immune senescence[108]. ABCs produce pro-inflammatory cytokines and inhibit B cell development but targeting pro-B cells for apoptosis[108–110]

In rheumatoid arthritis (RA) and SLE, disturbances in the B cell compartment are often seen, including the premature accumulation of ABCs[100,101]. These cells were subsequently identified in other autoimmune diseases including primary Sjögren's syndrome (pSS),

Crohn's disease and multiple sclerosis[111–113]. ABCs have also been found in infectious diseases such as malaria and HIV[91,114]. In viral infections, ABCs readily produce anti-viral IgG[91,114], and in chronic autoimmune diseases, ABCs can expand rapidly and produce autoantibodies[111–113]. In mouse models of autoimmunity, ABCs have been implicated as potent antigen presenting cells and the formation of spontaneous germinal centres[101,104,115].

1.2.7 FcRL4

In humans, the Fc receptor-like (FcRL) family consists of 6 surface proteins (FcRL1-6) and 2 intracellular proteins that reside within the endoplasmic reticulum (FcRLA and FcRLB). The FcRL family of receptors can also be found within mice, although only 3 surface proteins (FcRL1, FcRL5, and FcRL6), the two intracellular proteins, and a secreted FCRLS can be found[116].

The *IRTA1* gene which encodes for FcRL4 was first identified through their involvement in chromosomal translocations affecting band 1q21 in B cell non-Hodgkin's lymphoma[117,118]. FcRL4 expression defines a small subset of tissue-based memory B cells first identified within the mucosa-associated lymphoid tissues (MALT) of healthy individuals[95,119]. These are located within the tonsil epithelium and the dome epithelium of the Peyer's patches, which are sometimes regarded as the anatomical equivalent of the marginal zone[119]. However, they are rarely seen within the spleen and lymph nodes[119].

1.2.7.1 FcRL4 function

The FcRL4 receptor consists of 4 extracellular Ig-type domains and in the intracellular domain, 3 potential ITIM motifs (Figure 1.2.1). The inhibitory function of the ITIMs is mediated by the recruitment of SHP-1 (SH2 domain-containing tyrosine phosphatase 1) and

SHP-2[120]. SHP-1 and SHP2 prevent the recruitment of Syk to the Ig-α and Ig-β chain of the BCR which is necessary for its phosphorylation and subsequent activation. FcRL4 expression can be induced in peripheral blood B cells through BCR and TLR9 co-stimulation[121]. TLR9 binds endocytosed unmethylated CpG motifs common in bacterial and viral DNA which can be found on the mucosal surface.

Originally, FcRL4 was shown to be receptor for IgA aggregates[122], however a recent study found that FcRL4 binds to dimeric IgA but not secretory IgA (sIgA) and monomeric IgA[123]. FcRL4 competes with polymeric Ig receptor (pIgR) for binding to dimeric IgA (Figure 1.2.2). Therefore, the presence of FcRL4$^+$ cells could function to modulate the quantity of dimeric IgA that gets transported into the mucus as sIgA. FcRL4$^+$ B cells have been proposed to play a tolerogenic role in mucosal immunology. These cells have a preference for recognition of commensal antigens and the co-engagement of FcRL4 with BCR leads to inhibition of commensal specific B cell response[124].

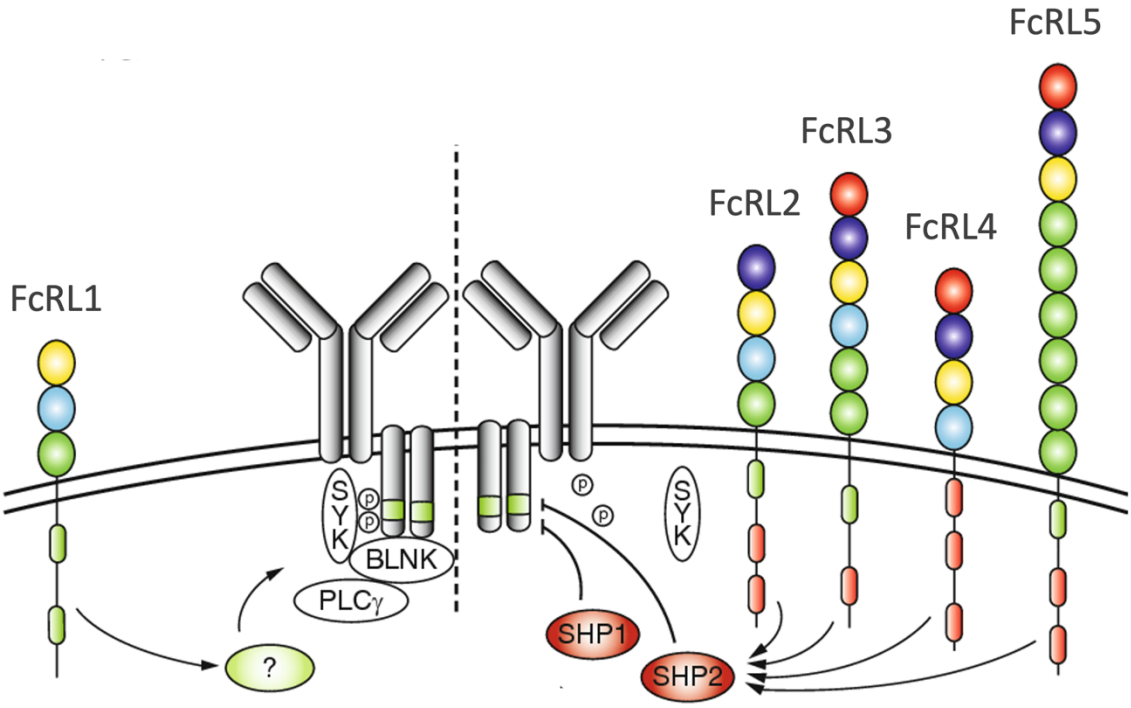


Figure 1.2.2 Protein structure of FcRL family of receptors and their signalling potential. *In human B cells, FcRL1-5 all modify BCR signalling. FcRL1 increases BCR signalling through an unknown pathway. FCRL2-5 all contain ITIMs that can inhibit BCR signalling through the recruitment of SHP1 and SHP2. SHP1 and SHP2 prevent the recruitment of Syk to the Ig-α and Ig-β chain of the BCR thus preventing activation of the BCR. Adapted from*[125]

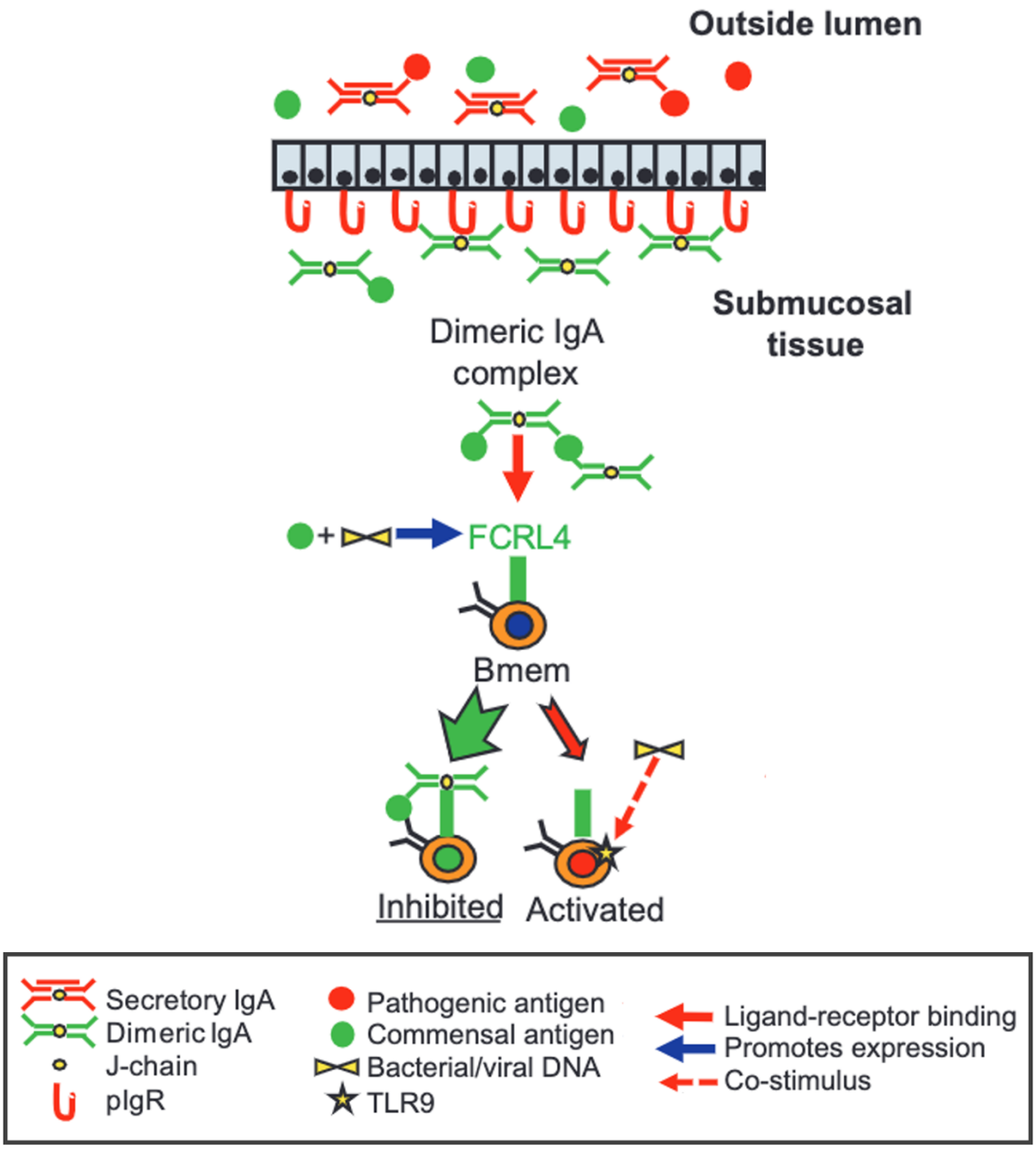


Figure 1.2.3 Potential FcRL4 function in the mucosa. *Dimeric IgA in the submucosal tissue binds to pIgR resulting in the transcytosis of IgA. IgA is released into the lumen as sIgA. Within the submucosal tissue, FcRL4 competes with pIgR for dimeric IgA. FcRL4 prefers commensal antigens. Co-stimulation of the BCR with FcRL4 results in the inhibition of the antigen specific activation, suggesting that FcRL4 plays a tolerogenic role in this pathway. Alternatively, TLR9 stimulation through bacterial and viral DNA leads to activation of the B cell. TLR9 pathway is independent of FcRL4 stimulation but requires FcRL4. In fact, TRL9 stimulation promotes the expression of FcRL4. Adapted from*[126]

1.2.7.2 FcRL4$^+$ B cells in disease

FcRL4$^+$ B cells have been identified in several diseases. In the blood of HIV-infected patients, FCRL4$^+$ B cells were described a double negative B cell population that exhibits an "exhausted" cell type[91] that do not proliferate upon antigenic stimulation. This is due to their limited response to BCR activation. On the other hand, these cells are highly proliferative. Phenotypically, these cells differ from FcRL4$^+$ B cells seen in the MALT of healthy individuals[91]. In autoimmune diseases, FcRL4$^+$ B cells are thought to contribute to disease progression[127–130]. FcRL4$^+$ cells can be located within the inflamed synovium in RA[128] and the inflamed salivary glands in pSS[130].

In RA, these cells are thought to play a role in disease pathogenesis through multiple pathways. First, FcRL4$^+$ B cells have been shown to produce the cytokine RANKL[127,128]. RANKL mediates the activation and differentiation of osteoclasts resulting in the bone erosion characteristic of RA[131]. Secondly, along with the function of FcRL4 as a receptor for IgA, FcRL4$^+$ cells from the inflamed synovium are significantly enriched for IgA expressing B cells[129]. This suggests that these cells could provide the link to the mucosal inflammation that precedes RA onset[132–134]. Thirdly, analysis of the BCR repertoire of FcRL4$^+$ B cells from the inflamed synovium of RA patients showed that these cells play a role in the recognition of citrullinated autoantigens in RA[129].

In pSS, FcRL4$^+$ B cells can be identified in the inflamed salivary glands[130,135]. CCR5 is expressed by FcRL4$^+$ B cells which aid in their migration towards the CCL3 and CCL5 producing ductal epithelial cells[135,136]. The IL-6 gene is upregulated in FcRL4$^+$ B cells isolated from pSS patients suggesting that these cells contribute to the pro-inflammatory microenvironment[135]. Treatment with the anti-CD20 monoclonal antibody rituximab has

been shown to be successful in eliminating FcRL4^{+} cells in patient salivary glands, which leads to subsequent reduction in inflammation[130]. Rituximab treatment also resulted in the reduction of Tfh and Th17 cells[137], suggesting that FcRL4^{+} B cells may have a complex role in pSS pathogenesis.

1.3 Mucosal immunology

1.3.1 The intestinal mucosal immune system

On a daily basis, the mucosal surface is exposed to a vast array of harmless food antigens, commensal microbes, and potentially harmful pathogens. The mucosal immune system protects these surfaces by using multiple layers of barriers; a tight monolayer of epithelial cells is covered by a mucus layer. This mucus layer is produced by goblet cells and is rich in antibacterial substances such as IgA and α defensins, preventing bacteria from attaching to the epithelial layer below.

The mucosa associated lymphoid tissue (MALT) can be found throughout the body situated along the surface of all mucosal tissues[138]. The MALT is subclassed depending on their location, these subclasses include bronchi-associated lymphoid tissue (BALT), gut-associated lymphoid tissue (GALT), and nasopharynx-associated lymphoid tissue (NALT). MALT can be divided functionally into effector sites and inductive sites[138,139]. Secondary lymphoid tissues where IgA class switching and B cell clonal expansion occurs are inductive sites. These activated B cells then migrate to effector sites[138], where IgA is secreted across the mucosal epithelium[140].

1.3.1.1 The gut epithelial barrier

The gut epithelium plays an active role in mucosal immunity. The mucus layer is the first line of defence against the large number of commensal bacteria found in the microbiome. Pathogen invasion is further thwarted by the epithelial monolayer's barrier function, which expresses toll-like receptors (TLR) and other pattern recognition receptors (PRR) that detect cellular injury or damage[141,142]. Intestinal epithelial cells release cytokines and chemokines in response to commensal bacteria, pathogens, or damage which allows them to shape the

local immune response and influence sub-epithelial DC and lymphocyte activity[143]. Under normal conditions, the epithelium produces anti-inflammatory cytokines such as IL-25[144]. However, a shift into a proinflammatory response occurs as a result of infection or epithelial damage. Activation of NFκB leads to the production of proinflammatory cytokines which mediate this shift[145].

Epithelial cells express MHC-II, suggesting that they are non-professional antigen presenting cells, although these cells do not express the co-stimulatory molecules CD80 and CD86[146], CD40 can be found on the epithelial cell surface[146]. In murine models, it has been shown that CD40 expressing dendritic cells or epithelial cells are required for the development of FoxP3$^+$ regulatory T cells[146]. Murine intestinal epithelial cells that express CD40 have also been demonstrated to be unable to promote antigen driven activation of CD4$^+$ T cells[147]. Together this shows that epithelial cells in the mucosa play an active role in establishing immune tolerance.

1.3.1.2 The lamina propria

The lamina propria is a highly vascularised connective tissue matrix found under the mucosal epithelium. Antigen presenting dendritic cells within the lamina propria are able to sample gut derived antigen[148]. CD103 expressing DCs then migrate to the draining mesenteric lymph nodes (MLN), or Peyer's patches where they activate naïve lymphocytes[149].

The balance between IFN-secreting CD4$^+$ T-cells, which drive inflammatory responses, and immunosuppressive regulatory cells, which regulate and restrict inflammation, determines the outcome of immunological activation in the lamina propria[150]. Peyer's patches, which

are the sites of IgA-producing B cell maturation, are found throughout the small intestine[151]. Within these patches, there is continuous production of IgA secreting plasma cells in response to gut derived antigen[152]. IgA produced by these cells are a major contribution to mucosal defence. T and B cells migrate to the lamina propria after activation and form part of the specific immune response[153].

1.3.2 IgA in the mucosa

1.3.2.1 Induction of IgA

Gut associated lymphoid tissue (GALT), which includes Peyer's patches, isolated lymphoid follicles, and mesenteric lymph nodes, is a characteristic sIgA inductive location. The GALT comprises at least 80% and 90% of the body's plasma cells and sIgA respectively[154].

Peyer's patches are located underneath a specialised epithelium, termed follicle-associated epithelium (FAE), which contain microfold cells (M cells). Within the Peyer's patches, the B cell follicles are covered by the subepithelial dome which lies under the FAE. DCs are found within the subepithelial dome[155] where they are able to collect mucosal antigens that have been transported across the epithelial barrier by M cells[155] or by extending their dendrites into the epithelium[156].

Subsequent antigen presentation by DCs to T and B cells results in activation and IgA class switching in mucosal B cells[157]. Activation-induced cytidine deaminase (AID) converts cytosines into uracils, leading to double stranded DNA breaks, resulting in the replacement of the Cμ gene with the Cα gene. TGF-β plays a critical role in class switching from IgM to IgA; downstream signalling of TGF-β receptor leads to activation of the Iα promotor of the IgA heavy chain gene[157].

Interactions between T and B cells via CD40/CD40L signalling results in the production of high affinity antigen-specific IgA[158]. The release of various cytokines, including IL-21, by T follicular helper cells, Tregs, and Th17 cells promotes class switching to IgA[159]. However, this involvement of T cells is not thought to be vital in the production of IgA. CD40 deficiency in both humans and mice does not oblate IgA production[160,161], instead innate immune cells through the production of BAFF and APRIL stimulate CSR to IgA[162].

1.3.2.2 Role of IgA

IgA is the predominant immunoglobulin found at the mucosal surface and the second most abundant in the circulation after IgG. The average human produces approximately 60mg of IgA per kilogram of body weight every day[163], most of which is located at the mucosal surface. The abundance of IgA at the mucosa, where the body is most exposed to the environment, demonstrates the importance of IgA in mucosal immunology.

There are two subclasses of IgA found in humans: IgA1 and IgA2. IgA exists in multiple molecular forms, in the serum IgA is monomeric and predominantly IgA1. In the mucosa, IgA1 and IgA2 are evenly distributed[164].

IgA has traditionally been non-inflammatory. IgA lacks the C1q binding site and so is unable to activate the classical caspase cascade. Instead, IgA provides passive immunity through pathogen neutralisation and antigen excretion. IgA produced by plasma cells within the lamina propria is transported into the lumen by poly Ig receptor (pIgR) on the surface of epithelial cells. Within the lumen sIgA bind to bacteria and bacterial products, preventing them from penetrating the epithelium by forming aggregates[165]. IgA is also able to capture antigen within the epithelial cell during transcytosis[166,167]. In addition, pIgR is able to

transport antigen-IgA immune complexes into the lumen[168], thus eliminating immune complexes from the mucosa preventing an immune response.

In addition to antigen neutralisation, IgA can also mediate effector function through binding to FCαR1. FcαR1, also known as CD89, is expressed on the surface of several innate immune cells and is able to bind both subclasses of IgA[168]. However, very few FcαR1 expressing cells are found within the mucosa during homeostasis[169]. To reduce overactive immune responses, monomeric serum IgA in the absence of antigen produces an inhibitory ITAM (ITAMi) response[170]. On the other hand, during infection, cross-linking of FcαRI by monomeric or dimeric IgA immune complexes, causing neutrophils and Kupffer cells to mount robust pro-inflammatory responses in order to clear the infection[171,172].

1.4 The human liver

1.4.1 Introduction

The liver is the largest solid organ of the human body; weighing approximately 1.5kg, it accounts for almost 2% of the weight of an adult body. Its importance is demonstrated not only by its size but that approximately 30% of the total blood volume in the body passes through the liver every minute[173]. Metabolism of amino acids, carbohydrates, lipids, and vitamins are important functions of the liver. Along with this, the liver is also tasked with the metabolism of drugs and alcohol, as well as the removal of infectious and foreign antigens from the blood. All these vital functions are facilitated by the central position of the organ and aided by its unique vasculature.

1.4.2 Liver anatomy and function

Proteins, carbohydrates, lipids, vitamins, and trace elements are all metabolised and stored by the liver. Thus, the liver is directly involved in blood glucose regulation, iron storage for erythrocyte synthesis, and the creation of plasma proteins and hormones[174]. Bile is produced and excreted by the liver, allowing lipids and fat-soluble vitamins to be emulsified and broken down[175]. Along with lipid metabolism, bile is also responsible for the excretion of bilirubin, a by-product of erythrocyte breakdown in the liver. The liver derives the majority of its blood supply from the gut in order to facilitate these metabolic functions. However, because of this, it is exposed to a wide range of exogenous pathogens and xenobiotics including drugs, that have the potential to cause damage to the organ. As a result, the liver has developed the ability to regenerate; only 25% of the residual liver is required for regeneration in a few months in humans[176].

In order to fulfil its many and varied tasks, the liver is composed of several cell types including hepatocytes, biliary epithelial cells (BECs), hepatic stellate cells (HSCs), Kupffer cells, and liver sinusoidal endothelial cells (LSECs). The most abundant cell type found in the liver are hepatocytes. These epithelial cells make up approximately 80% of the total liver tissue and perform the majority of the functions ascribed to the liver. BECs are the second most abundant epithelial cell type and are found lining the lumen of the bile ducts. Hepatic stellate cells are responsible for the storage of vitamin A. However, upon activation following liver injury, these cells are also responsible for the deposition of collagen, and it is this that leads to the scarring and eventual cirrhosis observed in end-stage liver disease. Kupffer cells are the resident macrophage population within the liver. They are situated within the lumen of the liver sinusoids and are the first immune cell encountered by bacteria, endotoxins, and microbial debris transported to the liver from the gut[177]. The liver sinusoids are lined by hepatic sinusoidal endothelial cells. These cells form larger (50-180nm) fenestrations that allow the exchange of material between the blood and hepatocytes[174].

The hepatic lobule is the functional and structural unit of the liver[178]. It is roughly hexagonal in shape, in the middle of which lies the central vein (Figure 1.4.1A). Liver sinusoids emanate from the central vein like the spokes of a wheel towards the portal triads at the vertices. Each portal triad consists of the hepatic artery, portal vein, and bile duct.

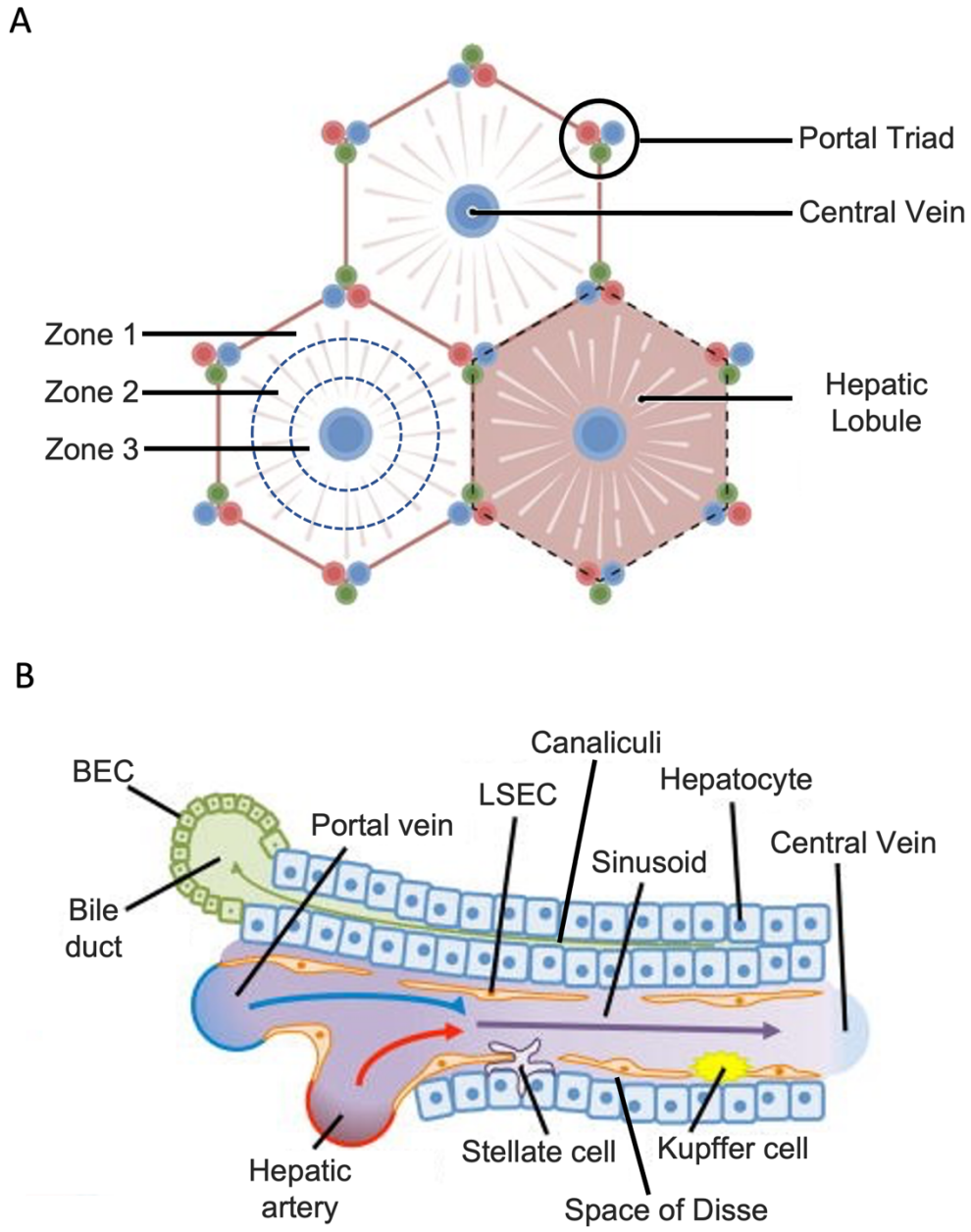


Figure 1.4.1. Anatomy of the liver. *(**A**) The functional unit of the liver can be described as a lobule (within the black dashed line). Each lobule is roughly hexagonal in shape with portal triads at each corner and a central vein at its centre. Each lobule can be subdivided into three zones according to the proximity of the arterial blood supply. (**B**) Within the liver lobule, the blood supply from the portal vein and hepatic artery mixes as it travels through the sinusoid towards the central vein. The sinusoid is lined by LESCs forming a permeable barrier between the blood supply and the single-cell layer of hepatocytes. The space of Disse is the space between the LSECs and the hepatocytes where hepatic stellate cells reside. Bile is produced by hepatocytes and is channelled out of the liver through canaliculi into the bile ducts, which are lined by BECs. Adapted from*[174].

Hepatocytes form one cell thick plates that are separated from the bloodstream by a barrier of LSECs[178]. The sinusoidal network functions to minimise the distance between each hepatocyte and the blood supply. To facilitate this, LSECs are permeable as they lack a basement membrane and form fenestrations that allow the exchange of particles between the sinusoidal blood and the space of Disse[179,180] (Figure 1.4.1B). Oxygenated blood from the hepatic artery mixes with the nutrient-rich blood travelling from the gut in the portal vein. As this blood makes its way through the sinusoids towards the central vein, oxygen and nutrients are removed while metabolites and waste products are added. This creates a gradient of the oxygenation, nutrient, and waste levels. As a result, the lobules are divided into zones depending on their proximity to the blood supply from the portal areas, with the hepatocytes from each zone having different metabolic capacities. This partitioning is known as "metabolic zonation"[174] (Figure 1.4.1A).

1.4.3 Bile

Bile production is an important function of the liver. Bile has two main functions: to facilitate the digestion and absorption of fats, and to eliminate waste products[181]. Large lipid droplets are broken down into smaller droplets by bile acids, allowing greater surface area for digestive enzymes[182]. Cholesterol is eliminated through its conversion into bile acids. Bilirubin, a waste product from erythrocyte breakdown, is also removed by secretion into bile[175].

Bile is produced by hepatocytes and is modified by biliary epithelial cells lining the bile ducts as it travels through the biliary tree. Hepatocytes are highly polarised; their plasma membrane is separated into a basolateral-sinusoidal and an apical-canalicular domain[183].

This allows the hepatocyte to secrete into the sinusoid and the canaliculi simultaneously[184]. Bile is emptied from the canaliculi into the canal of Hering, followed by a channel lined by cholangiocytes known as ductules[185] (Figure 1.4.2B). Ductules are connected to the interlobular bile ducts that form the portal triad along with the portal vein and hepatic artery. As bile passes through the small and large bile ducts, it is diluted and alkalinised by cholangiocytes. Eventually, it leaves the liver and enters the gallbladder and duodenum (Figure 1.4.2A).

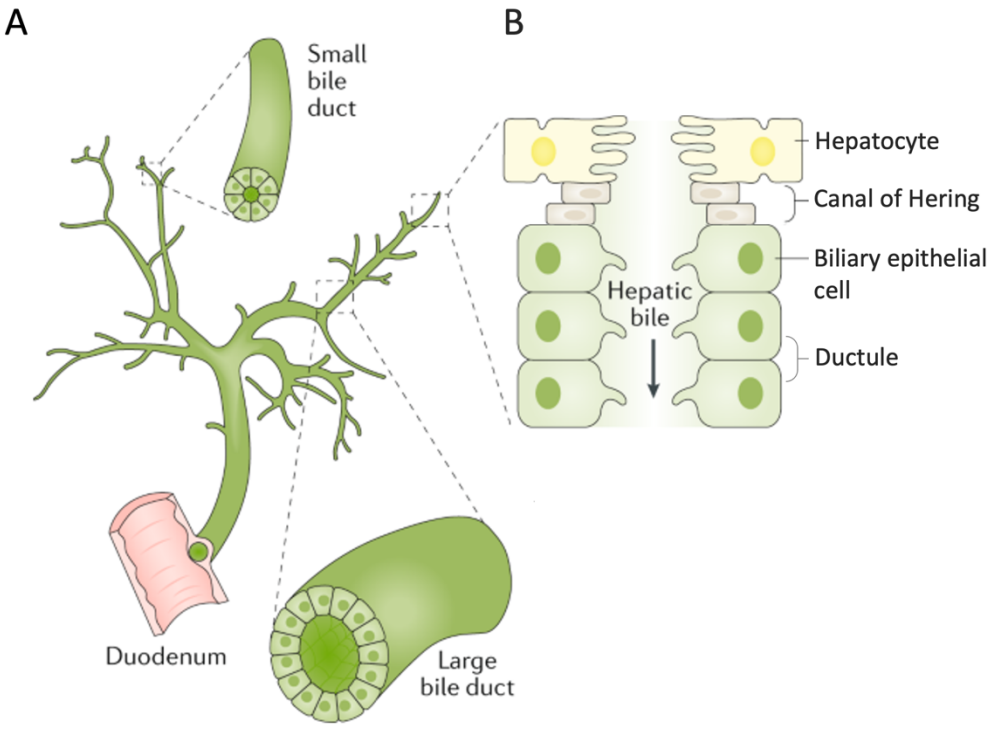


Figure 1.4.2 The biliary tree. *(**A**) Bile flows from small bile ducts that form part of the portal triad into large bile ducts. Bile is transported out of the liver and is either transported to the duodenum or stored in the gallbladder. (**B**) The apical-canalicular domain of hepatocytes secrete bile components into the canaliculi. The bile then travels through the canal of Hering and the ductules where it is modified by the BECs which line them. Adapted from*[186]

The transfer of IgA to the bile duct lumen is an important part of biliary humoral immunity. When compared to the upper intestinal fluid, bile has around twice the concentration of SIgA[187]. SIgA, which is made up of two IgA molecules, a peptide J chain, and a secretory component (SC)[188], is the most common type of IgA identified in bile. IgA binds to the pIgR on the basolateral side of the epithelial cell, before being transported to the apical or luminal surface. At the luminal surface, the IgA-pIgR complex is cleaved to release the mature SIgA and a free SC[189] (Figure 1.4.3). The heavily N-glycosylated SC of pIgR protects the SIgA from proteolytic digestion in the gastrointestinal tract, and its carbohydrate residues help anchor the SIgA to mucus[188]. SIgA protects the biliary through binding of both bacterial toxin and directly to bacteria to prevent their adhesion to the mucosal membrane[188].

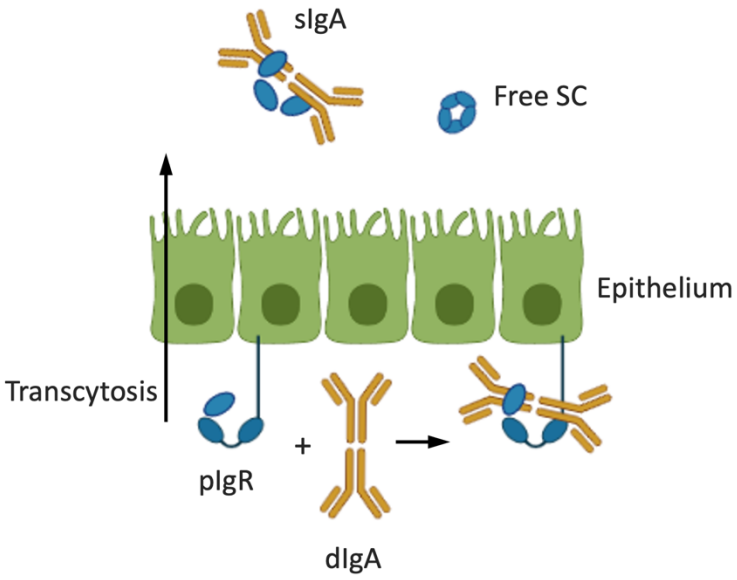


Figure 1.4.3 Transcytosis of IgA across the epithelium with pIgR. *Dimeric IgA binds to pIgR on the basolateral side of the epithelium. The IgA-pIgR complex is transported to the apical surface and cleaved to form the mature SIgA and a free SC. Created in BioRender.com*

1.4.4 Immune component of the liver

The liver contains a large compartment of immune cells. Kupffer cells are the largest population of resident macrophages consisting of 80-90% of all tissue macrophages in the body[190]. These cells reside within the sinusoidal space and are the first immune cells encountered by foreign antigens from the gut. Due to this, Kupffer cells play a vital role in phagocytosis, antigen presentation, and production of pro-inflammatory cytokines. Antigen capture and processing is also carried out by resident hepatic dendritic cells (DCs). These cells originate from the bone marrow[191] and reside around the central veins and portal tracts[192]. Scattered throughout the parenchyma, 10^{10} lymphocytes are contained within the average liver. Within this lymphocyte population are conventional T cells. Typically $CD4^+$ T cells are outnumbered by $CD8^+$ T cells and the frequency of effector and memory cells are higher than what is seen in peripheral blood[193]. The liver has more conventional and non-classical NKT cells than any other organ, accounting for up to 30% of the intrahepatic lymphocyte population[194]. NK cells, which are also seen in significant numbers among liver resident lymphocytes, govern their migration and expansion in the liver[195]. Lastly, only 6% of the liver lymphocytes are B cells, and little is known about their function within the liver.

LSECs make up around 50% of the nonparenchymal cells in the liver and line the sinusoids. These cells are capable of phagocytosis and express scavenger receptors. Receptors associated with antigen presentation such as MHC class I and II as well as co-stimulatory molecule CD80 and CD86 are also expressed by LSECs[196,197], and they have similar antigen processing and presentation capabilities as DCs[198]. The lack of a basement membrane and formation of fenestrations mean that LSECs allow direct contact between lymphocytes in the sinusoidal space with hepatocytes. Physical occlusion of the sinusoids by HSCs and

Kupffer cells creates stasis of the blood supply, thus allowing lymphocyte extravasation and increased contact time between lymphocytes and APCs[199,200].

1.4.5 Liver immunotolerance

As part of its functional role as a metabolic organ, the liver is constantly exposed to a myriad of antigens from commensal bacteria and food. This increased exposure comes with inherent risk of overactivation of the immune system resulting in chronic inflammation and disruption of cell homeostasis. As a result, the liver has a unique immunotolerant environment that can be switched to a responsive state at any given time[201]. This tolerogenic effect was first evidenced in the early history of experimental transplantation, where allogenic liver grafts were tolerated and did not require high doses of immunosuppressants[202] while other allografts were rejected.

Immune tolerance in the liver is facilitated by the numerous APCs found within the liver[203]. Hepatic DCs exhibit an immature phenotype[204], which is associated with reduced MHC class I and II expression as well as reduced expression of co-stimulatory molecules CD80 and CD86[205]. Together this mediates a tolerogenic effect on T cells leading to T cell deletion, anergy and the induction of Tregs[206]. Liver DCs have also been shown to secrete the anti-inflammatory cytokine IL-10[207] and is associated with reduced T cell proliferation. Additionally, Kupffer cells and LSECs also produced Il-10 and TGF-β which promotes an immature DC phenotype[190,207,208]. Furthermore, hepatocytes, Kupffer cells, and LSECs directly promote $CD8^+$ T cell death through expression of either programmed death-ligand (PD-L1) or first apoptosis receptor (Fas) ligand[209,210].

In normal livers, no MHC class II can be detected on BECs, however MHC class I has been observed at variable intensity across patient samples[211]. CD80 and CD86 are absent on the surface of BECs and could not induce a T cell response *in vitro*[212,213]. Although absent in healthy livers, TNF-related apoptosis-inducing ligand (TRAIL) is expressed on BECs from autoimmune cholestatic diseases[214]. TRAIL ligation with death receptor 5 (DR5) expressed on lymphocytes results in apoptosis[214]. PDL-1 is also expressed by BECs in autoimmune liver disease as well as in bile duct cancer[215,216], therefore cholangiocytes could directly induce apoptosis in lymphocytes thus limiting the immune response[187].

1.5 Liver disease

1.5.1 Non-alcoholic steatohepatitis

Non-alcoholic steatohepatitis (NASH) is a more aggressive form of non-alcoholic fatty liver disease (NAFLD). NASH is characterised by inflammation, fibrosis, and steatosis (the abnormal retention of fat within an organ). Progression of NASH to cirrhosis and hepatocellular carcinoma can lead to liver failure and the need for liver transplantation[217].

The aetiology of NASH remains unknown, however there are several risk factors have been shown to be associated with disease. The most common risk factor is being overweight or obese[218]. Obesity is associated with a less diverse intestinal microbiome compared to that seen in lean individuals[219]. Dysbiosis of the microbiome leads to the breakdown the intestinal barrier resulting in the exposure of the liver to gut derived toxins. Overgrowth of intestinal bacteria and increased intestinal permeability have been linked to the development of NASH[220]. Indeed, increased serum levels of LPS has been seen in NASH patients[220], suggesting that hepatic immune cells could be exposed to TLR ligands may be the trigger for hepatic injury in NASH. Other compounds such as fatty acids and damage associated molecular pattern released by hepatocytes, could also trigger liver resident Kupffer cells[221].

1.5.2 Polycystic liver disease

Polycystic liver disease (PLD) is a hereditary disease characterised by multiple cysts within the liver[222]. A number of genes are associated with PLD pathogenesis; however, the course of disease progression is the same across all PLD variation, which presents as an increasing number and volume of cysts within the liver[223]. Due to this progressive increase in cysts, the

volume of PLD livers can increase by 1.8% every 6 to 12 months[224,225]. Despite this, only 20% of patients report any clinical symptoms, these include abdominal distension, back pain, and gastroesophageal reflux[226]. PLD patients are at risk of developing portal hypertension due to the obstruction of hepatic venous flow by these cysts[227].

Liver transplantation is the only cure for PLD. This treatment is only available to patients with the most severe disease and symptoms that seriously affects their quality of life[226]. For patients with less severe disease, surgical and medical interventions are available to manage the disease[228].

1.5.3 Primary sclerosing cholangitis

Primary sclerosing cholangitis (PSC) is a chronic liver disease characterised by the stricturing of intrahepatic and extrahepatic bile ducts as a result of immune mediated inflammation and fibrosis[229].

The pathogenesis of PSC remains largely unknown, however there are a few proposed methods for disease progression. Due to the concentric fibrosis seen surrounding the bile ducts, defects in mechanisms protecting the liver against bile toxicity have been theorised as a method of disease pathogenesis. PSC has a strong association with inflammatory bowel disease (IBD); patients with PSC-IBD have a distinct intestinal microbiome compared to patients with IBD alone. This is has led to the theory that loss of tolerance in the gut of a shared liver antigen could also lead to PSC pathogensis[230].

Several autoantibodies have been linked to PSC, and evidence of their possible roles in pathogenesis is growing. Anti-neutrophil cytoplasmic antibodies (ANCA) are typically seen in

PSC, although their presence is not specific. It is unclear if the presence of ANCA antibodies in PSC is protective or harmful. In one cohort, ANCA specific for proteinase 3 (PR3) was found to be positively correlated with liver transaminase and ALP levels.

The link between PSC and IBD has led to several autoantibody targets to be investigated. In individuals with both PSC and IBD, autoantibodies of the IgA subclass targeting glycoprotein 2 (GP2) were discovered. Although GP2 is not known to be expressed on the biliary epithelium, it is found on intestinal microfold cells and is involved in the gut microbiome's antigen detection. This suggests that the gut-liver axis may play a role in PSC pathogenesis, and that tolerance loss may begin in the gut.

1.5.4 Primary biliary cholangitis

1.5.4.1 Introduction

Primary biliary cholangitis (PBC) is a chronic cholestatic autoimmune disease characterised by immune-mediated destruction of the small and medium-sized intrahepatic bile ducts[231]. PBC affects predominantly women at a female to male ratio of 10:1, with an average age of diagnosis of 40. Treatment with ursodeoxycholic acid (UCDA) is effective at inducing disease remission in a proportion of patients[232]. However, 20-30% of patients do not respond to UDCA resulting in eventual need for a liver transplant[233,234].

PBC was first described in an 1857 case report by Addison and Gull[235]. Traditionally, PBC was diagnosed late in disease onset when patients were already experiencing symptoms of cirrhosis such as jaundice. In 2014, the nomenclature for PBC changed from primary biliary "cirrhosis" to primary biliary "cholangitis". This was due to advances in our knowledge of the disease which has led to improvements in diagnostic procedures and therapeutic tools that

has resulted in patients being diagnosed at the asymptomatic stage prior to the onset of biliary cirrhosis[235].

1.5.4.2 Diagnosis

PBC diagnosis relies on the fulfilment of 2 out of 3 hallmark criteria of disease. These three criteria are: elevated alkaline phosphatase (ALP) in the absence of other hepatobiliary pathology, and either detection of anti-mitochondrial antibodies (AMAs) or a liver biopsy that identifies immune infiltrates of the small intrahepatic bile ducts[236].

1.5.4.3 Disease pathogenesis

Slow and progressive destruction of the small and medium sized intrahepatic bile ducts in PBC leads to cholestasis, the build-up of bile and other toxins within the liver. Progressive inflammation leads to fibrotic changes resulting in cirrhosis typically occurring 10-20 years post diagnosis. There is currently no cure for PBC, however standard treatment can reduce the risk of disease progression to end-stage liver disease[237].

The destruction of BECs is primarily attributed to autoreactive T cells[238–242]. However, B cells are also thought to play an important role in disease pathogenesis, predominantly in the autoantibody response. The presence of AMAs is a hallmark of PBC; 90-95% of patients have detectable levels of this disease-specific autoantibody in their blood[243]. Both genetic and environmental factors contribute to the development of PBC, however the aetiology of the disease remains elusive.

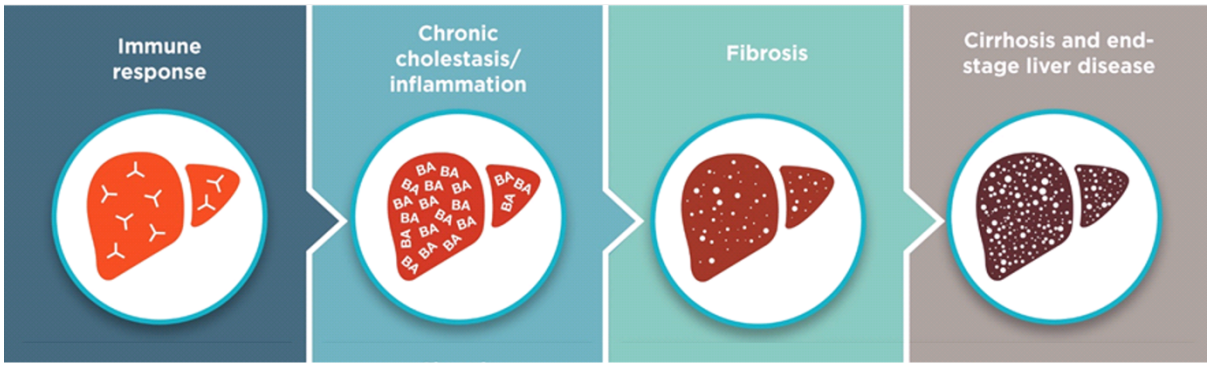


Figure 1.5.1 PBC disease progression. *Autoimmune destruction of the small bile ducts leads to the build of toxic bile acids resulting in cholestasis. Chronic cholestasis causes fibrosis and if left untreated results in cirrhosis and end-stage liver disease. Adapted from*[236]

1.5.4.3.1 Autoantibodies

AMAs are present in the sera of almost all PBC patients and have been used as a diagnostic tool since the 1970s[244]. The dominant target for AMAs is the E2 subunit of pyruvate dehydrogenase complex (PDC-E2). PDC-E2, which is aberrantly expressed on BECs in PBC[245] belongs to the 2-oxoacid dehydrogenase complex (2-OADCs) family of multi-enzyme complexes found in the inner mitochondrial membrane. Members of the 2-OADC family play vital roles in mitochondria function. In addition to PDC-E2, other members of the 2-OADC family have also been identified as targets of AMAs, including branched-chain 2-oxo-acid dehydrogenase complex E2 (BCOADC-E2), 2-oxo-glutarate dehydrogenase complex E2 (OGDC-E2), and dihydrolipoamide dehydrogenase-binding protein (E3BP)[246]. The observation of cross-reactivity between autoantibodies against PDC-E2 and E3BP highlighted a highly conserved structural motif present in both enzymes[247–249]. In fact, this motif containing a binding domain for lipoic acid (LA) is seen in all of the aforementioned E2 enzymes and plays an essential role in enzyme function[250–252].

AMAs are scarcely found in other liver or autoimmune diseases; indeed a positive AMA test in otherwise healthy individuals indicates substantial risk of developing PBC in the future[253]. Despite the importance of AMAs in PBC diagnostics, the role it plays in disease pathogenesis is unclear. The frequency of B cells specific to mitochondrial antigens were found to be correlated with increasing stage of PBC in the early inflammatory phase[254]. AMA titres correlate with PCs surrounding inflamed bile ducts on liver biopsies[255]. Liver infiltrating antibody secreting PBs and PCs isolated from PBC patients were able to create AMA *ex vivo*[256]. However, the presence of serum IgG anti-PDC-E2 in human infectious disease setting did not result in BEC damage[257], thus throwing into doubt the importance of AMAs in the destruction of BECs.

PBC has been associated with several other autoimmune diseases, including rheumatoid arthritis (RA) and primary Sjogren's syndrome (pSS). A common symptom seen in PBC patients is the presence of dry eyes and mouth. Indeed, studies into the secretory tissues in PBC have found pathology similar to BEC damage in the ductal epithelial cells of the pancreas, salivary, and lacrimal glands[258,259]. Furthermore, PDC-E2 has been found to be aberrantly expressed on salivary epithelial cells[260]. Examination of the antibody composition in PBC patient saliva found that most of the anti-PDC-E2 autoantibodies were IgA[261]. IgA-AMA can also be found within the bile of PBC patients[262]. Salivary ductule destruction in PBC has similar histological features as the destruction of biliary ductules in the liver[263]. Together, this raises the possibility of a shared mechanism of epithelial damage between the two sites. Plasma cells in the lamina propria produce IgA which is then internalised by epithelial cells as a complex with pIgR expressed on their basolateral surface. This IgA-receptor complex is transcytosed to the apical surface, the poly-Ig receptor is enzymatically

cleaved before it is secreted onto the mucosal surface. This process is carried out by both salivary epithelial cells and BECs to secrete IgA into the saliva and bile respectively. During its transcytosis, IgA has been shown to bind to newly synthesized viral proteins[264]. Co-localisation of IgA and PDC-E2 can be seen both intracellularly and at the apical cell surface in the PBC liver[265]. Moreover, IgA-AMAs derived from PBC patients were found to be able to bind intracellular PDC-E2 in Madine-Darby canine kidney cells (MDCK)[265]. In addition, these MDCK cells showed increased caspase activity after exposure to IgA-AMA[266]. Here, IgA-AMA increases caspase 9 and 3 compared to caspase 8 indicative of intracellular stress, suggesting that IgA-AMA could induce apoptosis of epithelial cells during transcytosis.

Binding of IgA-AMA to intracellular PDC-E2 could influence the metabolic pathway within the epithelial cell. *In vitro*, patient derived anti-PDC-E2 antibodies are highly effective at blocking PDC function[267]. PDC plays a vital role in glucose metabolism by linking glycolysis to the Krebs cycle. The presence of mitochondria dysfunction is associated with high anti-PDC-E2 titres in patient sera[268]. Fatigue is the most common symptom reported by PBC patients[269,270]. Rituximab, an anti-CD20 biological agent has been shown to reduce fatigue in immune conditions including pSS[271–274]. However, in PBC, rituximab treatment has been shown to reduce sera AMA titres[275,276], it is not effective at reducing fatigue in UDCA refractory patients[277,278].

AMAs are not the only autoantibodies seen in PBC. The presence of the anti-nuclear antibodies (ANAs) anti-Sp100 and anti-gp210 are associated with a more severe clinical course[279,280].

1.5.4.3.2 B cells

Despite AMAs being one of the main hallmarks of PBC and the presence of B cells within lymphoid structures close to bile ducts in the diseased liver, the role of B cells in disease pathogenesis is poorly understood.

High throughput sequencing of the peripheral B cell repertoire in PBC patients shows a lack of clonal diversity in the BCR[281]. Previous studies found that a reduction in clonal diversity follows the excessive expansion of lymphocyte repertoire[282], suggesting that PBC patients may have a compromised immune reserve repertoire. A negative correlation between serum ALP and clonal diversity also implies that the reduced clonal diversity could reflect disease severity as well as outcome[283,284].

In the periphery, there is an increase in $CD19^+$ B cells and activated $CD25^+$ B cells[285,286]. There is a correlation between increased numbers of circulating B cells and disease stage[285,286]. Changes in the B cell compartment is also seen, with an increase in naïve B cells and plasmablasts and decrease in memory B cells[285,287]. Within the liver, plasma cells expressing IgM are consistently found surrounding bile ducts close to CD8 and CD4 T cells, local interaction between the cells is therefore plausible[255].

It has been postulated that B cells could play a role in the breakdown of T cell tolerance. Autoreactive B cells in autoimmune arthritis have been shown to act as antigen presenting cells able to prime naïve T cells[288]. B cells isolated from PBC patients can also express the co-stimulatory molecule CD86[289], thus could potentially act as APCs.

Rituximab has been trialled as a potential treatment for patients who have demonstrated an unsatisfactory response to UDCA[276,290]. The anti-CD20 was able to confer significant

reduction in serum AMA titres and B cell numbers[276–278,290]. Patients also saw reductions in serum ALP levels. Although improvements in liver biochemistry were limited, this does suggest that B cells contribute to PBC pathogenesis.

1.5.4.3.3 T cells

Immune infiltration of mononuclear cells around damaged bile ducts is a hallmark of PBC. These infiltrates are composed of predominantly $CD4^+$ and $CD8^+$ T cells as well as B cells and NK cells. Like the AMA epitope, the T cell autoepitope is located within the LA binding domain of PDC-E2[241]. BECs in PBC liver expressed elevated levels of HLA class I and II, suggesting interaction with the infiltrating $CD4^+$ and $CD8^+$ T cells, thus contributing to disease pathogenesis. Moreover, autoreactive $CD4^+$ T cells can be identified even in AMA negative patients[291], thus highlighting the importance of autoreactive T cells in PBC pathogenesis.

$CD8^+$ T cell numbers are at their height within the liver at a time where there is the most damage to the biliary epithelium[292]. Adoptive transfer of T cells in a mouse model for PBC showed that infiltration of the bile ducts was mediated by $CD8^+$ T cells and not $CD4^+$ T cells[293], indicating that the cytotoxic T cell mediated response plays a role in biliary damage in PBC (Figure 1.5.2).

PBC patients display significantly lower frequency of $CD4^+CD25^+$ Tregs[294]. Tregs are established in their role in suppressing the activation and proliferation of autoreactive $CD4^+$ and $CD8^+$ T cells[295]. Functional assays demonstrated that numbers of PBC Tregs are comparable to control subjects[294]. However, due to the increased $CD8^+$/$FoxP3^+$ ratio, the relative deficiency in Treg numbers may contribute to the loss of tolerance in PBC.

The CXCR5$^+$ Tfh cell population is elevated in the blood and liver of PBC patients[296]. *Ex vivo*, these cells have been shown to enhance AMA production from autologous B cells in co-culture. Additionally, Tfh associated cytokine IL-21 is increased in the serum and liver of treatment naïve patients and is positively correlated with the percentage of circulating PBs[296]. PBC derived B cells have higher expression of the IL-21 receptor suggesting that they may be more sensitive to IL-21 signalling[296] (Figure 1.5.2). Together, this shows that T cells could potentially play a role in driving B cell expansion in PBC.

Recently, CXCR5$^-$ peripheral T helper (Tph) cells have been seen to be associated with PBC disease activity[297]. Functional assays also demonstrate that Tph cells can induce B cell differentiation[297]. Tph cell numbers have also been found to be elevated in other autoimmune diseases including RA[298] and SLE[299]. In RA, Tph cells assist B cell differentiation into plasma cells[298]. Although it is unclear what role Tph cells play in PBC pathogenesis.

1.5.4.3.4 BECs

PDC-E2 is ubiquitously expressed, however in PBC, only the BECs are affected within the liver. PBC can also reoccur after transplantation[300], suggesting that the immunopathology of PBC is not host specific, but rather a general feature of BECs. This raises the question as to whether BECs are innocent victims or facilitators of their own destruction.

Intrahepatic BECs keeps autoantigens intact in apoptotic blebs, an ability not seen in other epithelial cells[301]. During apoptosis, the production of apoptotic blebs is required to limit the escape of intracellular material and to prevent any subsequent immune responses to intracellular autoantigens that could result in inflammatory reactions. Apoptotic BECs overexpress B cell lymphoma-2 (Bcl-2) which inhibits the glutathiolation of PDC-E2, thus

keeping it intact within the apoptotic bleb[302,303]. This gives the opportunity for AMAs to encounter the autoantigen without the need to enter the cell. Defective post-apoptotic degradation in BECs is not limited to PDC-E2, PBC autoantigens OGDC-E2 and BCOADC-E2 are also intact within the apoptotic bleb[304]. Patient derived macrophages can be induced into pro-inflammatory cytokine production when cultured with BEC apoptotic blebs and AMAs[305] (Figure 1.5.2). Moreover, PBC derived BECs show increased apoptosis[306]. Overall, this suggests that BECs themselves participate in the immunopathogenesis of PBC.

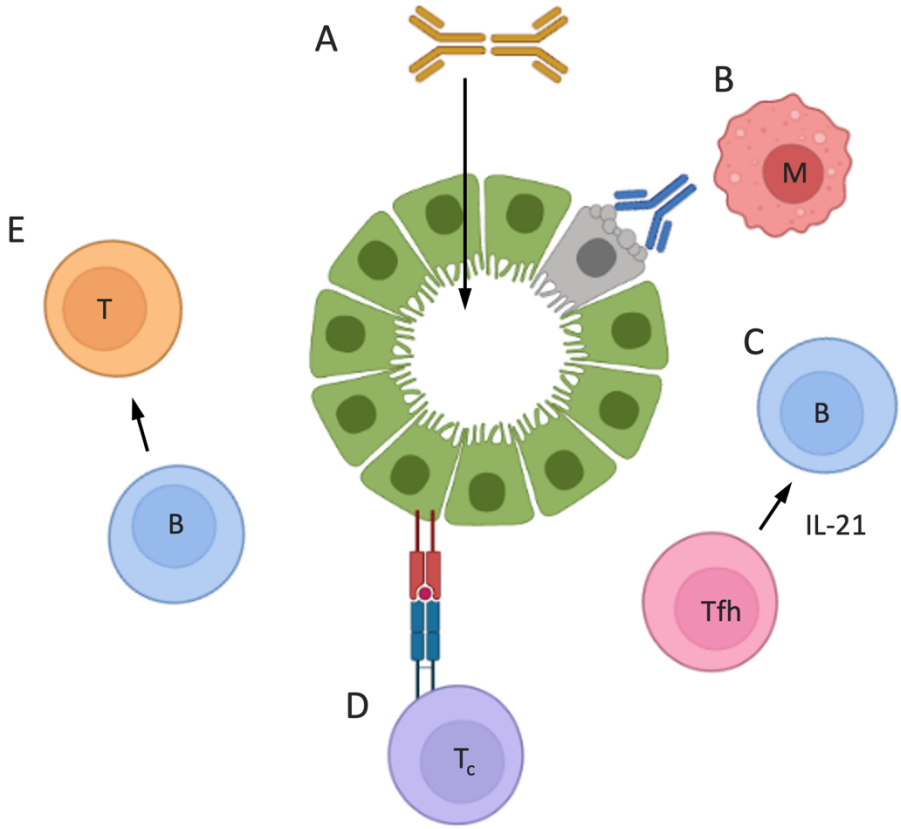


Figure 1.5.2 Potential mechanisms of BEC damage. *(**A**) Interaction between IgA-AMA and PDC-E2 through transcytosis of IgA-AMA through the BEC. Binding of AMA to PDC-E2 could lead to direct disruption in mitochondrial function as well as caspase induced apoptosis. (**B**) Defective post apoptotic degradation of autoantigens leads to the presence of intact PDC-E2 in apoptotic blebs. Resulting in pro-inflammatory macrophage response. (**C**) Production of IL-21 by Tfh cells results in the expansion of the B cell compartment (**D**) $CD8^+$ T cell mediated direct killing of BEC through MHC-class I restricted autoepitope of the LA domain of PDC-E2. (**E**) Potential of B cells to act as APC to activate the T cell response. Created using BioRender*

1.5.4.4 Disease aetiology

1.5.4.4.1 Genetics

Several genome-wide associated studies (GWAS) have been carried out to identify the risk genes for PBC[307–313]. HLA alleles show the strongest association with PBC onset; however, several non-HLA alleles have also been identified. Common pathways linked with these alleles include antigen presentation, T and B cell activation, IL-12 production, and IFN-γ production.

The female sex is the strongest inherited trait associated with PBC. Female PBC patients outnumber males at a ratio of approximately 10:1. X chromosome monosomy has been proposed as an explanation for this gender disparity. The X chromosome includes genes involved in immune tolerance[314], and an increase in incidence of X chromosome monosomy is seen in the peripheral white blood cells of female PBC patients[315]. Thus, haploinsufficiency for X-linked genes could increase disease susceptibility.

1.5.4.4.2 Epigenetic modifications

Methylation profiling has revealed several differences in gene promoters of T cells between PBC patients and controls[301,316]. *CXCR3* promoter in $CD4^+$ T cells has been found to be demethylated[317], resulting in significantly increased CXCR3 expression which is involved in leukocyte migration[318]. CXCR3 binds to CXCL9, CXCL10, and CXCL11, which facilitated the recruitment of T cells through IFN-γ[319]. Expression of CXCR3 is elevated in the PBC liver[320], leading to enhanced differentiation and recruitment of T helper 1 (Th1) cells.

Elevated serum IgM is commonly seen in PBC patients. T cell priming of B cells through the CD40/CD40L axis is thought to be responsible[321]. A mutation in CD40L has been seen in an

X-linked variant of immunodeficiency with hyper-IgM[322,323]. No such mutation was found in PBC, however significantly lower levels of DNA methylation of the *CD40L* promoter was found in $CD4^+$ T cells[324]. This hypomethylation of the promoter results in higher expression of CD40L on $CD4^+$ T cells and is inversely correlated with serum IgM levels in PBC patients. In addition, there is increased H4 histone acetylation in the same promoter region which would also lead to increased CD40L expression[325]. Therefore, in PBC, epigenetic modifications rather than genetic mutations may play an important role in increased IgM levels.

1.5.4.4.3 Environmental factors

Smoking and a history of urinary tract infections have been consistently demonstrated to associated with PBC[326]. Bacterial infections have been proposed to be the trigger for the breakdown in tolerance in PBC. *E. coli* has been identified as a potential culprit for molecular mimicry as there is significant conservation between *E. coli* and human PDC-E2[327]. PBC patient derived T and B cells cross-react with *E. coli* PDC-E2 and human mitochondrial autoantigens[242,328]. Furthermore, *E. coli* infections in mice can induce AMAs and liver pathology akin to PBC[329].

Novosphingobium aromaticivorans is another bacterium that has been investigated as a potential participant in PBC onset. A study found that all of the AMA positive and some AMA negative patients tested had sera AMA reactive to lipoylated proteins derived from *N. aromaticivorans*[330]. This reactivity was 10-fold stronger than that to *E. coli* with no reaction from control sera. *N. aromaticivorans* infection in mice was also able to induce PBC like liver pathology, although these mice appeared to have less severe disease and lower AMA titres compared to the E. coli infection model[331].

Epidemiological studies have identified several other environmental factors that could be involved in the aetiology of PBC[332]. The use of cosmetic products such as hair dye and nail polish have both been shown to be risk factors for PBC development[332]. Residing near certain geographic regions, such as toxic waste sites also carry significant risk for disease[333–335]. This led to subsequent studies into the modification of PDC-E2 epitope with xenobiotics found in these environmental toxins. Cross reactivity of PBC patient sera was seen on multiple peptides where LA is replaced by xenobiotics[336,337], suggesting that chemicals found in the environment can generate immunogenic neoantigens thus breaking immunotolerance in PBC.

1.6 Hypothesis and Aims

PBC is a chronic autoimmune disease with no current curative treatment. The presence of autoantibodies is a hallmark of PBC[244], and B cell infiltrates are observed within the diseased liver suggesting that B cells play a role in disease pathogenesis[255]. Indeed, depletion of the total B cell compartment in PBC patients who are refractory to UDCA treatment confers some, if limited, improvement in liver biochemistry[275,276,278].

FcRL4$^+$ B cells have been identified in several autoimmune diseases[127–130,135]. In RA and pSS, FcRL4$^+$ B cells contribute to the disease through the production of autoantibodies and pro-inflammatory cytokines[127–129]. FcRL4$^+$ B cells isolated from the RA synovium preferentially express IgA BCR suggesting a mucosal origin. Joint inflammation in RA is often proceeded by mucosal inflammation[132–134]. In PBC, molecular mimicry of enteric bacterial antigen has been proposed as a cause of loss of tolerance[242,327,328], thus implicating the gut as the origin of autoantigen priming in PBC. Thus, we hypothesize that **FcRL4$^+$ B cells contribute to PBC pathogenesis and contribute to the link between mucosal and liver inflammation in PBC**.

This project has 3 aims to test this hypothesis.

- To identify FcRL4$^+$ B cells in the liver of patients with inflammatory liver disease
- To phenotype B cells isolated from PBC livers.
- To elucidate a functional role for FcRL4$^+$ B cells in PBC disease pathogenesis.

2 MATERIALS AND METHODS

2.1 Patients and patients' materials

Liver explants from patients with PBC, PSC, NASH, and PLD as well as organ donors were collected through the liver transplant unit at University Hospital Birmingham in the Queen Elizabeth Hospital. Samples were obtained with patient consent and in accordance with local research ethics committee approval (LREC #06-Q2702-62). Liver explants from organ donors were used after these were deemed as unsuitable for transplantation.

Patient's clinical details are summarised in Supplementary Table 7.1.

2.2 Isolating liver infiltrating mononuclear cells (LIMCs)

Liver slices were weighed and cut into small pieces using scalpels. The tissue was then washed repeatedly with ice cold sterile PBS until the washes ran clear. 300mL of RPMI 1640 (Gibco) was added before the mixture was transferred to a stomacher bag. The bag was then sealed and placed into a stomacher machine for 6 minutes at 260rpm (Seward). The mixture was then poured through a fine mesh and washed thoroughly with sterile PBS. The filtrate was distributed evenly in to 50mL tubes and centrifuged at 400 *g* for 5 minutes. Pellets were washed repeatedly with PBS and gradually pooled until the number of tubes remining was reduced to 2. These two remaining tubes were centrifuged at 200 RPM for 5 minutes. The supernatant was removed, and each pellet resuspended fully in 30mL of PBS before being layered on to 15mL of Lympholyte (Cedarlane). The tubes were centrifuged at 800 *g* for 30 minutes with acceleration at 3 and deceleration at 0.

The buffy coat layer of cells was harvested into PBS. The cells were centrifuged at 2000rpm for 5 minutes and the pellet resuspended in sterile PBS. The cells were then counted using trypan blue and made up to 10 x 10^6 cells per mL with PBS.

2.3 Staining lymphocytes from the liver

1 x 10^6 LIMCs were aliquoted into FCS coated 96 well FlexiPlate. The cells were centrifuged at 300 *g* for 5 minutes. Cell pellets were resuspended in 100µL of Zombie Aqua™ Fixable viability dye (Biolegend) diluted 1 in 100 in PBS and incubated for 30 minutes on ice and in the dark. Cells were washed twice with PBS and resuspend in the relevant antibodies and isotype matched controls (Table 2.3.1) diluted in 100µL of FACS buffer (PBS, 2% w/v BSA, 8nM EDTA). After incubating for 30 minutes on ice and in the dark, the cells were washed and fixed by incubating with Medium A of Fix and Perm (Thermo Fisher Scientific) for 20 minutes in the dark at room temperature. Samples without intracellular staining were resuspended in 300µL of FACS buffer and stored at 4°C until processing on the Fortessa. Samples that required intracellular staining were washed and resuspended in intracellular antibodies diluted in Medium B of Fix and Perm. The antibodies and cells were incubated together for 20 minutes are room temperature. The samples were washed and resuspended in Medium A of Fix and Perm before incubating for a further 20 minutes. Cells were centrifuged and resuspended in 300µL of FACS buffer and stored at 4°C and in the dark until samples could be run on the BD LSR Fortessa X20 and analysed using FlowJo software.

2.3.1 Compensation

Compensation beads tubes were prepared using one drop each of comp beads (BD). Beads were incubated on ice for 30 minutes in the dark with the relevant antibody (Table 2.3.1) resuspended in 100µL of FACS buffer. The beads were centrifuged for 5 minutes at 300*g* and

resuspended in 300µL of FACS buffer and stored at 4°C and in the dark until samples could be run on the Fortessa. Sphero™ rainbow beads (ACEA) were used to calibrate voltages on the Fortessa before samples were run.

Antibody	Clone	Dilution	Supplier
Cell surface antibodies			
CD19 BV421	HIB19	1:50	BioLegend
FcRL4 PE	413D12	1:100	BioLegend
IgA APC	IS11-8E10	1:75	Miltenyi Biotec
CD11c APC-Cy7	BUL5	1:25	BioLegend
CD21 APC	HB5	1:100	eBioscience
CD27 BV711	O323	1:50	BioLegend
IgD FITC	IA6-2	1:100	BioLegend
RANKL APC	MIH24	1:100	BioLegend
CD80 FITC	2D10	1:50	BioLegend
CD86 BV711	IT2.2	1:100	BioLegend
CD24 APC-Cy7	ML5	1:25	BioLegend
CD21 FITC	HB5	1:50	eBioscience
T-bet APC	4B10	1:50	BioLegend
Ki67 BV711	Ki67	1:100	BioLegend
Isotype Controls			
Mouse IgG1 BV421			BioLegend
Mouse IgG2b PE			BioLegend
Mouse IgG2a APC			BioLegend
Mouse IgG1 APC-Cy7			BioLegend
Mouse IgG2a FITC			BioLegend
Mouse IgG1 BV711			BioLegend
Mouse IgG1 FITC			BioLegend
Mouse IgG2b BV711			BioLegend
Mouse IgG2a APC-Cy7			BioLegend
Mouse IgG2b APC			BioLegend
Mouse IgG1 APC			BioLegend

Table 2.3.1 Antibodies used for flow cytometry

2.4 IgA acid wash and IgA incubation

LIMCs were aliquoted into an FCS coated 20mL universal tube and centrifuged at 300 g for 5 minutes. The supernatant was aspirated until cell pellet was as dry as possible. The cell pellet was resuspended gently in 200µL of pH3 glycine wash (dH_20 with 100mM glycine, 100nM NaCl) and incubated on ice for 60 seconds. 20mL of cold complete RPMI was added to quench the cells and spun down. The supernatant was poured off. Human colostrum IgA (Sigma) was heat aggregated for 30 minutes at 63°C. HA-cIgA at 1mg/mL in RPMI was added to indicated samples and incubated at room temperature for 30 minutes. The cells were washed with PBS and stained and fixed according to the staining protocol.

2.5 Freezing and defrosting cells

Cells were centrifuged at 300 g for 5 minutes and resuspended in FCS. 20% DMSO in FCS was added dropwise to the cell suspension. Cells were aliquoted into cryovials and transferring to a -80°C freezer in a Corning freezing container.

Vials were defrosted in a 37°C water bath until thawed. The cell suspension was added dropwise to 20mL pre-warmed complete RPMI and centrifuged. The cell pellet was then resuspended in either PBS ready for staining or complete RPMI for culturing.

2.6 Cell culture

2.6.1 Culturing of cell lines

Cells were maintained in complete medium (RPMI 1640, 10% FCS, 1% penicillin/streptomycin) at 37°C. Raji cell line was passaged every 2-3 days and maintained

at a concentration of $0.5x10^6$ cells per mL of media. Passage numbers were recorded, cells were used in assays at passage 20-40.

2.6.2 Culturing biliary epithelial cells

BECs were culture on collagen coated plates in culture media containing 50% DMEM and 50% Ham's F12 media with 10% heat inactivated human serum, 2mM penicillin/streptomycin, 10µg/L epidermal growth factor, 124IU/L Insulin, 20µg/L hydrocortisone, 10µg/L cholera toxin, 0.2mM tri-odo-thyronine, and 10µg/mL hepatocyte growth factor. Cells were split when confluent and used at P3.

2.7 Cell sorts

Cells suspensions were defrosted and stained with antibodies. Tonsil derived cells were stained with anti-FcRL4 and anti-CD19 antibodies. Liver derived cells were stained with anti-FcRL4, anti-CD19, and anti-IgD antibodies. Antibodies used are listed in Table 2.7.1. Cells were sorted into FACS buffer containing 10% FCS.

Antibody	Clone	Dilution	Supplier
CD19 BV421	HIB19	1:50	BioLegend
FcRL4 PE	413D12	1:100	BioLegend
IgD FITC	IA6-2	1:100	BD Biosciences

Table 2.7.1 Antibodies used for cell sorting

2.8 Co-culture of FcRL4$^+$ B cells and BECs

BECs were seeded at 10,000 cells per well on a 96 well plate and cultured overnight at 37°C. Culture media was removed before sorted tonsil derived cells were added at a lymphocyte to BEC ratio of either 10:1, 5:1, or 2:1. Cells were cultured together for 24 hours with

complete RPMI. Supernatant was harvested and the BECs were harvested using trypsin. Cells were stained with cell viability dye and processed using the Fortessa.

2.9 Removing lipids from Bile

5mL of bile harvested from the attached gall bladder. Stored at -80°C in aliquots. Cleanascite™ was used to remove lipids from bile. Cleanascite™ selectively removes lipids and lipoproteins using solid-phase non-ionic absorbent suspended in saline. Bile, PBS, and Cleanascite were mixed at a 2:3:1 ratio and incubated on ice for 1 hour. The mixture was then centrifuged at 13000 *g* for 10 minutes. The supernatant is harvested, and the pellet discarded. The cleaned bile was then stored at -80°C until used in assays.

2.10 Bile assay

FcRL4 expression Rajis were spun down at 300g for 5 minutes and resuspended in patient derived bile at varying dilutions for 30 minutes at room temperature. The cells were then washed twice with cold PBS to remove excess bile. Zombie aqua was then added to the cells to identify dead and dying cells for 30 minutes on ice before an antibody panel consisting of anti-CD19 BV421, anti-FcRL4 PE, and anti-IgA APC were added to the cells. Excess antibodies were then washed off and cells fixed using Medium A of Fix & Perm™.

2.11 Antibody stimulation

$CD19^{+}IgD^{-}FcRL4^{+}$ and $CD19^{+}IgD^{-}FcRL4^{-}$ cells were sorted from frozen LIMCs and tonsils. The cells were counted and washed once in media before being resuspended at $20x10^{6}$ cells per mL in either plain culture media or a stimulation cocktail. Either complete RPMI or R5 media

(RPMI-1640 containing 10% heat inactivated FCS, 55µM β-mercaptoethanol, 1% glutamine/penicillin/streptomycin, 10mM HEPES, 1mM sodium pyruvate, 1% non-essential amino acids) used to culture sorted cells. The cells were then cultured for either 5 days, 7 days, or 10 days.

The whole cell suspension was harvested and spun down at 300g for 5 minutes. The cell free supernatant was removed and stored at -20°C and the cell pellets were either discarded or stained for cell viability.

Stimulant	Clone	Working concentration	Supplier
CpG ODN 2006 (TLR9 agonist)		2.5µM	Invivogen
Human IL-21		50ng/mL	Miltenyi Biotec
Anti-human CD40 antibody	HB14	0.1µg/1x10^5 cells	BioLegend
BAFF		100ng/mL	BioLegend
IL-4		50ng/mL	PeproTech

Table 2.11.1 Stimulation cocktail for antibody stimulation assay

2.12 ELISA

Sandwich ELISAs were performed using Thermo human IgA and IgG ELISA kits. ELISA plates were coated with either IgG or IgA coating antibody diluted at 1 in 250 in coating buffer. The plates were sealed and incubated overnight at 4°C before being washed twice with 400µL of wash buffer. To reduce non-specific protein binding, the plates were incubated for 2 hours at room temperature with blocking buffer. Blocking buffer was removed before standards and samples were added to the wells and incubated at room temperature with gentle shaking for 2 hours. The wells were then washed and incubate with a further 1 hour at room temperature with shaking with detection antibody diluted at 1 in 250. The plates were

thoroughly washed before the substrate solution was added, incubated time varied from 15 to 45 minutes. Stop solution of 1M H2SO4 was added to cease the colour reaction and the plates were read immediately using a Synergy™ HT plate reader.

2.13 Immunohistochemistry

2.13.1 Preparation of sections for Immunohistochemistry Staining

3µm sections were cut from paraffin embedded formalin fixed tissue harvested from donated livers. All sections were prepared in the same way before staining with the relevant antibodies. The slides were placed in 3 consecutive baths containing Histoclear to remove the paraffin wax. Excess Histoclear was washed off and the sections rehydrated by placing the slides in ethanol baths with decreasing ethanol concentration (100%, 90%, 80%, and 70%). The slides were then washed in dH_2O before being transferred into preheated Tris-EDTA pH9 and incubated for 1 hour at 96°C. The slides were allowed to cool to room temperature and washed in PBS-T. 2 drops of Bloxall® were added to the sections and incubated for 10 minutes in order to block the activity of endogenous peroxidase and alkaline phosphatase. Excess Bloxall was then wash off with PBS-T and the samples were incubated with PBS containing 10% human serum and 1x Casein for 10 minutes.

2.13.2 Single colour staining

The blocking solution was tipped off and the sections were incubated with primary antibody for 1 hour at room temperature. All reagents were diluted with PBS and wash steps were performed with excess PBS-T. The primary antibody (Table 2.13.1) was washed off before secondary antibody was added and incubated for 10 minutes. Once excess secondary antibodies had been washed off, the slides were incubated with Vector ImmPRESS anti-

rabbit Ig Peroxidase. After 30 minutes, the tertiary antibody was washed off. DAB IMPACT was prepared according to manufacturer's instructions and added to the sections. Incubation times can be found in Table 2.13.2. Sections were then place immediately in dH_2O.

2.13.3 Double staining

First colour staining was performed using the same protocol as for single colour staining, however after DAB incubation, sections were placed in TBS-T instead of dH_2O. All reagents from this point were diluted with TBS and wash steps were performed with excess TBS-T. The sections were then incubated for 10 minutes with blocking solution containing 10% human serum and 1x Casein. This was tipped off before a 1-hour incubation with the primary antibody (Table 2.13.1) diluted in TBS-T. Excess primary antibody was washed off before secondary antibody was added. The sections were incubated with secondary antibody for 10 minutes before another wash step was conducted. Vector ImmPRESS anti-rabbit Ig alkaline phosphatase was added and incubated for 30 minutes. Once the tertiary antibody was washed off, either Vector Red or Vector Blue was added to the sections. Incubation times are listed in Table 2.13.2. The sections were then placed in dH_2O to stop further colour development.

2.13.4 Mounting

All sections except those stained using Vector Blue were stained with Haematoxylin before mounting. Enough Haematoxylin was added to cover the whole tissue section and incubated for 45 seconds before washing with dH_2O until the washes ran clear. The sections were then dehydrated using 1-minute washes in 90% ethanol and 100% ethanol. Following this, the sections were washed 3 times in histoclear. The sections were then mounted using non-

aqueous Vectamount. Slides were then imaged using a Zeiss Axio Scan.Z1 scanner and analysed using Zen and ImageJ software.

Antibody	Clone	Dilution	Supplier
Primary antibodies			
CD20	L26	1:300	Dako
Cytokeratin 7	OVTL 12/30	1:2	Dako
FcRL4	M-IRTA1	1:40	-
Ki67	MIB-1	1:200	Dako
Isotype Controls			
Mouse IgG1			Dako
Mouse IgG2a			Dako
Secondary antibody			
Rabbit anti-mouse		1:150	Dako

Table 2.13.1 Antibodies used for immunohistochemistry

Tissue	Staining	Chromogen	Incubation time
Tonsil	CD20	DAB	1 min 45 sec
	FcRL4	DAB	2 min 40 sec
	Cytokeratin 7	Vector Red	4 min 30 sec
	Ki67	Vector Blue	8 min
Liver	CD20	DAB	3 min 40 sec
	FcRL4	DAB	6 min 10 sec
	Cytokeratin 7	Vector Red	6 min 50 sec
	Ki67	Vector Blue	13 min 40 sec

Table 2.13.2 IHC incubation times

2.13.5 Immunohistochemistry analysis

2.13.5.1 Identification of FcRL4$^+$ cells in end-stage livers

Whole slide scans were analysed using Zen image analysis software. FcRL4$^+$ cells were identified by eye across the whole tissue and counted. The surface area of the tissue section was also determined and the number of FcRL4$^+$ cells per mm^2 of tissue was calculated.

2.13.5.2 Quantification of Ki67 staining

Sequential sections were stained for either FcRL4 and Ki67 or CD20 and Ki67. Immune aggregates containing FcRL4$^+$ B cells were first identified across whole tissue sections. The same aggregates were then identified on the CD20 stained sections. The number of proliferating and non-proliferating FcRL4$^+$ and CD20$^+$ cells were counted.

2.13.5.3 Distance measurements between lymphocytes and the biliary epithelium

Sequential sections from PBC livers were stained for either FcRL4 and cytokeratin 7 or CD20 and cytokeratin 7. Lymphocyte aggregates that both contained FcRL4$^+$ cells and surrounded biliary epithelium were identified. The same aggregates were then determined on the sequential section stained with CD20 and cytokeratin 7. Regions of interest containing these aggregates were generated and imported into ImageJ. Distance measurements between the lymphocyte and the epithelium were calculated as the distance between the centre of the lymphocyte nucleus and the basolateral membrane of the cholangiocytes (Figure 2.13.1).

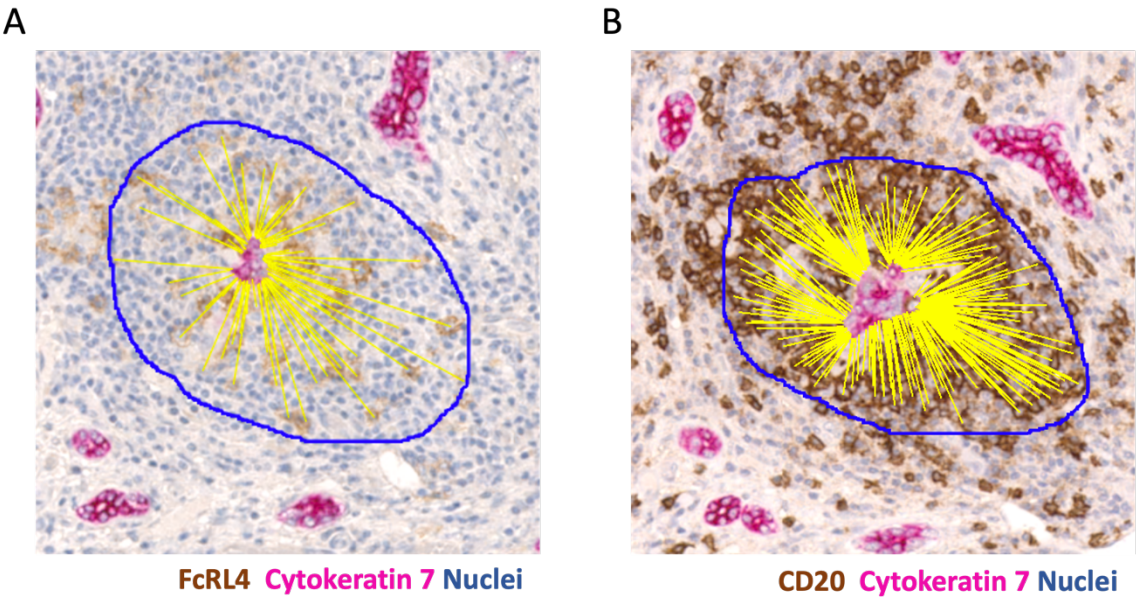


Figure 2.13.1 Method of measuring the distance between lymphocytes and the biliary epithelium. *Example of a matching lymphocyte aggregate from sequential staining of PBC tissue. Sections were stained with* ***(A)*** *FcRL4 and cytokeratin 7, or* ***(B)*** *CD20 and Ki67. The aggregate is demarcated within the blue lines. Yellow lines indicate the distance measured between the centre of the lymphocyte nucleus and the basolateral membrane of the biliary epithelium.*

3 IDENTIFICATION OF FCRL4^{+} CELLS WITHIN END-STAGE LIVER DISEASE

3.1 Introduction

FcRL4 expressing B cells were first identified by Falini et al. as CD27^{+} cells found within the tonsil epithelium and the dome epithelium of Peyer's patches[119]. Morphologically, FcRL4^{+} B cells are larger than FcRL4^{-} B cells[95,119]. They possess an extensive cytoplasm rich in mitochondria as well as prominent nucleoli[95].

FcRL4^{+} B cells have been identified in RA and pSS[127–130,135]. In both diseases, FcRL4^{+} B cells play a role in disease pathogenesis and are found within the infiltrating lymphocyte population. The presence of infiltrating lymphocytes in PBC is a main characteristic of the disease. Inflammatory infiltrates can be found surrounding small and medium sized bile ducts. Although these infiltrates are thought to consist of predominantly CD4^{+} and CD8^{+} T cells, B cell follicles have been observed in the portal tracts[338].

Both RA and pSS are known comorbidities of PBC. In PBC, dry eyes and dry mouths are common symptoms in patients. Histological studies show that damage in the salivary glands of PBC patients is morphologically similar to the damage of the cholangiocytes in the bile ducts[258,259,263]. This evidence indicates that there could be similarities in immune mediated damage between pSS and PBC. In pSS, FcRL4^{+} B cells within immune infiltrates are removed through rituximab treatment[130]. The loss of these cells within the salivary glands leads to a reduction in inflammation and restoration of the epithelium, which is suggestive of a pathological role for these cells[130]. The link between pSS and PBC, and the presence of

FcRL4^{+} B cells in other autoimmune diseases, indicates that these cells could be found within the PBC liver.

PSC, NASH, PLD, and donor organs that have not met the criteria for transplantation were used as control tissue. PSC is chronic liver disease where immune mediated damage to both intrahepatic and extrahepatic bile ducts leads to fibrosis and constriction of the bile ducts[229]. A strong association between IBD and PSC suggests that there may be a shared gut and liver antigen specific process involved in disease pathogenesis[339,340]. In PSC, the predominant infiltrating lymphocytes are T cells[341,342]. NASH is the progressive form of non-alcoholic fatty liver disease. It is characterised by liver steatosis, inflammation, and fibrosis. The inflammatory response seen in NASH is thought to be as a result of the uptake of modified lipids by Kupffer cells[221]. The presence of multiple diffuse cysts within the liver is the main characteristic of the hereditary disorder polycystic liver disease[222]. PLD does not typically affect liver biochemistry as the liver parenchyma is not completely destroyed[343]. Liver transplantation is the only cure available for PLD, and is only available to patients when quality of life is seriously affected[226].

In this chapter, I addressed the hypothesis that FcRL4^{+} B cells can be found within immune infiltrates in PBC livers. We also hypothesize that these cells will be absent within other end-stage liver diseases and donor organs that have been rejected for transplantation.

3.2 Results

3.2.1 Identification of FcRL4$^+$ cells in liver sections

Paraffin embedded liver tissue sections were obtained from patients with end-stage liver disease. Along with sections from PBC patients (n=20), 3 other disease groups were used as controls; PSC (n=10), NASH (n=10), donor organs that were not used for transplantation (n=9). FcRL4$^+$ cells were identified in these sections using IHC and counted by eye using Zen software.

In the PBC livers, FcRL4$^+$ cells were found exclusively within immune aggregates, and often within portal triad areas (Figure 3.2.1A). These cells were found in significantly fewer numbers in other end-stage liver diseases including PSC, NASH, and donor organs that did not meet the criteria for donation (Figure 3.2.1A-D). Within the PSC liver, the presence of immune aggregates was observed within portal triad areas (Figure 3.2.1B). However, significantly fewer FcRL4$^+$ B cells were found within these aggregates of the PSC liver compared to those located in similar areas of the PBC liver (Figure 3.2.1F). In NASH and donor livers, there was an absence of immune infiltrates and FcRL4$^+$ cells (Figure 3.2.1C, D, F).

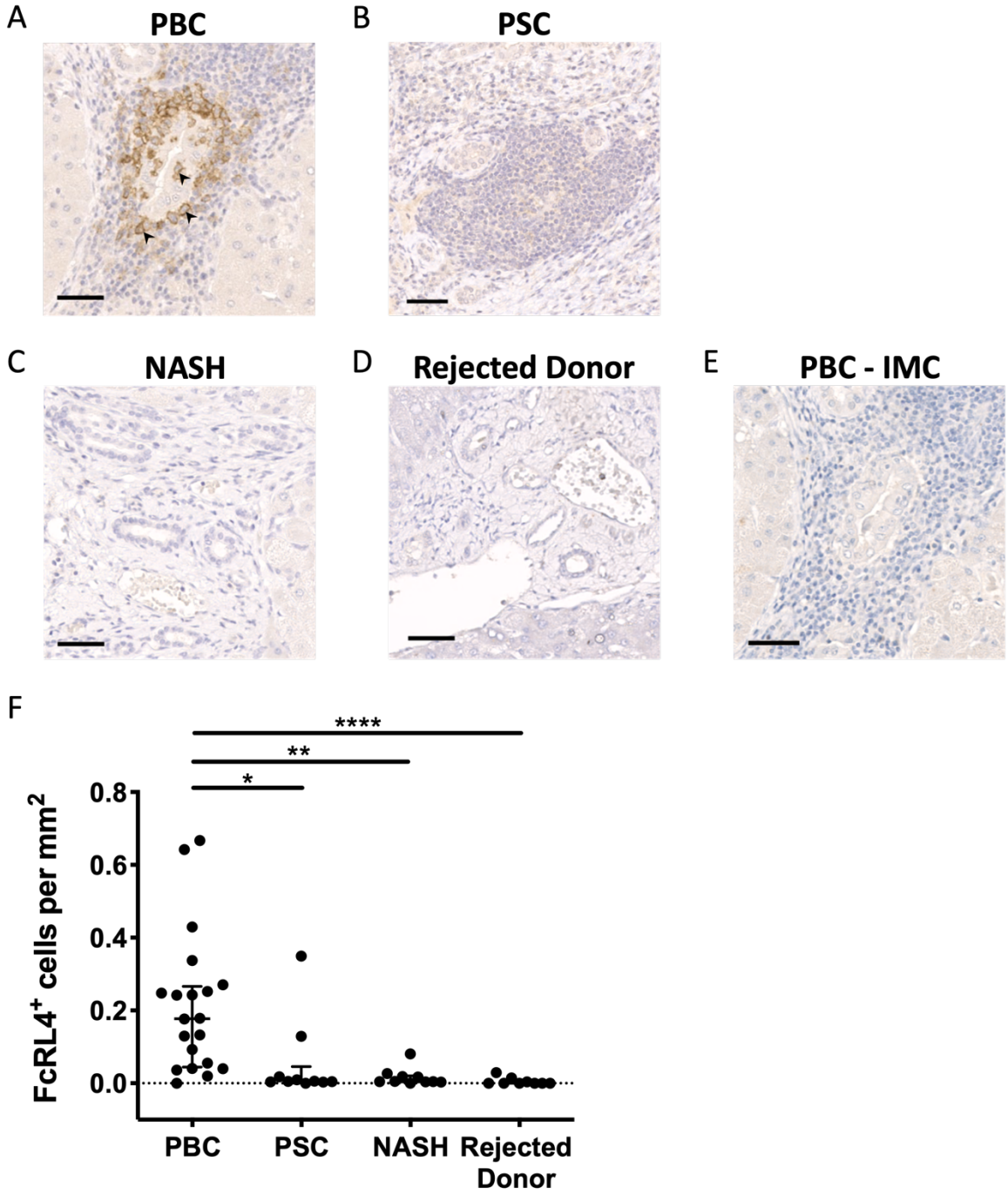


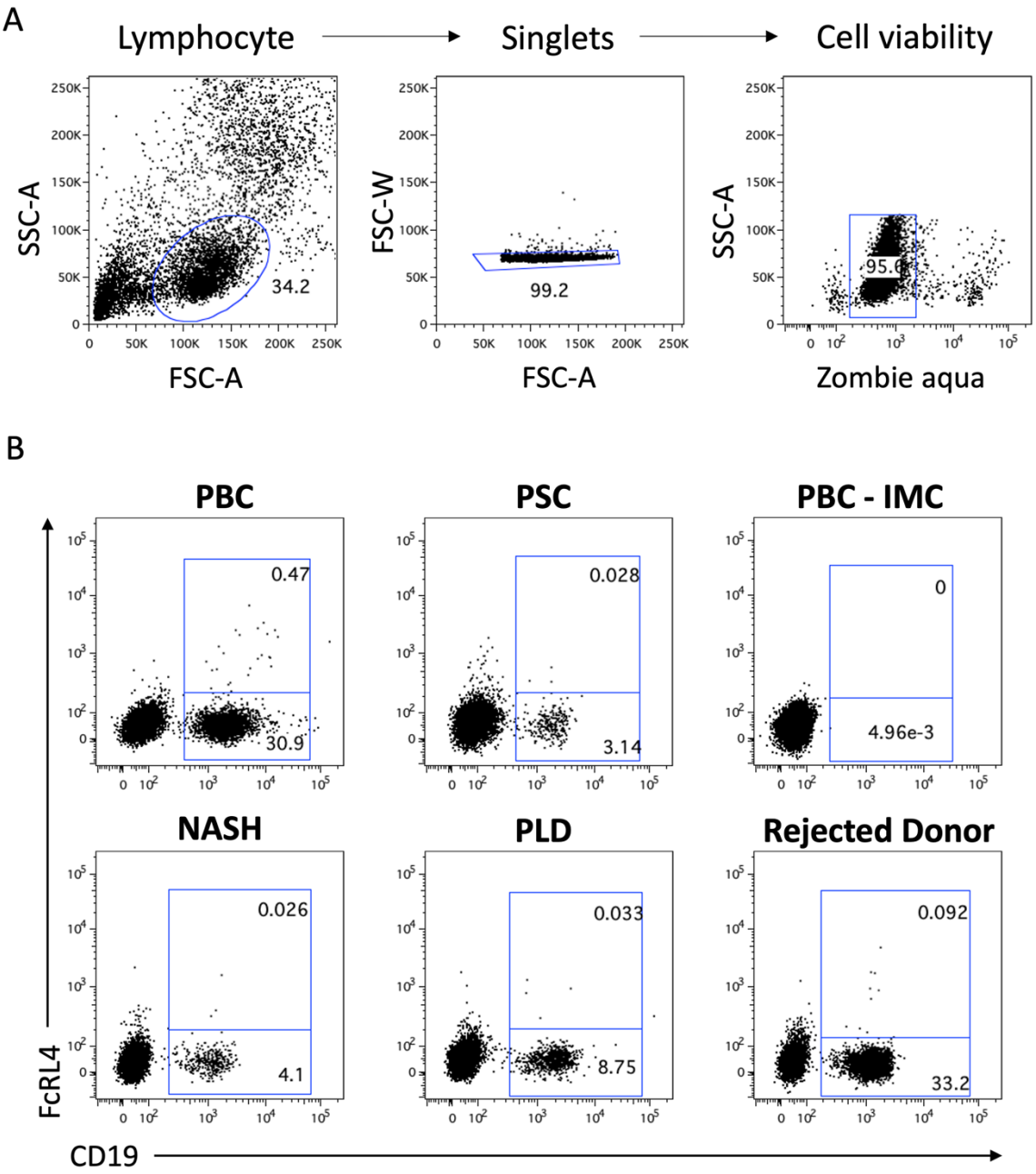
Figure 3.2.1. FcRL4⁺ cells can be identified in the PBC livers and are largely absent within other end-stage liver diseases. (A-D) *Staining of paraffin embedded sections of PBC, primary sclerosing cholangitis (PSC), non-alcoholic steatohepatitis (NASH), and rejected donor liver samples for FcRL4 (brown), with haematoxylin (blue) as a nuclear stain. Black arrows indicate example FcRL4⁺ cells.* ***(E)*** *Isotype matched control (IMC) of PBC section.* ***(F)*** *Quantification of FcRL4⁺ cells per mm² of tissue. Statistics – Kruskal-Wallis test followed by Dunn's post hoc test for multiple comparisons.*

3.2.2 Isolation of FcRL4$^+$ cells from fresh liver tissue

Fresh liver tissue was obtained from patients undergoing liver transplantations at the liver transplant unit of the Queen Elizabeth Hospital in Birmingham. In addition to PBC livers (n=15), livers from PSC (n=15), NASH (n=10), donor organs (n=10), as well as PLD (n=10) were used as controls. Liver infiltrating mononuclear cells (LIMCs) were isolated from these explant livers.

Using flow cytometry, FcRL4 expressing CD19$^+$ cells were identified within the livers of PBC patients. This population of cells is present in a significantly higher abundance compared to other end-stage liver diseases. FcRL4$^+$ cells were enriched in both the CD19$^+$ cell population (Figure 3.2.2C) as well as in the total LIMCs population (Figure 3.2.2D).

There was no significant difference in the proportion of B cells within the infiltrating lymphocyte population across all end-stage liver diseases (Figure 3.2.3A). This was also reflected in the absolute number of B cells per gram of tissue (Figure 3.2.3B). Additionally, the absolute number of infiltrating lymphocytes per gram of tissue was comparable between the diseased groups (Figure 3.2.3C). Absolute numbers per milligram of tissue show that there is a slight increase in FcRL4$^+$ B cells in the PBC liver compared to other end-stage liver diseases (PBC median = 344.0, PSC median = 162.6, NASH median = 29.29, PLD median = 45.3, rejected donor median = 47.76). The comparison between NASH and PBC reached statistical significance ($p = 0.0108$) (Figure 3.2.3D)


A
Lymphocyte
Singlets
Cell viability
SSC-A
FSC-A
34.2
FSC-W
FSC-A
99.2
SSC-A
Zombie aqua
95.6
B
PBC
PSC
PBC - IMC
0.47
30.9
0.028
3.14
0
4.96e-3
NASH
PLD
Rejected Donor
0.026
4.1
0.033
8.75
0.092
33.2
FcRL4
CD19

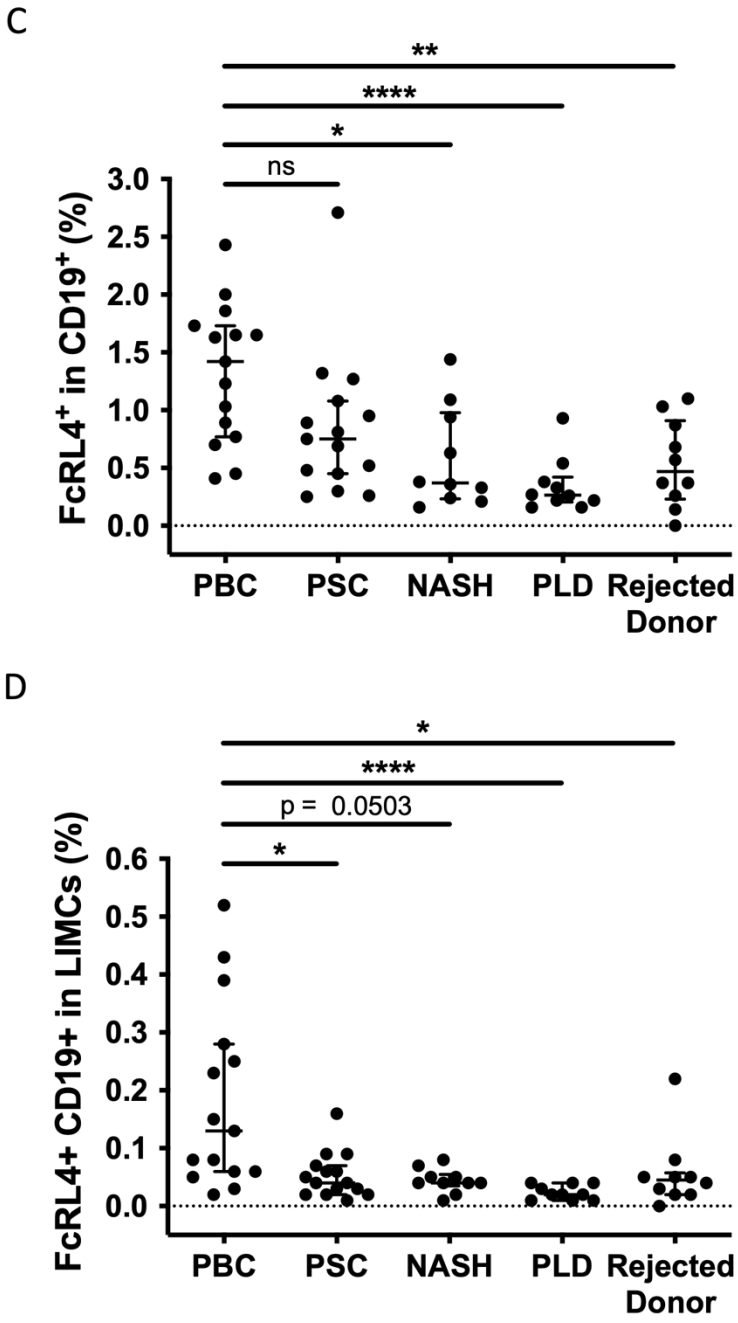
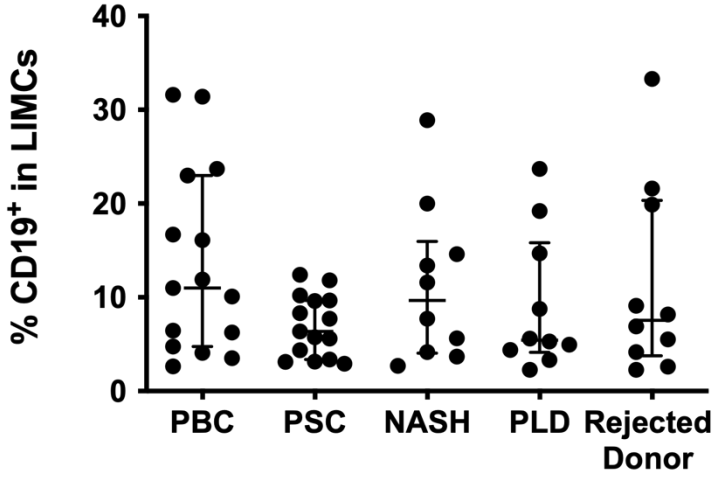
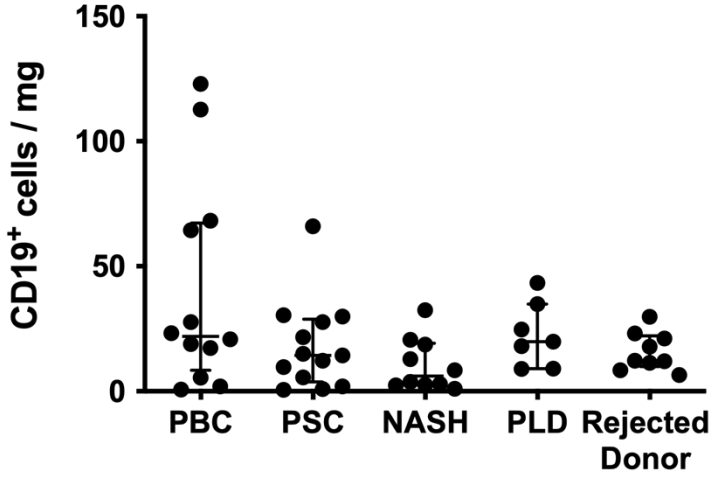


Figure 3.2.2. FcRL4⁺ cells can be isolated from PBC livers. (A) *Gating strategy. Lymphocyte gate was first applied, singlets were then identified, and finally a cell viability dye was used to gate on live cells.* ***(B)*** *Example of gating on FcRL4 and CD19 expression by LIMCs from PBC, PSC, NASH, polycystic liver disease (PLD) and rejected donors.* ***(C)*** *Percentage of B cells that express FcRL4.* ***(D)*** *Percentage of liver infiltrating mononuclear cells that are FcRL4 expressing B cells. Statistics – Kruskal-Wallis test followed by Dunn's post hoc test for multiple comparisons.*

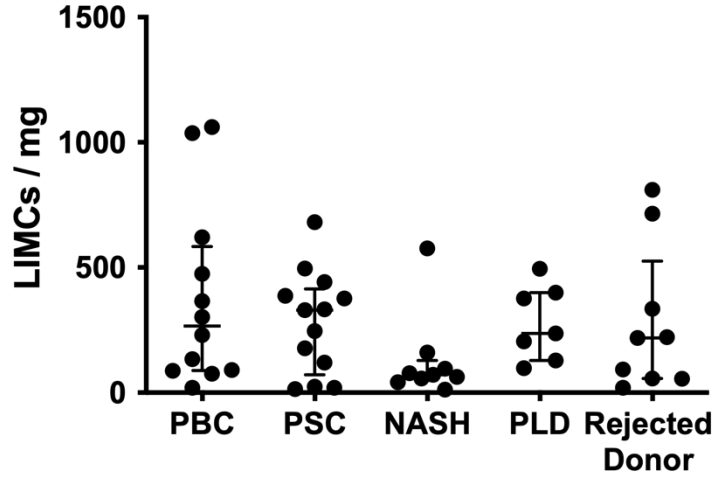
A


% CD19+ in LIMCs
40
30
20
10
0
PBC
PSC
NASH
PLD
Rejected Donor

B


CD19+ cells / mg
150
100
50
0
PBC
PSC
NASH
PLD
Rejected Donor

C


LIMCs / mg
1500
1000
500
0
PBC
PSC
NASH
PLD
Rejected Donor

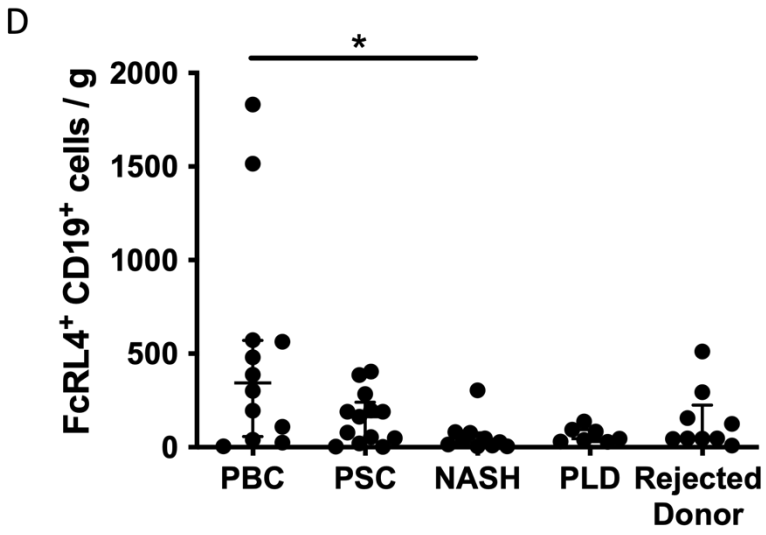


Figure 3.2.3. B cells are not enriched in end-stage PBC. (A) *B cell population within LIMCs isolated from end-stage livers.* ***(B)*** *Absolute number of CD19⁺ cells.* ***(C)*** *Absolute number of LIMCs per gram of tissue.* ***(D)*** *Absolute number of FcRL4⁺ B cells per gram of tissue. Statistics – Kruskal-Wallis test followed by Dunn's post hoc test for multiple comparisons.*

3.2.3 Association of FcRL4$^+$ B cell numbers with clinical parameters

Alkaline phosphatase (ALP) is an enzyme released into the blood by damaged bile ducts and is monitored as part of patient care. No correlation was observed between the proportion of FcRL4$^+$ B cells in the infiltrating lymphocyte population and ALP levels in PBC patients (Figure 3.2.4A). No correlation between the proportion of FcRL4$^+$ B cells in LIMCs and other patient clinical information was seen, including tests for liver function and damage (Supplementary Figure 7.1).

Within the PBC patient cohort, female patients have a slightly higher percentage of FcRL4$^+$ B cells within the total infiltrating lymphocyte population compared to male PBC patients. Although this was not statistically significant, there is no difference in FcRL4$^+$ B cell numbers between male and female patients in any other end-stage liver diseases (Figure 3.2.4B).

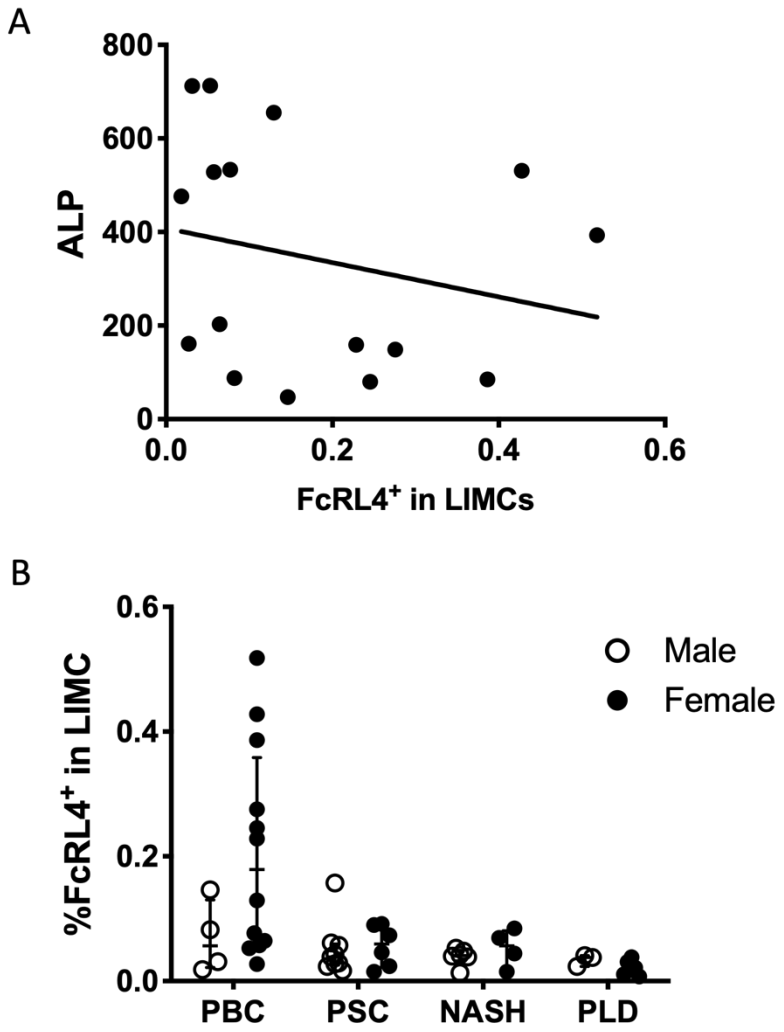


Figure 3.2.4 Clinical significance of FcRL4⁺ B cells. (A) *Correlation between FcRL4⁺ B cells in the LIMC population with liver alkaline phosphatase levels. Spearman rank correlation coefficient = -0.4118, p = 0.1144.* ***(B)*** *FcRL4⁺ B cell numbers in male and female end-stage liver disease patients.*

3.3 Discussion

We addressed the hypothesis that FcRL4$^+$ B cells are present within end-stage PBC liver. FcRL4$^+$ B cells can be found within immune aggregates often surrounding bile ducts. These cells are absent or present in very small numbers in other end-stage liver diseases including PSC, NASH, and PLD. FcRL4$^+$ B cells can be isolated from fresh liver tissue. Although there is no correlation between liver ALP levels and the proportion of these cells within the PBC liver, there is a non-significant trend towards more in FcRL4$^+$ B cells in female patients with PBC compared to males.

In paraffin fixed sections of PBC livers, FcRL4$^+$ cells were often located close to bile ducts. In PBC, immune mediated destruction of bile ducts leads to the build-up of toxic bile acids within the liver, resulting in the development of cirrhosis. The observation of these cells at the site of epithelial destruction indicates that they could be participating in disease pathogenesis. Although, there was no correlation between FcRL4$^+$ cell numbers and ALP levels, this could be because only end-stage PBC livers that required transplantation were tested. Testing of liver biopsies from patients at earlier stages of disease may show the stage at which FcRL4$^+$ B cells become relevant in disease.

Most PBC patients in this study have been treated with UDCA. UDCA is a secondary bile acid and is the only approved treatment for PBC, although approximately 20-30% of patients are refractory to treatment and will require subsequent liver transplantation[233]. Therefore, it is probable that the patients studied here are those that did not respond well to treatment. The presence of FcRL4$^+$ B cells could be indicative of disease that is more resistant to treatment. Conversely, UDCA treatment has been shown to reduce serum IgM levels in patients[344] as well as reduce the capacity of B cells to produce IgM *ex vivo*[345]. The ability of

UCDA to modulate B cells in PBC could have impacted on FcRL4$^+$ B cell numbers. Liver biopsy samples of PBC patients prior and post treatment with UDCA could elucidate whether this treatment influences FcRL4$^+$ B cell numbers. Additionally, liver biopsies of patients who respond well to UDCA treatment could show whether the presence of FcRL4$^+$ B cells could be an indicator of more difficult-to-treat disease.

FcRL4$^+$ B cells have been identified in both RA and pSS. In the rheumatic joint, FcRL4$^+$ B cells can be predominantly found in lymphocyte aggregates underneath the synovial lining layer[128]. In pSS, these cells can be found within the inflamed salivary glands[130]. Within the parotid glands, FcRL4$^+$ cells are located within lymphoepithelial lesions[130], showing a clear association between these cells and the epithelium. In this study, we also show that in PBC, FcRL4$^+$ B cells associate closely with the biliary epithelium. A common feature between the salivary and biliary epithelium is the expression of pIgR. FcRL4 acts as a receptor for IgA, and together this suggests that FcRL4$^+$ cells could participate in the destruction of epithelium.

In summary, FcRL4 expressing B cells are enriched within the PBC compared to other end-stage liver diseases. These cells can be found within immune filtrates close to the small bile ducts. Although there is no correlation between the presence of these cells and liver ALP levels, further investigation is required to determine the role of FcRL4$^+$ B cells in PBC pathogenesis.

4 PHENOTYPING FcRL4$^+$ B CELLS IN END-STAGE LIVER DISEASE

4.1 Introduction

In healthy individuals, FcRL4 is expressed by memory B cells located within the MALT and is only expressed at very low levels in the peripheral blood. Approximately 90% of MALT FcRL4$^+$ B cells are class switched[95,119], with most cells class switching to IgG and some to IgA[95,119]. Although expression of the classical memory B cell marker CD27 by tonsillar FcRL4$^+$ B cells is contested[95,119]. These cells are also thought to express high levels of CD20 and intermediate levels of CD21 but lack expression of plasma cell markers. FcRL4$^+$ B cells also express high levels of the co-stimulatory molecules CD80 and CD86, suggesting that they could function as antigen-presenting cells. Upon *in vitro* stimulation, they can quickly differentiate into antibody secreting cells[95,119].

FCRL4$^+$ B cells have also been found within peripheral blood of HIV patients[91]. These peripheral blood derived cells share some phenotypic similarities with those found within the MALT, including high expression of CD20 and the absence of CD27[95]. However, there are some marked differences. FcRL4$^+$ B cells from HIV-infected patients express low levels of CD80 and CD86[91] unlike those found within healthy patients[95]. Tissue based FcRL4$^+$ cells are also Ki-67$^+$ and are therefore dividing, whereas those derived from HIV-infected blood are Ki-67$^-$, suggesting that they are quiescent cells. Functionally, these cells also differ in that they cannot be stimulated to become plasmablasts after *in vitro* stimulation. Together, this suggests that FcRL4$^+$ B cells from HIV-infected patients represent an "exhausted" cell type that differs from the FcRL4$^+$ B cell population found within healthy individuals.

FcRL4$^+$ B cells have been characterised in several autoimmune diseases. In pSS, FcRL4$^+$ B cells can be found within the inflamed salivary glands[130]. Transcription analysis of gene expression has revealed that FcRL4$^+$ B cells highly express CD11c and T-bet[135]. Treatment with rituximab reduced the frequency of FcRL4$^+$ B cells and leads to the restoration of the glandular epithelium[130]. Our group were the first to show that in RA, synovial fluid derived FcRL4$^+$ B cells are CD27$^+$IgD$^-$ classical class switched memory B cells[128]. These cells express higher levels of CD11c and lower levels of CD21 compared to FcRL4$^-$ B cells. Further characterisation showed that FcRL4$^+$ B cells from the synovial fluid of RA patients also express higher levels of the costimulatory molecules CD80 and CD86[128]. FcRL4$^+$ B cells in RA also preferentially express IgA BCR, indicative of a mucosal origin for these cells[230]. In healthy gut associated lymphoid tissue (GALT), FcRL4 is expressed by a mixture of naïve transitional B cells, CD27$^-$CD45RB$^+$ memory B cells, CD27$^+$IgM$^+$IgD$^+$ marginal zone B cells, and CD27$^+$IgM$^-$IgD$^-$ class switched memory cells[346].

Identified in 2011, age-associated B cells (ABCs) have since been linked to a number of autoimmune diseases including SLE[100], MS[112], RA[101] and pSS[113]. In mice, ABCs appear earlier in autoimmune prone models suggesting that they are involved in the development of autoimmune disease[101]. These cells are characterised phenotypically as CD21$^-$ CD11c$^+$CD11b$^+$T-bet$^+$. A functional role for ABCs in autoimmune disease remains largely unclear. However the depletion of CD11c$^+$ ABCs in mouse models of lupus shows a reduction in autoantibody titres[101]. In human SLE, CD11c$^+$T-bet$^+$ B cells are linked to autoantibody producing plasma cells[96], suggesting that these cells are intrinsically linked to SLE pathogenesis.

Phenotyping of FcRL4$^+$ B cells within end-stage PBC livers could help elucidate a functional role for these cells in disease pathogenesis. We hypothesise that FcRL4$^+$ B cells derived from end-stage PBC are phenotypically similar to those identified within other autoimmune diseases. We also hypothesise that FcRL4$^+$ B cells derived from PBC livers would be phenotypically different to those identified within the blood of HIV-infected patients, as well as those isolated from other end-stage liver diseases.

4.2 Results

4.2.1 Ki-67 expression

FcRL4$^+$ B cells in several other diseases have been suggested to represent an exhausted cell population. To investigate if FcRL4$^+$ cells within the PBC livers were exhausted, Ki67 staining was used to identify proliferating cells. Two paraffin embedded sections each from 10 end-stage PBC livers were stained for either FcRL4 or CD20, before staining for Ki67. Both FcRL4 and CD20 are surface markers and Ki67 is present within the cell nucleus, thus double positive cells would appear to have a blue nucleus with a brown halo (Figure 4.2.1A-B). The number of proliferating and non-proliferating FcRL4$^+$ and CD20$^+$ cells were then counted by eye. The proportion of proliferating cells within the FcRL4$^+$ cell population was significantly higher, with a median of 18% of cells expressing Ki67 compared to only 1% in the CD20$^+$ population (Figure 4.2.1D). Intracellular staining of LIMCs isolated from fresh PBC livers (Figure 4.2.1E) also showed that the FcRL4$^+$ B cell population (median 16.7%) is significantly more proliferative than the total B cell population (median 1.8%) (Figure 4.2.1F).

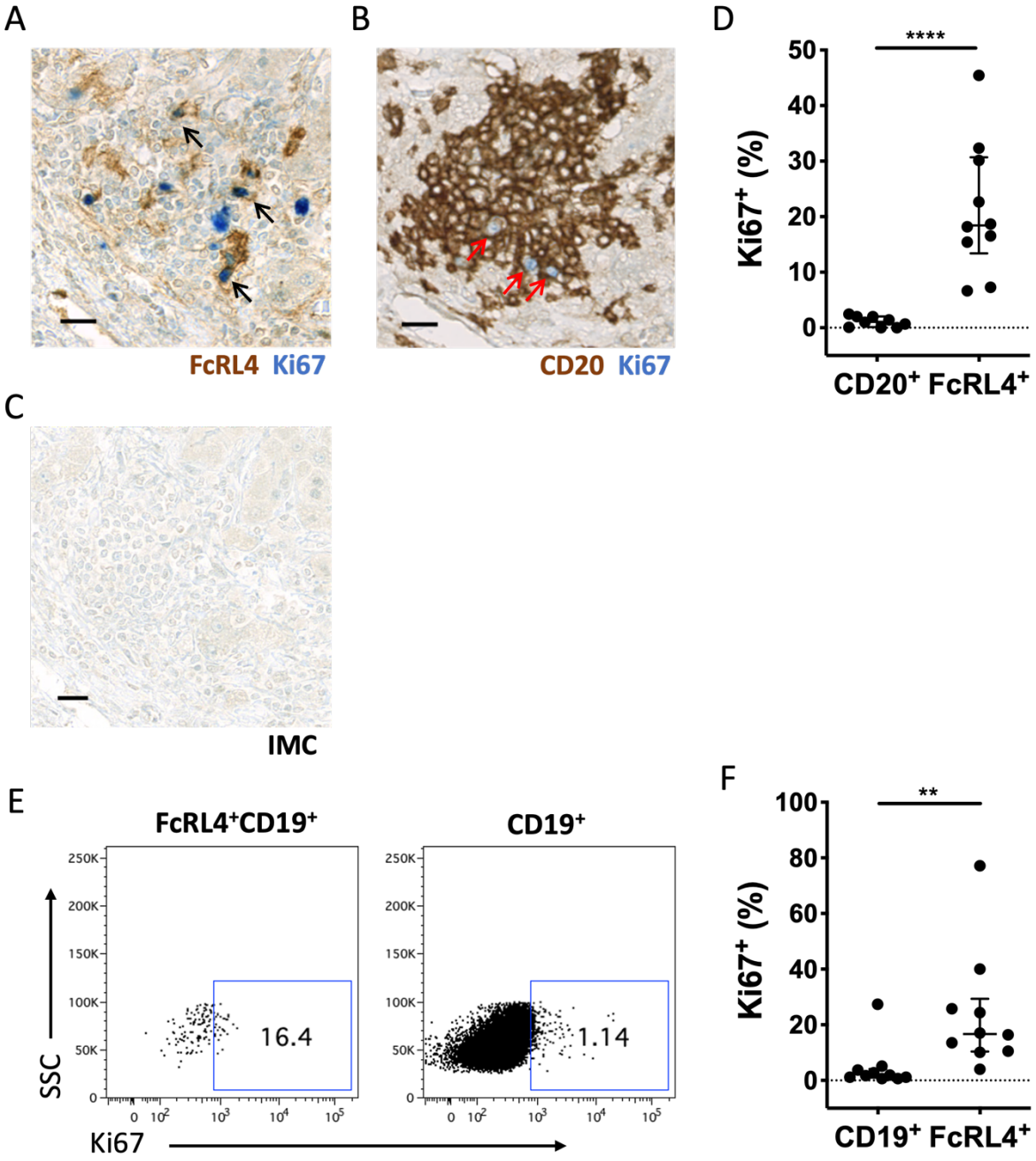

A
FcRL4 Ki67
B
CD20 Ki67
C
IMC
D
****
Ki67+ (%)
50
40
30
20
10
0
CD20+ FcRL4+
E
FcRL4+CD19+
CD19+
250K
200K
150K
100K
50K
0
SSC
Ki67
16.4
1.14
F
**
Ki67+ (%)
100
80
60
40
20
0
CD19+ FcRL4+

Figure 4.2.1. Proliferation of FcRL4$^+$ cells within PBC liver. *Staining of paraffin embedded PBC liver samples.* ***(A)****,* ***(B),*** *and* ***(C)*** *show the same region within a PBC liver from sequential paraffin sections (20µm scale).* ***(A)*** *Staining with FcRL4 (brown) and the proliferation marker Ki67 (blue). Arrows indicate FcRL4$^+$Ki67$^+$ cells.* ***(B)*** *CD20 (brown) and Ki67 (blue) double stain of PBC liver. Red arrows indicate double positive cells.* ***(C)*** *Staining with isotype matched controls.* ***(D)*** *Quantification of Ki67 expression within the FcRL4$^+$ and CD20$^+$ population. (n=10).* ***(E)*** *Representative flow plots of isolated liver infiltrating mononuclear cells were stained for CD19, FcRL4, and Ki67 and analysed using flow cytometry. Gating strategy outlined in Chapter 3 was used.* ***(F)*** *Quantification of Ki67 expression in FcRL4 expressing B cells and the total B cell population. (n=10). Statistics – Wilcoxon matched-pairs signed rank test.*

4.2.2 IgA expression

Although it is not known how the loss of tolerance occurs in PBC, several theories have suggested that the breakdown of tolerance occurs within the gut. IgA staining of LIMCs showed there is an enrichment of IgA^+ B cells in PBC livers (median 1.2%) compared to other end-stage liver disease (Figure 4.2.2A). Although some of this could be caused by the slight increase in total B cell numbers within the PBC liver, there is also an enrichment of IgA^+ cells within the B cell population compared to other end-stage liver diseases (Figure 4.2.2B). There is also no significant difference in IgA expression within both the total LIMC and B cell population in PBC livers compared to rejected donor livers (Figure 4.2.2A, B). There are significantly more IgA^+ B cells in PBC liver (median 10.9%) compared to PSC (median 4.8%). Within the PBC liver, $FcRL4^+$ B cells are also enriched for IgA isotype, a median of 22.2% of $FcRL4^+$ B cells expressing IgA compared to 11% in the $FcRL4^-$ B cell population (Figure 4.2.2D).

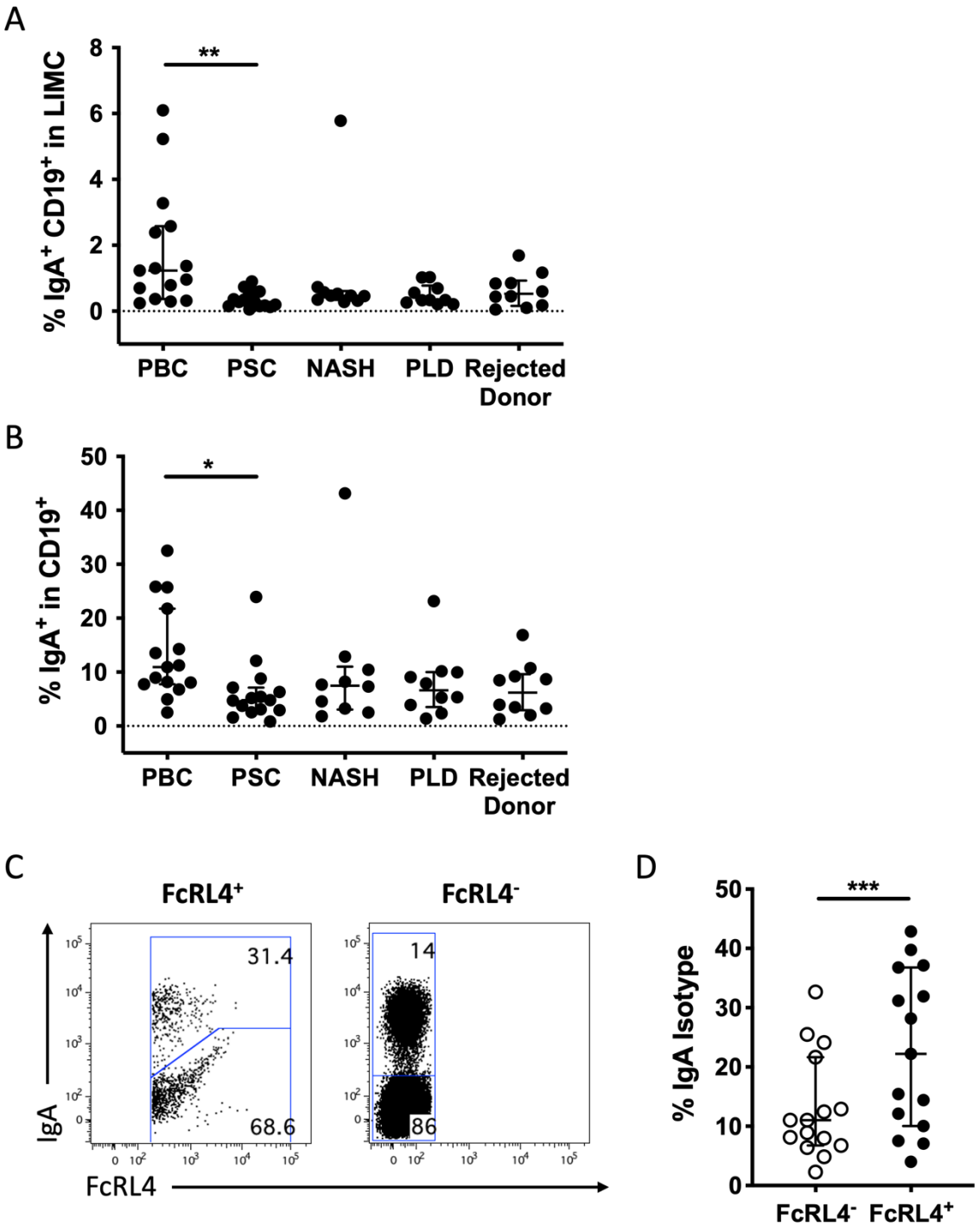

A
% IgA+ CD19+ in LIMC
**
PBC
PSC
NASH
PLD
Rejected Donor
B
% IgA+ in CD19+
*
PBC
PSC
NASH
PLD
Rejected Donor
C
FcRL4+
FcRL4-
31.4
68.6
14
86
IgA
FcRL4
D
% IgA Isotype
***
FcRL4-
FcRL4+

Figure 4.2.2. FcRL4$^+$ B cells are enriched for IgA BCR. *LIMCs were isolated from end-stage livers.* ***(A)*** *IgA expression by B cells in end stage liver disease. PBC (n=15), PSC (n=15), NASH (n=10), PLD (n=10), rejected donor (n=10). Statistics – Kruskal-Wallis test followed by Dunn's post hoc test for multiple comparisons.* ***(B)*** *IgA$^+$ B cells in the total LIMCs population in end stage liver disease. Statistics – Kruskal-Wallis test followed by Dunn's post hoc test for multiple comparisons.* ***(C)*** *Representative plot of IgA expression by FcRL4$^+$ and FcRL4$^-$ B cells isolated from PBC livers. Gating strategy outlined in Chapter 3 was used.* ***(D)*** *IgA expression by FcRL4$^+$ and FcRL4$^-$ B cells. (n=15). Statistics – Wilcoxon matched-pairs signed rank test.*

4.2.3 Differentiation stage

Further phenotyping of FcRL4^{+} cells was conducted using frozen LIMCs from: PBC (n=10), PSC (n=7), NASH (n=2), and donor livers (n=4). The PSC, NASH, and donor livers were grouped together and termed "end-stage liver disease" (ESLD). Flow cytometry staining was used to investigate the differentiation stage. Previous work from our group has shown that RA derived FcRL4^{+} B cells are mostly CD27^{+}IgD^{-}[128]. Here we show that PBC derived FcRL4^{+} cells are mostly CD27^{+}IgD^{-} class switched classical memory B cells (median 53.1%) (Figure 4.2.3B). Few FcRL4^{+} B cells are CD27^{-}IgD^{+} (median 16.3%), however this naïve B cell subset is enriched within the FcRL4^{-} B cell population (median 45%) (Figure 4.2.3B). This enrichment of class switched memory B cells within the FcRL4^{+} B cell population was only seen within the PBC liver (Figure 4.2.3C). In other end-stage liver disease and within the tonsil, there were significantly fewer CD27^{+}IgD^{-} B cells (median 37.7% and 45.6% respectively), although there is no significant enrichment in the naïve B cell subset (Figure 4.2.3D).

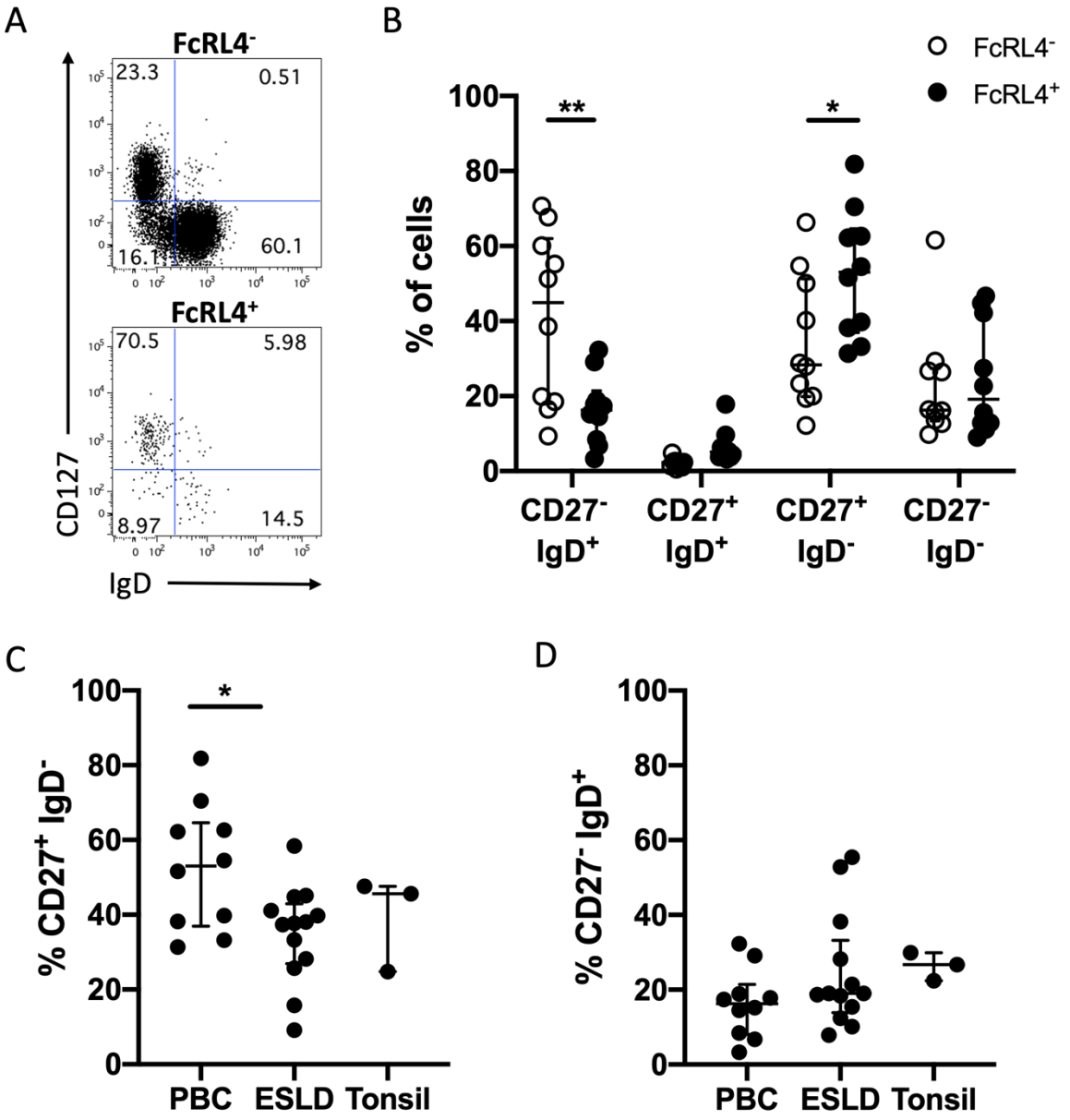


Figure 4.2.3. Most FcRL4⁺ B cells in the PBC liver are class switched memory B cells. *LIMCs isolated from liver tissue were stained and analysed using flow cytometry.* ***(A)*** *Example flow plot of CD27 IgD staining in end-stage PBC. Gating strategy outlined in Chapter 3 was used.* ***(B)*** *Comparison of CD27 and IgD staining of FcRL4-expressing B cells and total B cells. (n=10). Statistics – Wilcoxon matched-pairs signed rank test.* ***(C)*** *Proportion of CD27⁺IgD⁻ cells within the FcRL4⁺ population in PBC liver compared to other end stage liver diseases (ESLD) and inflamed tonsils. Statistics – Mann-Whitney test.* ***(D)*** *Proportion of CD27⁻IgD⁺ cells within the FcRL4⁺ B cell population in PBC liver compared to other end-stage liver diseases and inflamed tonsils. PBC (n=10), ESLD (n=13), tonsil (n=3).*

4.2.4 CD11c, CD21, and T-bet expression

A growing body of research has linked the presence of ABCs to several infectious and autoimmune diseases. These cells are characterised as $CD21^{-}CD11c^{+}CD11b^{+}CD23^{-}$T-$bet^{+}$. CD11c, CD21, and T-bet staining was conducted on frozen LIMCs to identify the presence of ABCs within end-stage PBC. FcRL4 staining was able to enrich for $CD11c^{+}CD21^{-}$ B cells within PBC livers (median 42.1%) (Figure 4.2.4A). Within other end-stage liver diseases investigated, there were significantly higher proportion of $CD11c^{+}CD21^{-}$ B cells within the $FcRL4^{+}$ population compared to the $FcRL4^{-}$ population (median 25.2% and 5.0% respectively). However, this $FcRL4^{+}$ ABC population is significantly smaller than what is found in PBC livers.

T-bet expression by total B cells was slightly elevated in end-stage PBC (median 5.3%) compared to tonsils (median 0.7%), although no significant difference was observed between PBC derived cells and the other end-stage liver diseases (median 4.2%) (Figure 4.2.4C). However, in all end-stage liver derived cells, a significantly higher proportion of $FcRL4^{+}$ B cells were T-bet expressing compared to $FcRL4^{-}$ B cells, with the highest T-bet expression seen in the PBC derived cells (median 55.15%). A median number of 81.7% of PBC derived ABCs express T-bet (Figure 4.2.4E), and there is no difference in T-bet expression between $FcRL4^{+}$ ABCs and $FcRL4^{-}$ ABCs (Figure 4.2.4F). Within the inflamed tonsil, $FcRL4^{+}$ B cells did not enrich for ABCs. This may be because the $CD21^{-}CD11c^{+}$ subset represented only a very small population in the tonsils (Figure 4.2.4B). T-bet expression within the tonsil was also low, with few tonsils derived cells expressing T-bet (Figure 4.2.4C-D).

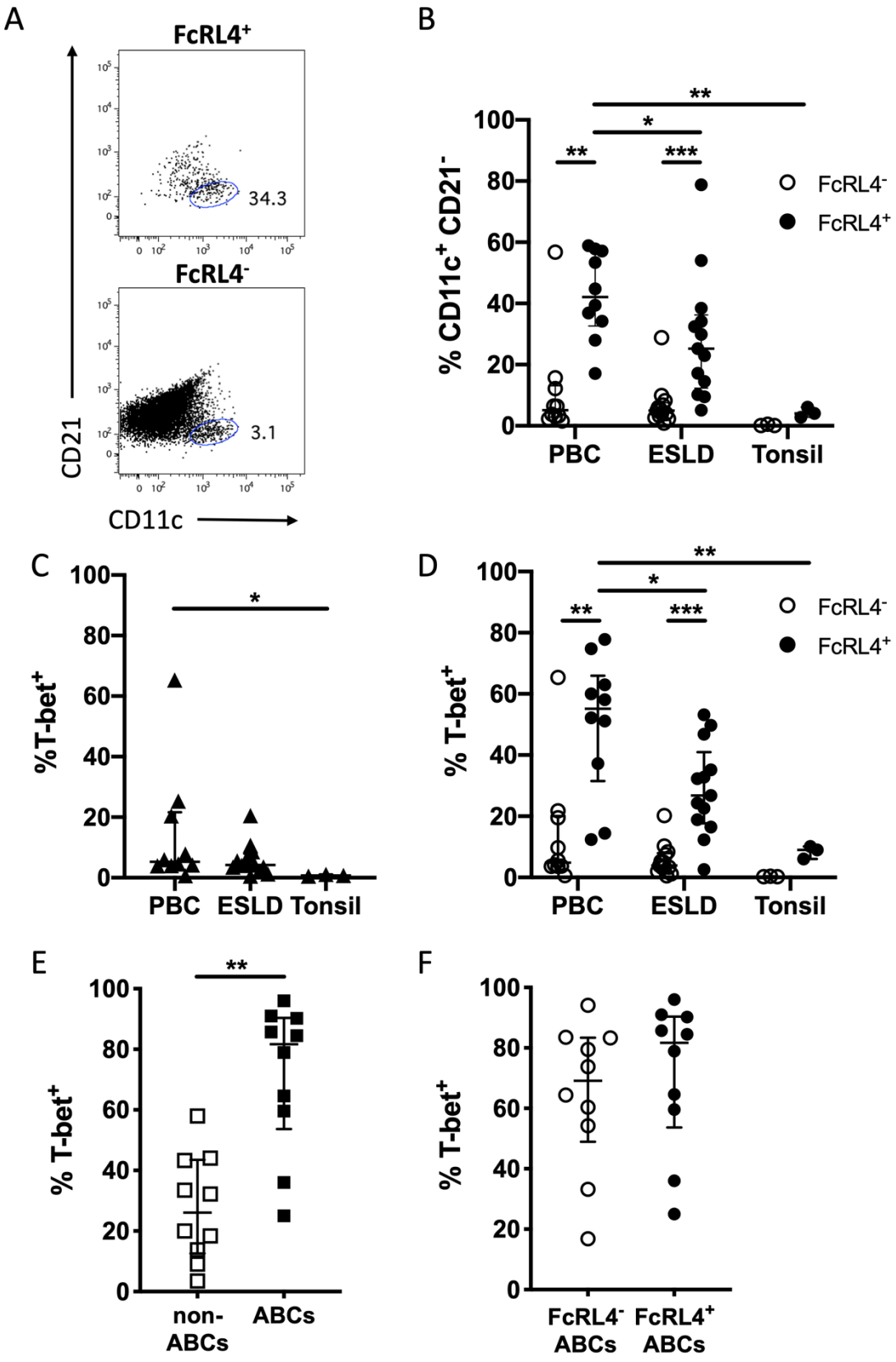

A
FcRL4+
34.3
FcRL4-
3.1
CD21
CD11c
B
% CD11c+ CD21-
FcRL4-
FcRL4+
PBC
ESLD
Tonsil
C
%T-bet+
PBC
ESLD
Tonsil
D
% T-bet+
FcRL4-
FcRL4+
PBC
ESLD
Tonsil
E
% T-bet+
non-ABCs
ABCs
F
% T-bet+
FcRL4- ABCs
FcRL4+ ABCs

Figure 4.2.4. FcRL4$^+$ B cells in the PBC liver are enriched for CD11c$^+$CD21$^-$ ABCs. *LIMCs isolated from liver tissue were stained and analysed using flow cytometry.* ***(A)*** *Representative flow plot of CD11c and CD21 staining on FcRL4$^+$ and FcRL4$^-$ B cells. Gating strategy outlined in Chapter 3 was used.* ***(B)*** *CD11c$^+$CD21$^+$ population within the FcRL4$^+$ and FcRL4$^-$ B cell population in PBC livers compared to ESLD and tonsils. Statistics – Wilcoxon matched-pairs signed rank test and Mann-Whitney.* ***(C)*** *T-bet expression by B cells in end-stage liver disease. Statistics – Mann-Whitney test.* ***(D)*** *T-bet expression by FcRL4$^+$ and FcRL4$^-$ B cells in end-stage liver disease. Statistics – Wilcoxon matched-pairs signed rank test and Mann-Whitney.* ***(E)*** *T-bet$^+$ B cell population in CD11c$^+$CD21$^-$ ABCs compared to non-ABCs in end-stage PBC. Statistics – Wilcoxon matched-pairs signed rank test.* ***(F)*** *T-bet expression by FcRL4$^+$ ABCs compared to FcRL4$^-$ ABCs in end-stage PBC livers. PBC (n=10), ESLD (n=13), tonsil (n=3).*

4.2.5 Ki67 expression of ABCs

Like in PBC, FcRL4^{+} B cells derived from other end-stage liver diseases are also more proliferative than their FcRL4^{-} counterparts (median 5.2% and 0.8% respectively) (Figure 4.2.5B). However, the same was not observed within the tonsil, as very few B cells expressed Ki67. ABCs from PBC livers were more proliferative than in other end-stage liver disease (median 5.1% and 1.4% respectively). Within the PBC derived ABC population, FcRL4 expressing ABCs were more proliferative than FcRL4^{-} ABCs (median 16.3% and 4.5% respectively) (Figure 4.2.5D). This trend was seen in all end-stage liver diseases, however PBC derived FcRL4^{+} ABCs were significantly more proliferative than those found in other end-stage liver disease (Figure 4.2.5C).

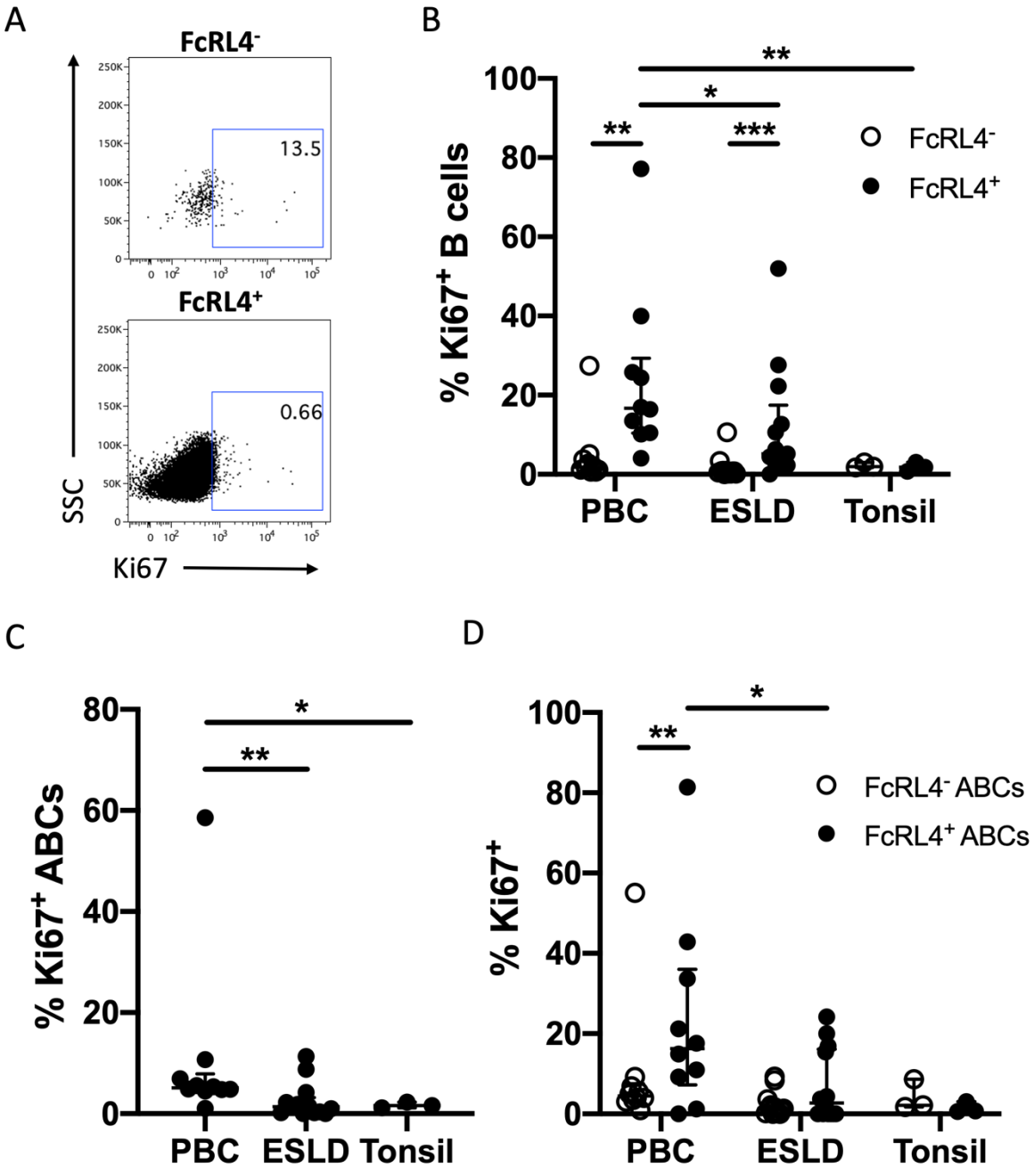
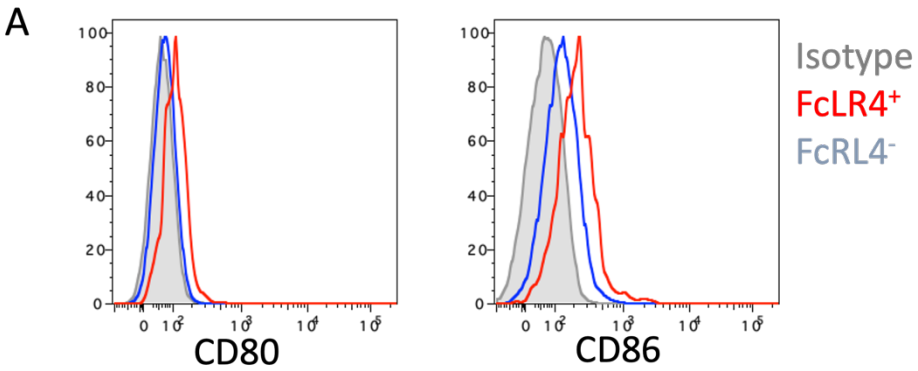
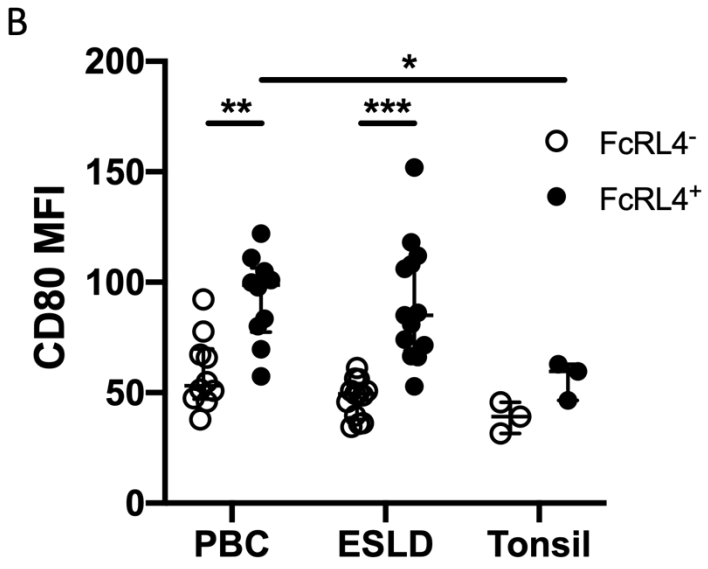


Figure 4.2.5. Ki67 by ABCs in end-stage liver disease. *LIMCs isolated from liver tissue were stained and analysed using flow cytometry.* ***(A)*** *Representative flow plot of Ki67 on FcRL4$^+$ and FcRL4$^-$ B cells. Gating strategy outlined in Chapter 3 was used.* ***(B)*** *Ki67 expression by FcRL4$^+$ and FcRL4$^-$ B cells derived from end-stage liver diseases and tonsils. Statistics – Wilcoxon matched-pairs signed rank test and Mann-Whitney.* ***(C)*** *Ki67 expression by CD11c$^+$CD21$^-$ ABCs. Statistics – Mann-Whitney test.* ***(D)*** *Ki67 expression of FcRL4$^+$ and FcRL4$^-$ ABCs. Statistics – Wilcoxon matched-pairs signed rank test and Mann-Whitney. PBC (n=10), ESLD (n=13), tonsil (n=3).*

4.2.6 CD80 and CD86 expression

FcRL4$^+$ cells in healthy tonsils have previously been shown to express high levels of the co-stimulatory molecules CD80 and CD86. In RA, these cells also express higher levels of both CD80 and CD86 than FcRL4$^-$ B cells. Here, we show that FcRL4$^+$ B cells from PBC livers express significantly more CD80 and CD86 compared to FcRL4$^-$ B cells (Figure 4.2.6). The same increase in CD80 and CD86 expression was also seen in FcRL4$^+$ B cells derived from other end-stage liver diseases. We also see that liver derived FcRL4$^+$ B cells expressed higher levels of these two costimulatory molecules compared to tonsil derived cells.


A
CD80
CD86
Isotype
FcLR4+
FcRL4-


B
CD80 MFI
FcRL4-
FcRL4+
PBC
ESLD
Tonsil

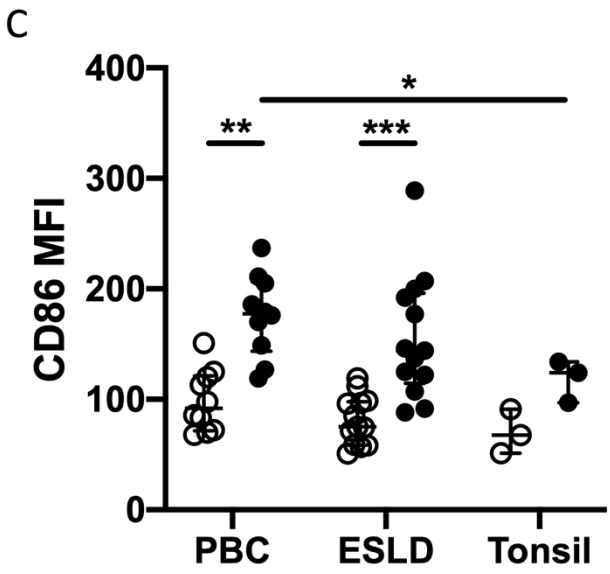

C
CD86 MFI
PBC
ESLD
Tonsil

Figure 4.2.6. FcRL4^{+} B cells have higher expression of CD80 and CD86 than FcRL4^{-} B cells. *Stained PBC derived LIMCs were gated using gating strategy outlined in Chapter 3.* ***(A)*** *Example histogram of CD80 and CD86 expression by FcLR4^{+} and FcRL4^{-} B cells compared to isotype control.* ***(B)*** *CD80 and* ***(C)*** *CD86 MFI of FcRL4^{+} FcRL4^{-} B cells in PBC, other end-stage liver diseases and inflamed tonsil. Statistics – Wilcoxon matched-pairs signed rank test and Mann-Whitney test. PBC n=10, ESLD n=13, tonsil n=3.*

4.3 Discussion

We hypothesised that PBC derived FcRL4$^+$ B cells would be phenotypically similar to those identified within other autoimmune diseases such as RA. In RA FcRL4$^+$ B cells are predominantly class switched classical memory B cells with reduced expression of CD21, and elevated expression of CD11c, CD80, and CD86. Consistent with our findings in RA, PBC derived FcRL4$^+$ B cells are mostly CD27$^+$IgD$^-$, enrich for CD21$^-$CD11c$^+$ ABCs, and have increased expression of CD80 and CD86 compared to FcRL4$^-$ B cells. It is important to note that although FcRL4 enriches for ABCs, our data show that not all FcRL4$^+$ cells are ABCs, and not all ABCs express FcRL4. So, although the phenotyping data suggest an overlap between the characteristics of these cells, they cannot be considered to be the same subset of cells.

FcRL4$^+$ B cells identified within the blood of HIV-infected patients have been shown to be non-proliferative[91]. Our data suggest that FcRL4$^+$ B cells within PBC livers are in fact highly proliferative compared to the total B cell population. The absence of CD80 and CD86 expression in these cells from HIV-infected individuals[91] suggests that PBC derived FcRL4$^+$ cells may have closer resemblance to those identified in other autoimmune diseases than in viral infection.

Although the number of FcRL4$^+$ B cells are lower in end-stage PSC, NASH, and donor livers, our data showed that phenotypically, FcRL4$^+$ B cells derived from all livers share some similarities. There is no significant difference in CD80 and CD86 expression by FcRL4$^+$ across all the end-stage liver diseases investigated in this study. Although there are fewer CD11c$^+$CD21$^-$T-bet$^+$ ABCs within the FcRL4$^+$ B cell subset in other end-stage liver diseases than in PBC, ABCs are still more abundant in the FCRL4$^+$ subset compared to FcRL4$^-$ B cells. There were also significantly fewer CD27$^+$IgD$^-$FcRL4$^+$ B cells in the non-PBC group.

It is becoming increasingly recognised that the gut microbiota plays an important role in the development of chronic liver illnesses such as non-alcoholic fatty liver disease, alcoholic liver disease, cirrhosis, and PSC[230,347–349]. The liver is exposed to the microorganisms and microbial metabolites of the gut as its primary function is to filter blood arriving through the portal vein from the intestine. Dysbiosis of the gut can increase intestinal permeability, leading to bacterial infiltration which in turn can result in chronic hepatic inflammation and fibrosis. PDC-E2 is the principal target of AMAs in PBC sera[350]. As a result of autoantibody, B cell, and T-cell cross-reactivity with a related version of this enzyme found in intestinal bacteria[242,328,351], molecular mimicry has been proposed as a possible explanation for the breakdown of tolerance in PBC[242,329,352]. This theory is supported by the increase in recurrent urinary tract infections in PBC[353], as well as the induction of AMA and PBC-like liver pathology in mouse models following *E. coli* infection[329]. FcRL4$^+$ cells isolated from healthy tonsils react to commensal microbiota[124], implying that these cells have a role in the mucosal immune system's maintenance. Here we show that a substantial proportion of the FcRL4$^+$ B cells in PBC livers express IgA BCR, indicating that the cells may originate in the MALT, where they may be primed against the bacterial PDC-E2 before moving to the liver. Indeed FcRL4$^+$ B cells have been identified within the GALT of healthy individuals. Here FcRL4 expressing CD27$^+$IgM$^-$IgD$^-$ class switched memory B cells occupy the sub-epithelial space[346]. We were however unable to obtain matched samples to confirm the presence of FcRL4$^+$ B cells in the gut of PBC patients.

Increased serum IgM is commonly observed in PBC patients, which correlates with infiltrating IgM$^+$ plasmablasts can also be seen in the portal tracts[354,355]. The polyclonal IgM response in PBC has been shown to be affected by changes in the faecal microbiome. A

recent study showed that a reduction in sera IgM levels correlates with changes to the bile acid composition after UDCA treatment[356]. The same study found that UDCA treatment was able to alter the gut microbiota in PBC patients[356]. Together, this suggests that IgM expressing B cells may play an important role in PBC pathogenesis. Therefore, our study would have benefitted from IgM staining of the FcRL4^{+} B cell subset to determine if they participate in the production of IgM in PBC.

CD24^{hi}CD38^{hi} are immature transitional B cells that have been identified at frequencies in peripheral blood of PBC patients[357]. CD24 and CD38 expression has also been used to describe regulatory B cells which have been shown to suppress the CD4^{+} T cell response[34]. Altered numbers and function of these cells have been shown in autoimmune diseases including RA[358], SLE[359], and ulcerative colitis[360]. In PBC, the increased frequency of these regulatory B cells is coupled with a reduced capacity to inhibit CD4^{+} T cell function[357]. Although we stained our PBC derived B cells for CD24 and found that the majority of B cells in the liver expressed CD24, we did not investigate CD38 expression (Supplementary Figure 7.2). Future work is required to identify the CD24^{hi}CD38^{hi} B cell population in PBC.

In summary, we show that PBC derived FcRL4^{+} B cells are enriched in highly proliferative, IgA expressing, classical class-switched memory B cells. FcRL4 expression enriches for the ABC phenotype, however, not all FcRL4^{+} B cells are ABCs. These cells express the co-stimulatory molecules CD80 and CD86 suggesting that they have the potential to be antigen presenting cells.

5 FcRL4$^+$ B CELL PARTICIPATION IN PBC PATHOGENESIS

5.1 Introduction

PBC is characterised by the progressive destruction of small bile ducts. Immune infiltration into the bile ducts is a hallmark of PBC[231,236]. Previously, we showed that FcRL4$^+$ B cells can be found within these aggregates, indicating that they could participate in the destruction of the small bile ducts. In the experimental work shown in this chapter we have explored several aspects of the potential functional contribution that FcRL4$^+$ B cells may make to the pathomechanism of PBC.

FcRL4$^+$ B cells have been shown to participate in disease pathogenesis of RA[127–129] and pSS[130,135]. Both RA and pSS are known comorbidities of PBC[332]. In pSS, rituximab treatment can eliminate FcRL4$^+$ B cells from inflamed salivary glands, leading to the normalisation of the epithelial lining and the significant reduction of lymphoepithelial lesions[130].

In RA, FcRL4$^+$ B cells in the synovium express high levels of RANKL and TNFα mRNA[127,128]. Production of the pro-inflammatory cytokine TNFα indicates that these cells play a significant role in the chronic inflammation seen in RA[128]. Receptor activator NFκB ligand (RANKL) mRNA is elevated in the RA synovium compared to normal tissue[361]. RANK is a type II membrane receptor found on the surface of osteoclasts, dendritic cells, and epithelial cells[362]. The binding of RANKL to RANK is a key player in osteoclast differentiation and activation[131], which in RA, leads to characteristic bone erosion. Osteoprotegerin (OPG) is a decoy receptor for RANKL[362]. Both RANKL and OPG are produced by osteoblasts, and the ratio of RANKL and OPG influences osteoclastogenesis[363].

FcRL4$^+$ B cells isolated from the RA synovium have been shown to contribute to the autoantigen response[129]. Among a series of monoclonal antibodies derived from FcRL4$^+$ B cells in the RA synovium several were reactive against citrullinated peptides. Analysis of Ig isotype also showed significant enrichment of IgA expressing cells within the FcRL4$^+$ B cell population[129]. Indeed, IgA autoantibodies in RA are a predictor for aggressive disease[364,365], indicating that these cells could play an important role in disease pathogenesis.

Although the presence of autoantibodies is a hallmark of disease in PBC, the precise role that B cells play in disease pathogenesis remains elusive. UDCA, the current therapy for PBC, has been shown to be able to modulate the B cell compartment despite not being a known immune modulator. Patients treated with UDCA show improvements in serum IgM levels[345,366], suggesting that this treatment may have some indirect effects on B cells in PBC.

Despite treatment with UDCA significantly increasing transplant-free survival in PBC, approximately 20-30% of patients are refractory to treatment[233]. Rituximab has been trialled in PBC patients who are refractory to UDCA[275–278]. The anti-CD20 monoclonal antibody treatment is well tolerated by patients, was effective at depleting peripheral B cells, and led to a significant reduction in serum AMA titres[275,276]. There were limited improvements in liver biochemistry in these patients, indicating that B cells may participate in disease pathogenesis.

We hypothesise that FcRL4$^+$ B cells in end-stage PBC contribute to the pathomechanism. We aimed to identify the method by which these cells participate in the destruction of the small bile ducts. We investigated the ability of FcRL4$^+$ B cells to capture IgA complexes, directly interact with BECs, and to recognise the AMA autoantigen.

5.2 Results

5.2.1 Proximity of FcRL4$^+$ to the biliary epithelium

To determine the proximity of FcRL4$^+$ cells to the site of inflammation in PBC, cytokeratin 7 staining was used to identify biliary epithelial cells. This staining identified FcRL4$^+$ B cells within the wider context of immune aggregates. Co-staining with cytokeratin 7 demonstrated that these immune aggregates often surrounded bile ducts (Figure 5.2.1A). Moreover, cytokeratin 7 staining revealed residual biliary epithelial cells, likely remainders of destroyed bile ducts in the centre of aggregates (Figure 5.2.1B).

In order to further explore the spatial proximity of these FcRL4$^+$ B cell populations to biliary epithelium, the distance between B cells and the biliary epithelium was measured. A minimum of 2 B cell aggregates surrounding biliary epithelium were identified from 6 PBC patients. The distance between either FcRL4$^+$ or CD20$^+$ cells to the basolateral membrane of the biliary epithelium was then measured. Across all 6 patients, the mean distance between FcRL4$^+$ cells and the bile duct was significantly shorter than the distance seen with total CD20$^+$ cells (median 52.46µm and 85.02µm respectively) (Figure 5.2.1I). In fact, in some cases, FcRL4$^+$ B cells were seen embedded within the bile ducts, suggesting a pivotal role in the inflammatory process.

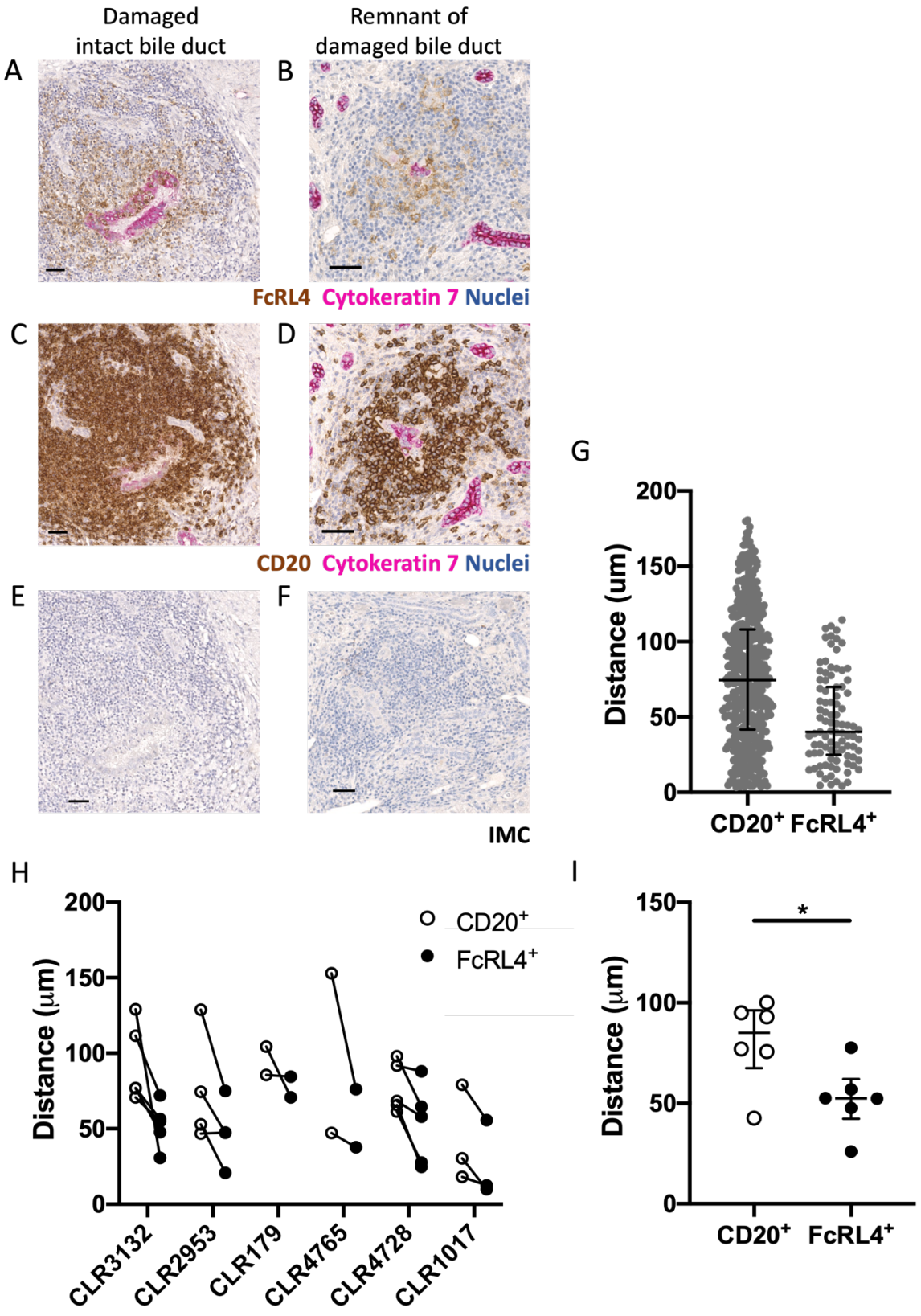

Damaged intact bile duct
Remnant of damaged bile duct
A
B
FcRL4 Cytokeratin 7 Nuclei
C
D
CD20 Cytokeratin 7 Nuclei
E
F
IMC
G
Distance (um)
200
150
100
50
0
CD20+ FcRL4+
H
Distance (μm)
CD20+
FcRL4+
CLR3132
CLR2953
CLR179
CLR4765
CLR4728
CLR1017
I
*
Distance (μm)
CD20+ FcRL4+

Figure 5.2.1 In PBC FcRL4$^+$ B cells form aggregates around inserted in biliary epithelium. *Paraffin-embedded PBC sections. Scale bar = 50um* ***(A)*** *and* ***(B)*** *Sections were stained for FcRL4 (brown) and Cytokeratin 7 (pink).* ***(C)*** *and* ***(D)*** *Sections were stained for CD20 (brown) and Cytokeratin 7 (pink).* ***(E)*** *and* ***(F)*** *isotype matched controls.* ***(G)*** *Distance from the epithelium to FcRL4$^+$ cells and total B cells of one immune aggregate.* ***(H)*** *Mean distance of B cells to the epithelium from a minimum of 2 aggregates identified from 6 PBC livers.* ***(I)*** *Median distance of FcRL4$^+$ cells and CD20$^+$ cells to the biliary epithelium. n=6. Statistics – Wilcoxon matched-pairs signed rank test.*

5.2.2 FcRL4 binding to IgA

FcRL4 has been shown to be a receptor for IgA[122,123]. Given the proximity of these cells to the biliary epithelium in PBC where IgA transcytosis occurs[266], we sought to investigate the ability of PBC derived FcRL4$^+$ B cells to bind IgA aggregates.

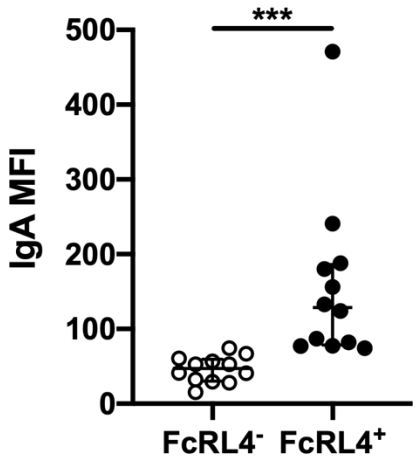
IgA staining of FcRL4$^+$ B cells derived from PBC livers showed that there is a close association between FcRL4 and IgA (Figure 5.2.2A). The staining pattern observed when plotting FcRL4 and IgA staining shows a direct correlation between FcRL4 and IgA (Figure 5.2.2B), suggesting that FcRL4 is directly binding IgA. To test this, PBC derived LIMCs were washed with a pH3 glycine buffer to remove surface bound antibodies. After this acid wash, the previously observed correlation between FcRL4 and IgA staining was no longer present and there was a significant reduction in IgA MFI of FcRL4$^+$ cells (Figure 5.2.2B, C). To further demonstrate the binding of IgA by FcRL4, acid washed cells were subsequently incubated with heat aggregate colostrum IgA. As expected, a significant increase in IgA MFI was observed (Figure 5.2.2B, C). Acid washing did not reduce IgA MFI on FcRL4$^-$ B cells, however, subsequent incubation with HA-IgA did result in an increase in IgA MFI (Figure 5.2.2B, C).

The gating strategy outlined in Chapter 3 was used for this acid washing experiment. A strict live/dead gate was important for the exclusion of dead cells from this experiment to eliminate any non-specific antibody binding to non-viable cells.

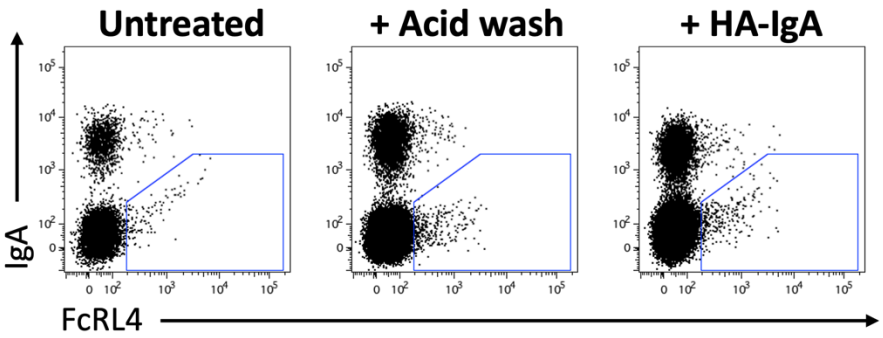
IgA AMAs have been found within the bile of PBC patients. Transcytosis of IgA AMAs has been proposed as one possible mechanism of disease pathogenesis. This led us to believe that IgA-PDC-E2 immune complexes can be found within the bile of PBC patients which may be captured by FcRL4. Raji B cells transfected to express FcRL4 were incubated with human

bile. Bile samples were collected from rejected donor (n=2), PSC (n=2), and PBC (n=2) patients. Patient bile was first washed to remove lipids and cell debris before incubation with Rajis. FcRL4^{+} Rajis were able to capture IgA from patient bile. At a bile concentration of 1 in 15, IgA binding by FcRL4 is comparable to 1mg/mL of heat aggregated colostrum IgA (median MFI 113.5 and 158.5 respectively) (Figure 5.2.3B). The binding of bile derived IgA by FcRL4^{+} cells was dosage dependent with a lot of variability in IgA binding seen across patient samples. The lowest levels of IgA binding were observed in the PBC bile samples.

A


***
500
400
300
200
100
0
IgA MFI
FcRL4- FcRL4+

B


Untreated
+ Acid wash
+ HA-IgA
IgA
FcRL4

C

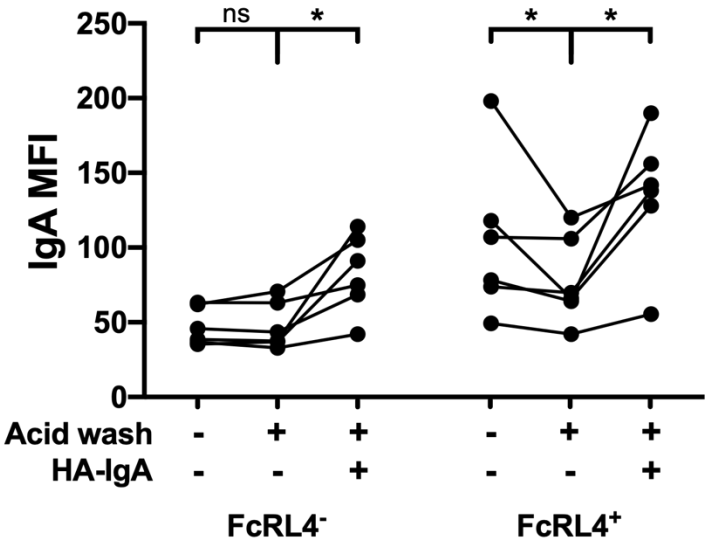

ns
*
*
*
250
200
150
100
50
0
IgA MFI
Acid wash - + + - + +
HA-IgA - - + - - +
FcRL4-
FcRL4+

Figure 5.2.2 FcRL4$^+$ as a receptor for IgA aggregates. *LIMCs isolated from PBC livers were stained for CD19, FcRL4, and IgA.* ***(A)*** *IgA MFI of FcRL4$^-$ and FcRL4$^+$ B cells. (n=12). Statistics – Wilcoxon matched-pairs signed rank test.* ***(B)*** *FcRL4$^+$ B cells isolated from PBC liver were washed with pH3 glycine wash to remove surface-bound IgA. The cells were then incubated with 1mg/mL colostrum IgA that had been heat aggregated. Example flow plots of FcRL4$^+$ and FcRL4$^-$ B cells before acid washing, after acid washing, and after replenishing with heat aggregated IgA.* ***(C)*** *IgA MFI of FcRL4$^-$ and FcRL4$^+$ B cells before acid washing, after acid washing, and after replenishing with heat aggregated IgA. Statistics – Wilcoxon matched-pairs signed rank test.*

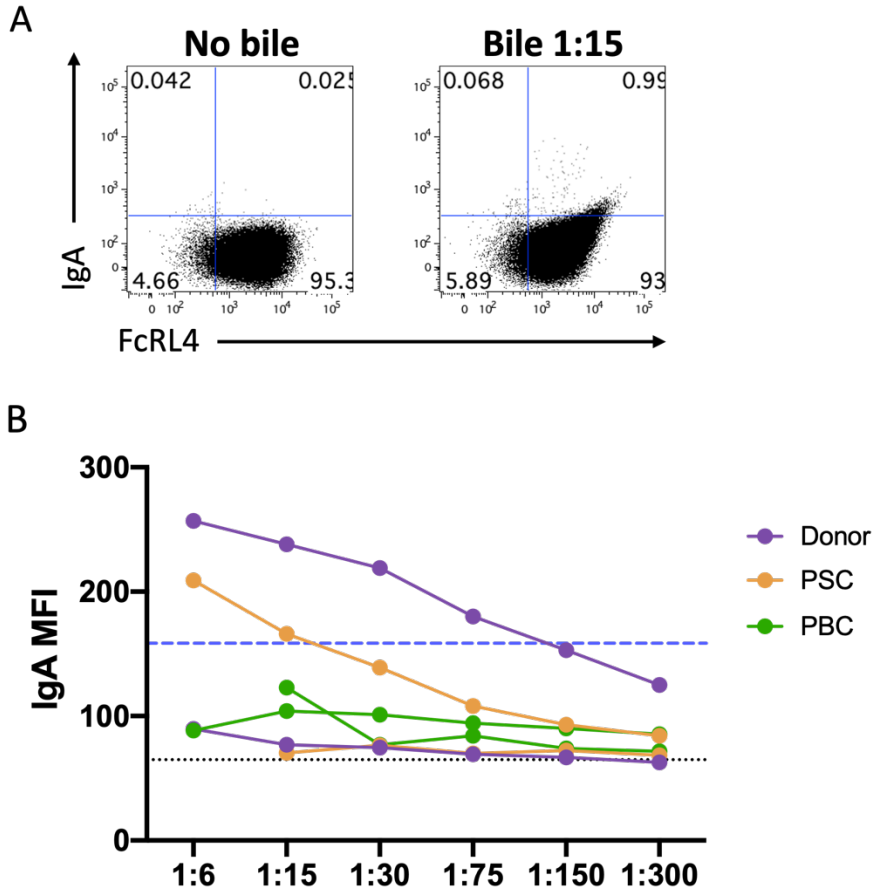


Figure 5.2.3 FcRL4 captures IgA from bile. *FcRL4 expressing Rajis were incubated with patient derived bile.* ***(A)*** *Representative flow plots of FcRL4 expressing Rajis.* ***(B)*** *IgA MFI of FcRL4 expressing Rajis after culturing with bile from 4 patients. Black dotted line represents median IgA MFI of Rajis alone. Blue dashed line represents the median MFI of Rajis incubated with 1mg/mL of heat aggregated colostrum IgA. Donor (n=2), PBC (n=2), PSC (n=2).*

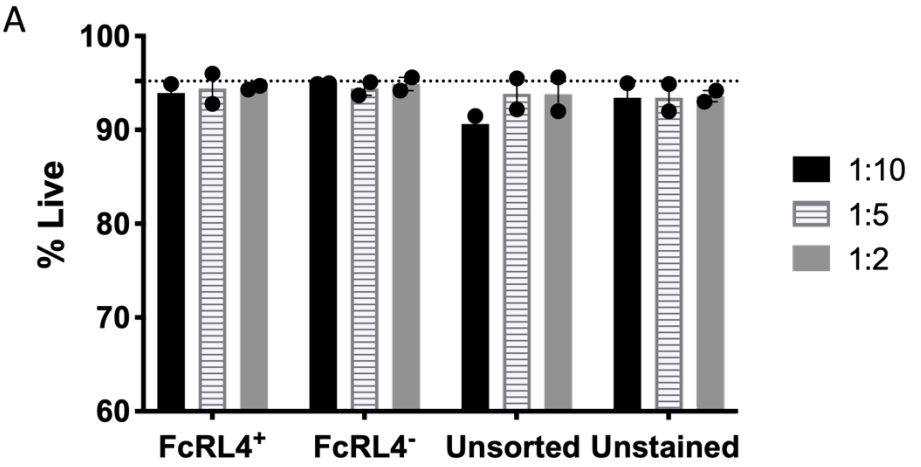
5.2.3 Co-culture of FcRL4$^+$ B cells and BECs

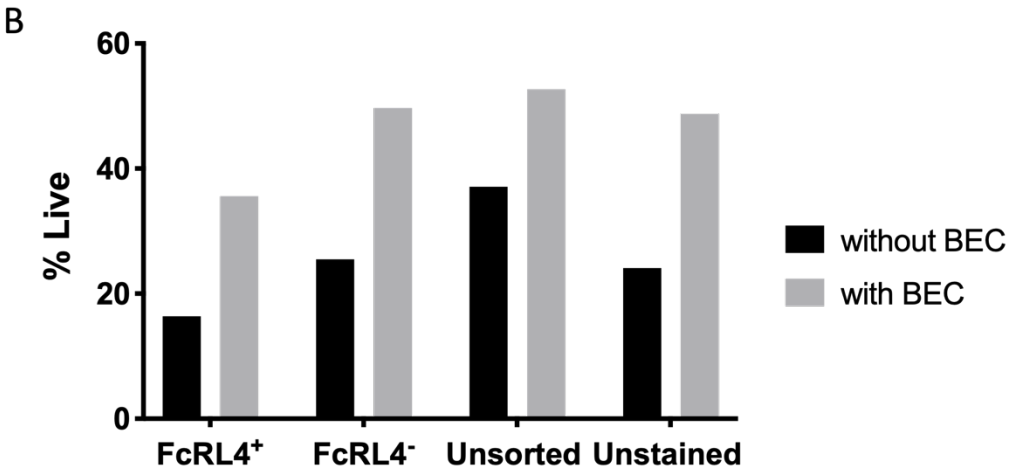
The proximity of FcRL4$^+$ B cells to the damaged biliary epithelium led us to investigate the possibility of direct killing of BECs by FcRL4$^+$ B cells. We set out to develop an assay to measure the viability of both FcRL4$^+$ B cells and epithelial cells after co-culture. FcRL4$^+$ and FcRL4$^-$ B cells were sorted from tonsil lymphocytes and co-cultured with human primary BECs for 24 hours. B cell and BEC viabilities were tested using a live/dead cell dye. After 24 hours of co-culture, no difference in BEC viability was observed between those cultured with and without FcRL4$^+$ and FcRL4$^-$ B cells (Figure 5.2.4A). Unsorted tonsil-derived cells and unstained cells were also used as a control. A slight reduction in BEC viability was seen in these wells, with the lowest cell viability observed in unsorted but antibody-stained tonsil cells at a BEC to lymphocyte ratio of 1:10.

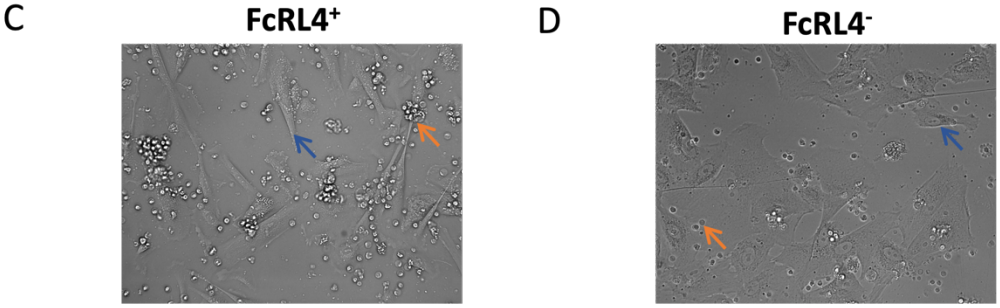
B cell survival was improved when cultured in the presence of BECs compared to B cells cultured alone (Figure 5.2.4B). This increase in cell viability after 24 hours of culture was seen across all B cells used in this assay. However, FcRL4$^+$ B cell survival was lower compared to FcRL4$^-$ B cells, tonsil lymphocytes that were stained but not sorted, and lymphocytes that were not stained with antibodies (Figure 5.2.4B).

Imaging of the B cell and BEC co-culture assay showed that FcRL4$^+$ B cells formed cell clusters with the biliary epithelial cells (Figure 5.2.4C). These cell clusters were not observed in the wells that contained FcRL4$^-$ B cells (Figure 5.2.4D). Direct interaction between FcRL4$^+$ B cells and BECs could be mediated by the expression of RANKL by FcRL4$^+$ B cells and RANK by BECs. FcRL4$^+$ B cells in the PBC liver express higher amounts of RANKL compared to FcRL4$^-$ B cells (Figure 5.2.4F). A similar trend was seen in cells derived from other end-stage

liver diseases, although only a slight increase in RANKL expression was seen in tonsil derived FcRL4^{+} cells.


A
100
90
80
70
60
% Live
FcRL4+
FcRL4-
Unsorted
Unstained
1:10
1:5
1:2


B
60
40
20
0
% Live
FcRL4+
FcRL4-
Unsorted
Unstained
without BEC
with BEC


C
FcRL4+
D
FcRL4-

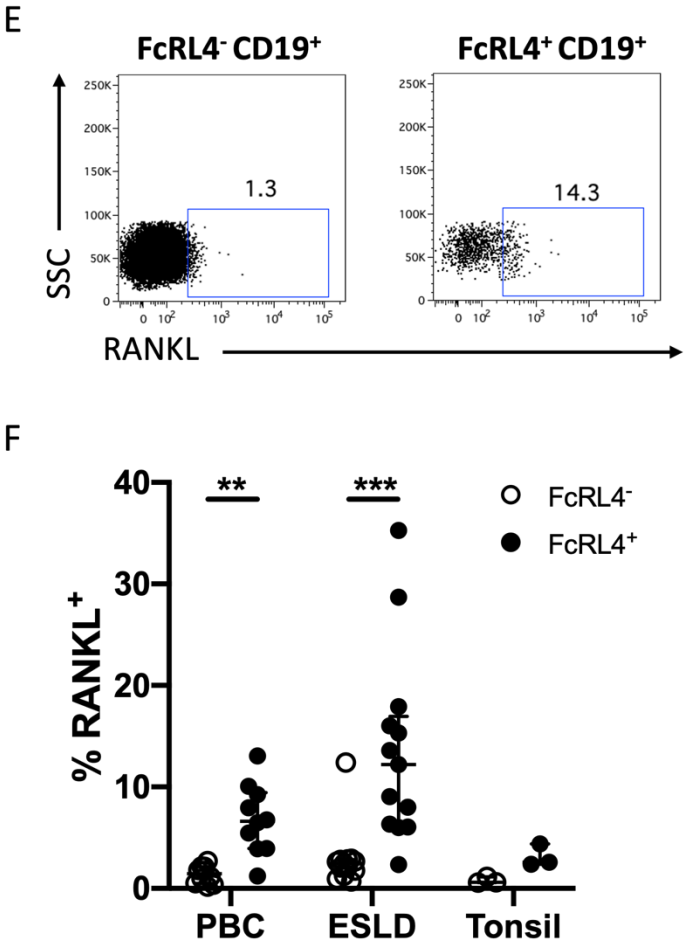


Figure 5.2.4 Co-culture of BECs with FcRL4⁺ B cells. *FcRL4⁺ B cells sorted from the tonsil were incubated with BECs.* ***(A)*** *Viability of BECs after incubation with sorted cells. (n=2).* ***(B)*** *Viability of B cells after incubation with BECs. (n=1).* ***(C)*** *and* ***(D)*** *Microscopy of B cell culture with BECs, orange arrows are lymphocytes, blue arrows indicate BECs.* ***(E)*** *Representative flow plots showing gating of RANKL⁺ cells. Cells were initially gated using gating strategy described in Chapter 3.* ***(F)*** *RANKL expression by FcRL4⁺ and FcRL4⁻ B cells in end-stage livers. Statistics – Wilcoxon matched-pairs signed rank test.*

5.2.4 Antibody production by PBC derived FcRL4$^+$ B cells

In RA, FcRL4$^+$ B cells have been shown to participate in disease pathogenesis through the autoantibody response. PBC derived FcRL4$^+$ B cells were sorted and stimulated to produce antibodies using of simulation cocktail containing CpG, IL-21, anti-CD40, IL-4, with and without BAFF.

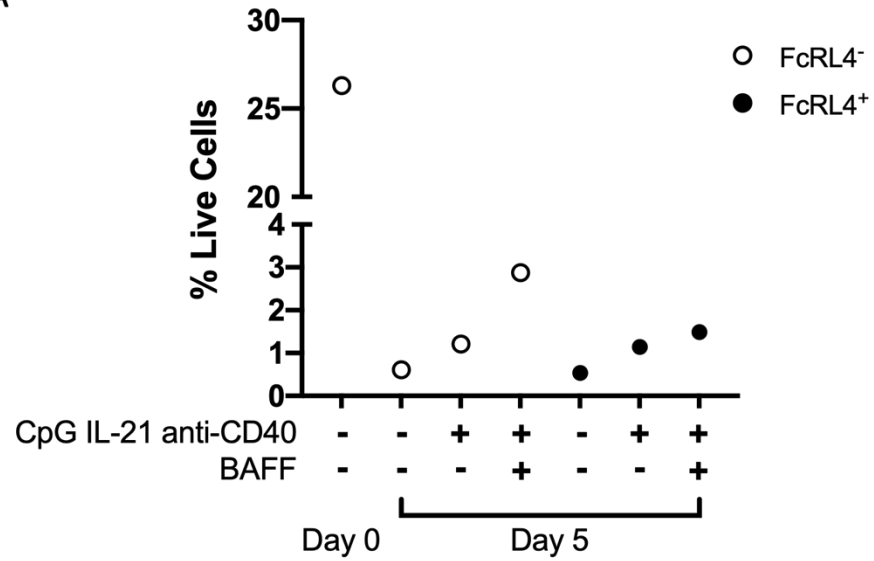
Firstly, tonsil-derived cells were used to assess the protocol and to investigate cell survival in culture. CD19$^+$IgD$^-$FcRL4$^+$ and CD19$^+$IgD$^-$FcRL4$^-$ cells were sorted from human tonsils. Previous culturing experiments showed low survival of FcRL4$^+$ B cells in culture (Figure 5.2.4B) so B-cell-activating factor (BAFF), a B cell survival factor[367] was used to test if its inclusion could improve B cell survival.

Both FcRL4$^+$ and FcRL4$^-$ B cells had better survival after 5 days in culture with the addition of BAFF to the stimulation cocktail (Figure 5.2.5A). Additionally, both IgA and IgG production by FcRL4$^+$ B cells were increased when BAFF was included in the stimulation cocktail. For FcRL4$^-$ B cells, an increase if IgA production was seen after BAFF stimulation, however no difference in IgG production was observed (Figure 5.2.5B).

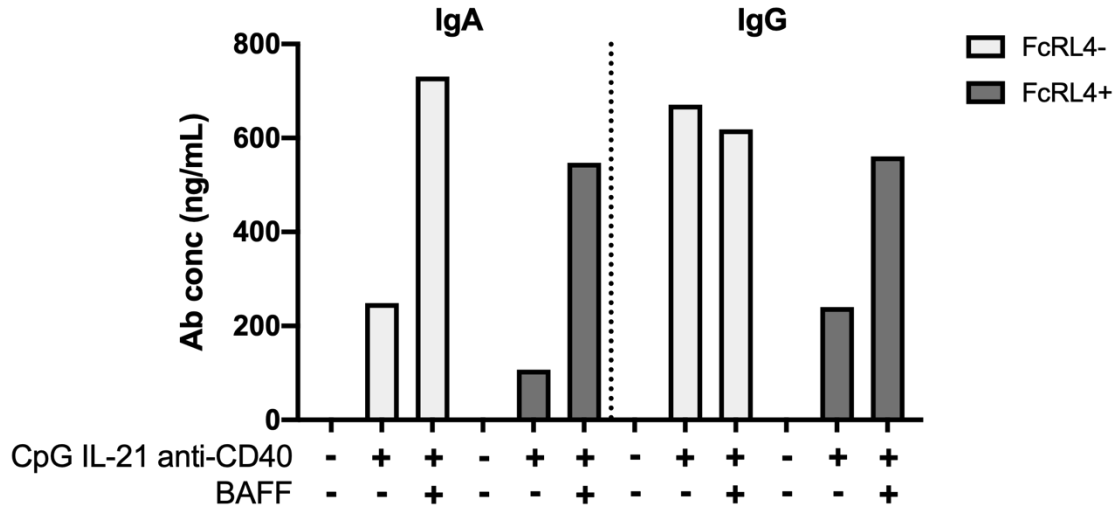
Different culture media were also tested for their effects on B cell survival and antibody production. FcRL4$^+$ B cell viability after 5 days of culture was higher when cultured in R5 media (Figure 5.2.5C) containing additives of HEPES, sodium pyruvate, non-essential amino acids, and β-mercaptoethanol in addition to the FBS, L-glutamine, penicillin, and streptomycin found in cRPMI. The use of R5 media also increased IgA production by FcRL4$^-$ B cells after 5 days of culture, although no difference was seen after 10 days in culture (Figure 5.2.5D).

Subsequently, a stimulation cocktail containing BAFF diluted in R5 media was used to stimulate B cells derived from PBC and PSC livers. Cryopreserved lymphocytes from PBC and PSC patients were sorted for $CD19^{+}IgD^{-}FcRL4^{+}$ and $CD19^{+}IgD^{-}FcRL4^{-}$. $FcRL4^{+}$ B cells isolated from both diseases produced fewer antibodies compared to the $FcRL4^{-}$ B cell population (Figure 5.2.6A-D). Although not statistically significant, B cells from PBC livers showed a trend towards higher IgA antibody production compared to IgG antibody production (Figure 5.2.6A-B). Whereas B cells from PSC livers produced similar levels of IgA and IgG (Figure 5.2.6C-D).

A


% Live Cells
30
25
20
4
3
2
1
0
FcRL4-
FcRL4+
CpG IL-21 anti-CD40 - - + + - + +
BAFF - - - + - - +
Day 0
Day 5

B


IgA
IgG
Ab conc (ng/mL)
800
600
400
200
0
FcRL4-
FcRL4+
CpG IL-21 anti-CD40 - + + - + + - + + - + +
BAFF - - + - - + - - + - - +

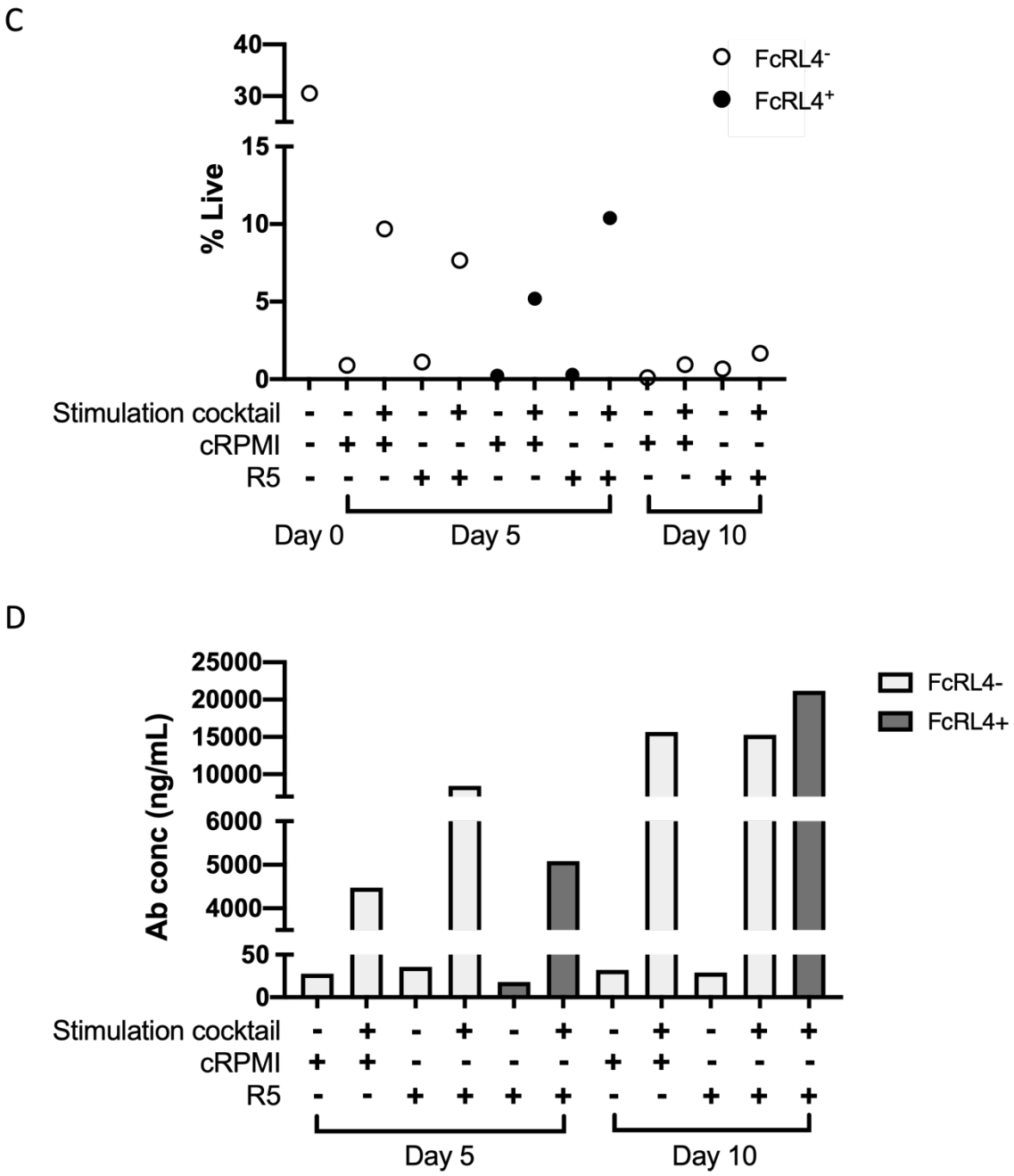


Figure 5.2.5 Antibody production assay development. *$CD19^+IgD^-FcRL4^+$ cells and $CD19^+IgD^-FcRL4^-$ were sorted from frozen tonsil lymphocytes.* ***(A)*** *B cell viability with and without BAFF in stimulation cocktail after 5 days in culture.* ***(B)*** *IgA and IgG production by cells after 5 days of stimulation with and without BAFF. (n=1).* ***(C)*** *B cell viability using either complete RPMI or R5 media after 5 and 10 days in culture.* ***(D)*** *IgA production by B cells after 5 and 10 days in culture in either complete RPMI or R5 media. (n=1).*

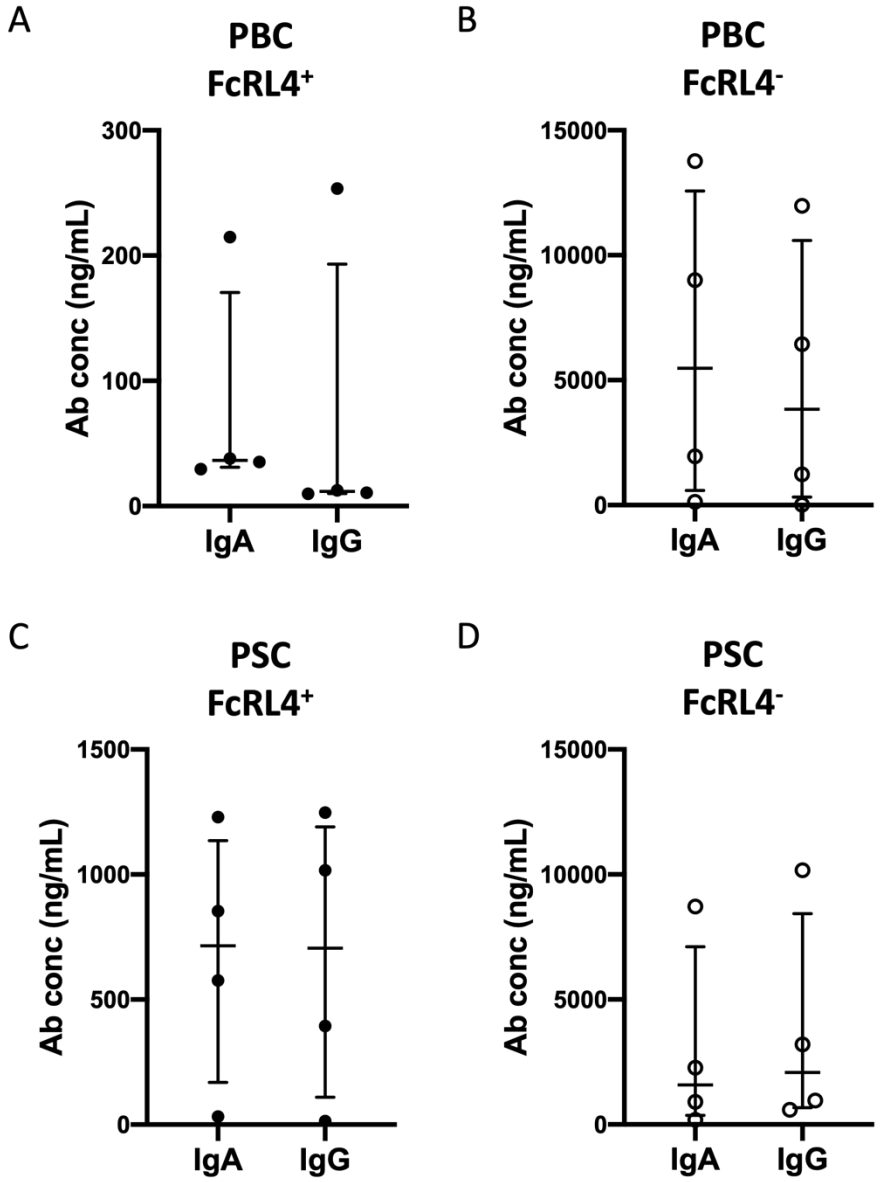


Figure 5.2.6 Antibody production by FcRL4⁺ B cells. *$CD19^{+}IgD^{-}FcRL4^{+}$ and $CD19^{+}IgD^{-}FcRL4^{-}$ B cells were sorted from end-stage PBC and PSC livers and cultured for 7 days in a stimulation cocktail. Antibody concentrations were measured using IgA and IgG ELISAs.* ***(A)*** *and* ***(B)*** *IgA and IgG production by B cells derived from PBC livers.* ***(C)*** *and* ***(D)*** *IgA and IgG production by B cells derived from PSC livers. PBC (n=4), PSC (n=4).*

5.3 Discussion

We hypothesised that FcRL4$^+$ B cells play a role in disease pathogenesis through either the direct killing of BECs, capture of immune complexes, or through the generation of autoantibodies. FcRL4$^+$ B cells can be found near the damaged epithelium in end-stage PBC livers. FcRL4 itself can capture IgA aggregate *in vivo* and *in vitro*, moreover, FcRL4 can capture IgA from patient derived bile. Tonsil derived FcRL4$^+$ B cells do not affect direct killing of BECs *in vitro* over a period of 24 hours. However, these cells do aggregate around the BECs as observed through microscopy. This could be as a result of the interaction between RANKL on the surface of FcRL4$^+$ B cells and RANK on BECs. PBC derived FcRL4$^+$ B cells can be stimulated *ex vivo* to produce antibodies, however the low antibody concentration yielded meant that autoantibody testing could not be carried out.

Co-culture of FcRL4$^+$ B cells and BECs showed that after 24 hours, there was no change in BEC viability. A longer time point for BEC death could be more helpful to elucidate BEC death, along with the use of counting beads to determine a more accurate cell count. FcRL4$^+$ B cell survival over 24 hours is much higher when in the presence of the epithelial cells, suggesting that the assay time point could be extended to better determine if FcRL4$^+$ B cells could be directly killing BECs. There was a slight reduction in BEC viability when culturing with total tonsil cells. This could be due to the presence of cytotoxic T cells or NK cells, as the lymphocytes and BECs derive from different patients, there is likely to be an HLA mismatch.

Additionally, live/dead cell dye was used as an indicator for cell viability in these co-culture assays. This methodology may not account for cells that have committed to apoptosis.

Activated or cleaved caspase 3 staining would have been an improved marker to identify such cells, as it is an early indicator for apoptosis[368].

This co-culture assay was still in the validation stages, so tonsil FcRL4$^+$ B cells were used as tonsils are a plentiful source of FcRL4$^+$ B cells. However, as demonstrated in the previous chapter, there are some phenotypical differences between tonsil derived FcRL4$^+$ B cells and those derived from the PBC liver. Additionally, the BECs used in these assays derived from NASH patients and not PBC patients. Biliary epithelial cells in PBC are thought to contribute to disease as PBC can reoccur after transplantation[300]. The lack of BEC death could be a result of these differences.

Despite the lack of direct BEC killing, microscopy of the co-cultures showed that FcRL4$^+$ B cells homed and aggregated to the BECs, which was not seen in the wells containing FcRL4$^-$ B cells. This direct interaction could be due to the expression of RANKL by FcRL4$^+$ B cells. Previous work has demonstrated that among the infiltrating immune cells in the RA joint, FcRL4$^+$ B cells are the main source of RANKL. RANK is expressed on the surface of BEC[369], thus the RANK/RANKL operon could be a method of interaction between these cells. Indeed, damaged BECs expressed higher levels of RANK leading to the recruitment of RANKL expressing lymphocytes[369], thus potentially exacerbating the immune-mediated damage. Further, expression of RANKL within the PBC liver correlated with stage of disease[369], and could be related to a decrease in bone marrow density and osteoporosis seen in PBC[370]. The use of either an anti-RANKL antibody or the natural decoy ligand for RANK, OPG, could be introduced to the co-culture assay to potentially elucidate the role of this interaction.

Intriguingly RANKL has been implicated in the development of lymph nodes[131,371]. RANKL deficient mice have altered lymphocyte populations and have been found to lack lymph nodes. Therefore, FcRL4$^+$ B cells could contribute to the formation of lymphoid structures in RA[372] and the immune aggregates that are one of the hallmarks of disease in PBC.

Moreover, suppression of the RANK/RANKL pathway in colitis results in a reduction in CD4$^+$CD25$^+$ regulatory T cells thus abolishing the Treg mediated suppression of inflammation[373]. RANKL is expressed by CD4$^+$CD25$^+$ Tregs and RANK is found on DCs[374]. In the PBC liver, RANKL expressing FcRL4$^+$ B cells could compete with regulatory T cells to bind to RANK expressing DCs. This could lead to a reduction in T regulatory cells in PBC, indeed FoxP3 expression in the damaged portal tracts is reduced[375]. Furthermore, spontaneous colitis is observed in a mouse model with increased RANKL and the absence of regulatory T cells, where OPG treatment can reduce colitis[376]. Together, this could indicate that FcRL4$^+$ B cells may be exacerbating inflammation in the bile duct through the expression in RANKL. Although staining for RANK expressing DCs at FcRL4 rich aggregates would be required.

We showed in Chapter 4 that FcRL4$^+$ B cells express the co-stimulatory molecules CD80 and CD86, indicating that they could be antigen presenting cells. Here we demonstrated that FcRL4$^+$ B cells from the PBC liver have IgA bound to their surface. FcRL4 has been shown to preferentially bind to IgA aggregates[122]. These captured complexes could contain the autoantigen. Further experiments need to be carried out to determine whether these aggregates can be internalised by the FcRL4$^+$ B cell and subsequently presented to autoreactive T cells with the help of costimulatory signalling via CD80 and CD86.

Recently, FcRL4 has been suggested to be a receptor for dimeric IgA but not secretory IgA or monomeric IgA[123]. Bile contains both dimeric and sIgA (IgA associated with SC and not associated with SC). However, the majority of bile derived IgA is sIgA (75-95%)[377]. This variability could explain the differences in IgA binding by FcRL4 seen in our assay. Testing is required to determine whether the IgA binding seen by incubating Rajis with bile is due to secretory IgA or systemic IgA.

Previously our group has shown that in RA, FcRL4$^+$ B cells participate in the autoantibody response[129]. FcRL4$^+$ B cells isolated from the RA synovium are reactive to citrullinated antigen, a known antigen in RA. Here, we isolated FcRL4$^+$ B cells from the PBC liver and stimulated them to produce antibodies. Although we were successful in generating both IgG and IgA from these cells, the antibody concentration was too low to test for the presence of AMAs. Improvements in the assay could be made, including increasing the density of the cells and the use of freshly isolated cells instead of cryopreserved cells. Previous data from co-culture assays suggest that B cell viability could be significantly improved with the addition of epithelial cells. Culturing sorted FcRL4$^+$ B cells with a layer of epithelial cells could have increased cell survival in culture and thus increased antibody yield.

In summary, we show that FcRL4$^+$ B cells are nearby to the site of epithelial inflammation in PBC. FcRL4$^+$ B cells isolated from end-stage PBC livers capture IgA complexes. In addition, these cells are able to produce antibodies post stimulation, however it is unclear if these antibodies include AMAs. Further, more work is required to determine where FcRL4$^+$ B cells can induce BEC death.

The experimental work for this chapter was interrupted by the COVID19 pandemic which led to a temporary shutdown of our laboratory and a temporary discontinuation of liver transplantation in PBC patients.

6 DISCUSSION

6.1 Summary

FcRL4^{+} B cells can be identified in immune infiltrates within end-stage PBC livers and are rarely observed within other end-stage liver diseases including PSC, PLD, and NASH. These cells are found near to the biliary epithelium within lymphoepithelial lesions. FcRL4^{+} B cells isolated from end-stage PBC livers are predominantly class-switched memory B cells and enriched for CD21^{+}CD11c^{-} ABCs. The costimulatory molecules CD80 and CD86 are expressed on the surface of these cells suggesting these cells could act as antigen presenting cells. The ability of FcRL4 to bind to IgA aggregates and the location of these cells close to the site of inflammation illustrates that these cells could participate in the autoimmune response. FcRL4^{+} B cells preferentially express IgA as their BCR receptor compared to FcRL4^{-} B cells indicating a mucosal origin. Multiple theories of xenobiotic and molecular mimicry at the onset of PBC involve mucosal inflammation. FcRL4^{+} B cells also express RANKL. RANKL levels have been shown to correlate with increasing stage of disease and could play a role in the osteoporosis observed in some PBC patients. Furthermore, expression of RANKL could allow these cells to directly interact with RANK expressing biliary epithelial cells, thus leading to direct killing.

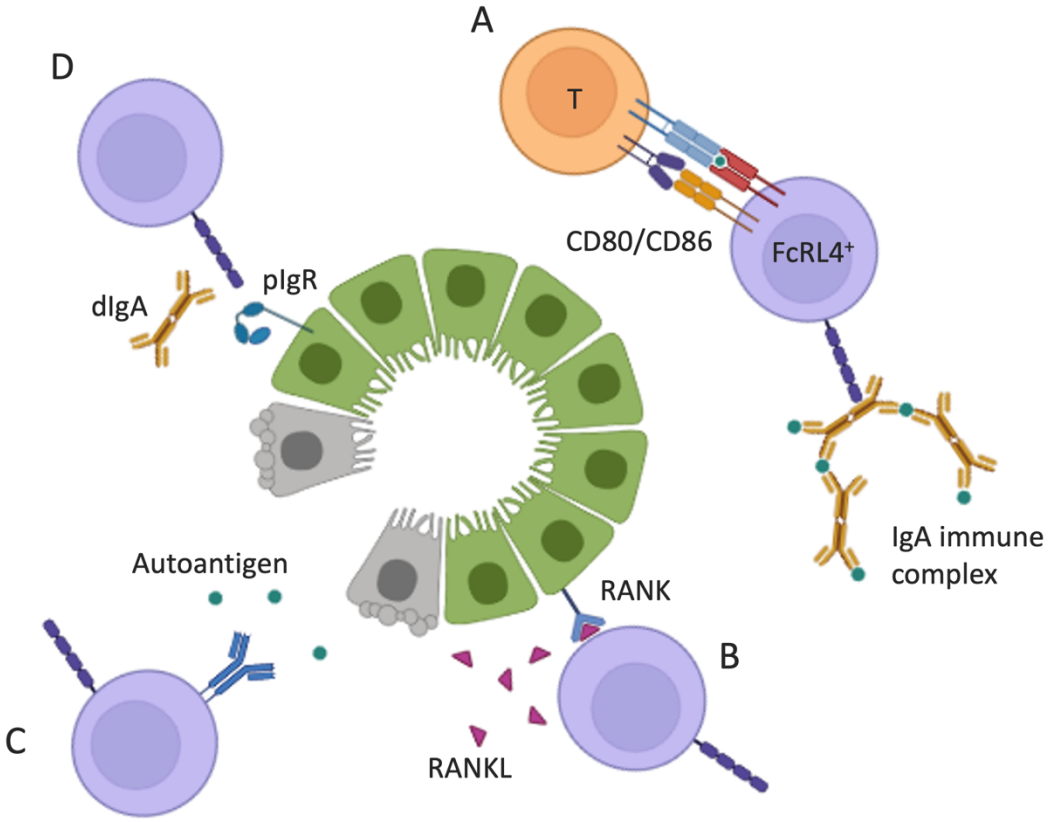


Figure 6.1.1 Potential pathogenic functions of FcRL4 expressing B cells in PBC. *FcRL4⁺ B cells can be found within immune aggregates near damaged biliary epithelium suggesting a pathogenic role for these cells.* ***(A)*** *FcRL4 is a receptor for IgA aggregates. FcRL4⁺ B cells isolated from end-stage PBC livers have IgA captured on their FcRL4 receptor. FcRL4⁺ B cells express the co-stimulatory molecules CD80 and CD86 indicating that these cells can act as antigen presenting cells. Therefore, if FcRL4⁺ B cells can internalise captured IgA immune complexes they could present autoantigen to T cells.* ***(B)*** *PBC derived FcRL4⁺ B cells express RANKL. BECs express RANK, indeed RANK expression is increased in damaged BECs. Direct interaction between FcRL4⁺ B cells and the damaged biliary epithelium could occur through RANK/RANKL binding. RANKL also plays a role in lymph node development, therefore, FcRL4⁺ B cells could contribute to the formation of lymphoid structures in the PBC liver.* ***(C)*** *FcRL4⁺ B cells could contribute to the autoantibody response. The antigen specificity of these cells is still unknown.* ***(D)*** *One possible method by which IgA autoantibodies encounter the autoantigen is through transcytosis of the biliary epithelium. FcRL4 could compete for binding of dimer IgA with pIgR thus acting to dampen the autoantigen response. Therefore, FcRL4 could have an anti-inflammatory role in PBC. Created in BioRender.com*

6.2 FcRL4$^+$ B cells

For both RA and PBC, the prevailing theory on the initiation of disease pathogenesis points at the involvement of the mucosa associated immune response in the breakdown of immune tolerance[242,326,328,330]. For example, smoking is a major risk factor for RA development and inflammatory changes in the lung have been observed before clinical onset of arthritis[326]. Similarly, molecular mimicry from immune responses to gut associated bacteria and environmental xenobiotics have been hypothesised to initiate production of antibodies to the PDC-E2 antigen recognised by the AMA antibodies associated with PBC onset. How this link between mucosal and systemic inflammation works is not yet clearly understood.

FcRL4$^+$ B cells in RA and PBC preferentially express IgA as their BCR and FcRL4 acts as an IgA receptor[129]. Both observations indicate a link to the mucosal immune response. It is possible that these cells were originally activated at the mucosal site where tolerance is lost before migrating to either the liver or joint respectively. This requires further experimental work which was beyond the scope of this project.

FcRL4 expressing B cells were first identified as a subset of memory B cells within the tonsil and Peyer's patches[119]. Subsequently, these cells have been identified in the blood of HIV-infected patients, and within some autoimmune diseases. FcRL4$^+$ B cells within the blood of HIV-infected patients are non-proliferative and express low levels of costimulatory molecules CD80 and CD80[91]. The phenotype of PBC derived FcRL4$^+$ cells resemble that found in other autoimmune illnesses such as RA and pSS more than those found in viral infection.

ABCs were first described in 2011 and have since been linked to a range of autoimmune disorders[100,101,112,113]. These cells appear at an earlier age in autoimmune prone mouse models compared to wild-type mice, implying that they have a role in autoimmune disease development[101], although a functional role for these cells is yet to be determined. In SLE, these cells are thought to be producers of autoantibodies. Here, we showed that FcRL4^{+} B cells were enriched for ABCs. However, there are FcRL4 expressing cells that are not CD11c^{+}/CD21^{Low} and vice versa. It is conceivable but untested that the population of FcRL4^{+} ABCs are pathogenic in disease, and not FcRL4^{+} cells nor FcRL4^{-} ABCs.

The gut microbiota is gradually becoming recognised as a key player in the development of chronic liver diseases like non-alcoholic fatty liver disease, alcoholic liver disease, cirrhosis, and PSC[230,347–349]. Because the liver's primary role is to filter blood from the intestine, it is exposed to bacteria and microbial metabolites. Intestinal permeability can be increased through dysbiosis, allowing bacteria to infiltrate and cause chronic hepatic inflammation and fibrosis. Dysbiosis in the intestine also leads to inflammation in the gut. This could result in the activation or generation of FcRL4^{+} B cells. Although FcRL4^{+} B cells were significantly enriched in PBC livers, small numbers of these cells were also observed in NASH and PSC livers. This suggests that the presence of FcRL4^{+} B cells could simply be an indication of mucosal inflammation.

6.3 Role of FcRL4^{+} B cells in PBC

The role of B cells in PBC pathogenesis is not fully understood. Rituximab treatment was overall ineffective as a treatment for PBC patients who were refractory to UDCA treatment. However, limitations in these studies mean that B cell depletion cannot be ruled entirely

ineffective. All the patients who have participated in these trials are refractory to UDCA treatment. UCDA treatment has been shown to modulate IgM expressed plasmablasts. Failure to respond to UDCA in these patients could be due to an expansion of this subset of cells - rituximab would be ineffective at depleting plasmablasts due to their low expression of CD20. Secondly, rituximab is a very efficient drug in the depletion of peripheral CD20 expressing cells. Although these studies have demonstrated a complete depletion of B cells within the periphery, there is no information on the B cells compartment within the liver and how they have been affected. Serum AMA levels were also measured, and shown to have been reduced post treatment, however local AMA levels were not measured. In other autoimmune diseases, rituximab treatment has been followed by an increase in serum BAFF levels. BAFF is a survival signal produced by macrophages that is required by B cells. The elevation in BAFF levels post the depletion of B cells shows that there is a feedback mechanism between B cells and monocytes. Without a negative signal from B cells, monocytes continue to produce BAFF, which could lead to a rapid repopulation of autoreactive B cells after treatment. Indeed, a randomised control of a combined rituximab-belimumab treatment in SLE patients who are refractory to conventional treatment has shown significant reduction in serum autoantigen and reduced risk of severe flares[378].

Rather encouragingly, however, rituximab treatment in these PBC patients did show some reduction in ALP levels, indicating a small improvement in liver biochemistry. Although a return to baseline ALP levels is seen at 52-week follow-up which could be indicative of the hypothesised repopulation of B cells.

FcRL4 has been proposed to be a receptor for systemic IgA and not sIgA[123]. That is not in agreement with our finding that aggregated colostrum derived IgA does bind to FcRL4. One

of the proposed mechanisms of how autoantibodies encounter the autoantigen is through the transcytosis of IgA by BECs. Intracellular co-localisation of IgA and PDC-E2 can be observed in the biliary epithelium of the PBC liver[265]. Additionally, exposure of Madine-Darby canine kidney cells to IgA-AMA results in apoptosis through increased caspase activity[266]. Binding of secretory IgA by these cells could function to remove these autoantibodies from the liver prior to contact with the autoantigen. FcRL4$^+$ B cells could compete with pIgR expressed by BECs to bind systemic IgA. Thus, these cells could be actively removing IgA autoantibodies from the liver. Clinically the presence of IgA-AMAs correlates with disease progression, suggesting that a failure for these cells to remove IgA AMAs could result in disease progression.

Within mucosal biology, FcRL4$^+$ B cells have been proposed to play a tolerogenic role. Within the tonsil, FcRL4$^+$ cells recognise commensal antigens. Co-engagement of FcRL4 and BCR leads to the inhibition of commensal specific B cell response[124], thus contributing to maintenance of tolerance. From our data, we have shown that FcRL4 binds to IgA within the PBC liver. If these cells recognise the autoantigen, then they could be trying to inhibit the autoantigen response. This would mean that FcRL4$^+$ B cells migrate into immune infiltrates after the biliary epithelium has been damaged and the autoantigen exposed.

In RA, these cells have been shown to produce the proinflammatory cytokine TNF-α, which contradicts the idea that FcRL4$^+$ B cells could be anti-inflammatory. Indeed, within the PBC liver, these cells express the CD80 and CD86 indicating that they could play a role in antigen presentation and activation of T cells. Additionally, FcRL4$^+$ B cells within the RA joint and in the PBC liver produce RANKL. RANKL is responsible for the differentiation of osteoclasts leading to bone erosion. In PBC, serum RANKL levels correlate with disease stage[369] and

could contribute to the development of osteoporosis seen in some PBC patients[370]. RANKL is also required for the development of lymph nodes[131,371], which suggests that it could play a role in maintaining the immune infiltrates which surround the bile ducts in PBC. As epithelial cells can express RANK, there may be a direct effect of RANKL released or expressed on the surface by FcRL4$^+$ B cells.

Although serum AMA is used in diagnosis, a small percentage of PBC patients have no detectable serum AMA. PDC-E2 autoreactive CD4 T cells, on the other hand, were seen in all tested PBC patients, including those who are AMA negative[291]. This suggests that AMA may not be harmful themselves, and that immunopathogenesis is driven by T cell responses to PDC-E2. If FcRL4$^+$ B cells can act as APC, they could therefore be responsible for driving the T cell response.

FcRL4$^+$ B cells are a potential target as a therapy for PBC and other autoimmune diseases. Although we were not able to demonstrate any direct killing of the biliary epithelium by these cells within the PBC liver, their phenotype suggests that they could be contributing to disease progression. Selective depletion of this subset of cells could also alleviate some of the side effects associated with broader B cell therapies such as rituximab.

6.4 Future work and limitations

Although mouse models of both spontaneous and induced PBC show some difference to human PBC, they may be useful in the study of early PBC[379]. FcRL4 is however absent within mice[116], so we were unable to utilise knockout mouse models to determine if these cells are actively promoting damage to the biliary epithelium at disease onset.

Throughout this study "reject donors" were used as a non-disease control group. However, it is not strictly accurate to describe these livers as "healthy". These livers were originally intended to be donated for transplantation, but for unknown reasons have failed to meet the strict criteria for transplantation[380,381]. Subsequently these organs were instead donated to science research. As a result, we have no metadata from these individuals and undiagnosed diseases are possible. Comparisons made between the end-stage liver disease groups and "rejected donors" should consider both the heterogeneity of the group and possibility of undiagnosed liver disease.

Ki67 staining suggested that few B cells were proliferating within the tonsil. Lymphoid follicles within the human tonsil contain 2 distinct zones: the mantle zone and the germinal centre. The mantle zone is populated by memory B cells, while the germinal centre contains both non-proliferating centrocytes and highly proliferative centroblasts[382]. Clonal selection occurs within the germinal centres, the ability of centroblasts to rapidly proliferate plays a central role in this process. Therefore, we expected to see numerous $Ki67^+$ B cells within these tonsil samples. The lack of these cells requires further investigation, for example immunohistochemistry staining of paraffin embedded tonsil sections could be used to validate this finding.

Phenotyping of the FcRL4-expressing cells isolated from the liver indicate that these cells express the co-stimulatory molecules CD80 and CD86. This suggests that $FcRL4^+$ B cells are capable of antigen presentation. Immune infiltrates containing both B cells and T cells can be identified within PBC livers[383], moreover, these infiltrates have been shown to be surrounding bile ducts. Together, this suggests that FcRL4 expressing B cells could act as antigen presenting cells. This question is currently being addressed by a PhD student

exploring FcRL4$^+$ B cells as APC in RA. To investigate the potential ability of FcRL4$^+$ B cells to act as APCs in an autoimmune response, we need to first demonstrate the ability of these cells to internalise the autoantigen. We have identified FcRL4$^+$ B cells close to damaged epithelium where these cells could be exposed to the autoantigen. FcRL4 expressing B cells could bind directly to the autoantigen through their BCR. Through stimulation of antibody production *in vitro*, we were unable to ascertain whether FcRL4$^+$ B cells isolated from PBC livers are autoreactive. Further optimisation of this assay is required to resolve this. Alternatively, autoantigens could be internalised through the FcRL4 receptor. FcRL4 itself is a receptor for IgA aggregates and IgA AMAs are present within the liver of PBC patients[262]. PBC derived FcRL4 expressing cells are observed to have surface bound IgA. Internalisation of FcRL4 after IgA binding could lead to the subsequent presentation of autoantigens. IgA immune complexes with PDC-E2 would need to be generated to test this theory. Co-stimulation assays need to be conducted to investigate which method of internalisation leads to antigen presentation and activation of T cells by FcRL4 expressing B cells. Crosslinking of B cell receptor and FcRL4 by IgA immune complexes combining both auto-antigen and IgA would be another intriguing option. As an inhibitory receptor signalling through the ITIM motif in the intracellular portion of FcRL4 will alter the signalling strength coming through the BCR.

While our studies in RA showed that IgM expression was very rare in FcRL4$^+$ B cells[129], it may be interesting to repeat this experiment in PBC liver B cells as a potential role for IgM has been described in PBC; serum IgM is increased in PBC patients, and IgM$^+$ plasmablasts can be seen in immune infiltrates in the portal tracts[354,355]. UDCA treatment has been shown to

reduce serum IgM levels[356], which suggest that IgM expressing B cells may be pathogenic in PBC.

RANKL has been implicated in disease pathogenesis of PBC. Levels of serum RANKL in PBC correlate with the stage of disease[369]. Surface staining of FcRL4 expressing B cells isolated from PBC livers, shows that these cells express higher levels of RANKL compared to $FcRL4^-$ B cells. Although only a median of 6.6% of liver $FcRL4^+$ B cells express RANKL on their surface (Figure 5.2.4E). Cytokine profiling of PBC derived $FcRL4^+$ B cells or quantification of soluble RANKL levels in PBC liver tissue compared to other end-stage liver diseases is required.

The proximity of $FcRL4^+$ B cells to the damaged epithelium raises the question of whether these cells are causing direct damage to the cholangiocytes. Co-culture assays of FcRL4 expressing B cells and biliary epithelial cells in this thesis were not conclusive. However, since biliary epithelial cells (BEC) from PBC patients were not available, BEC cells from normal donors were used. These may have lacked a necessary trigger which initiates the induction of apoptosis by B cells. Further development of this assay is required. A live/dead cell viability dye was used to determine the viability of BECs after incubation with B cells. Mitochondrial dyes such as JC-1 could be an alternative marker for the detection of cells in early stages of apoptosis or activated caspase 3 can also be used to detect dying cells. Additionally, the release of granzyme B or perforin at the cell-cell interface could demonstrate cytotoxic properties of $FcRL4^+$ B cells.

Within the tonsil, $FcRL4^+$ B cells have been proposed to be tolerogenic[124]. Therefore, CD24 and CD38 staining could be performed to identify if in PBC these cells are regulatory B cells. $CD24^{hi}CD38^{hi}$ immature transitional B cells have been shown to inhibit $CD4^+$ T cells[34]. In RA,

UC, and SLE, changes in numbers and function of these cells have been observed[358–360]. Regulatory B cells produce IL-10 which acts to suppress $CD4^+$ T cells[359]. In PBC, although there is an increase in $CD24^{hi}CD38^{hi}$ B cells in the periphery, these cells produced significantly less IL-10 after stimulation compared to regulatory B cells from healthy individuals[357]. This suggests that in PBC these cells are functionally abnormal and thus lead to a breakdown in tolerance. These cells could be part of the $FcRL4^+$ subset of cells and potentially be a target for therapeutic intervention.

Throughout our sampling of PBC tissue, both in paraffin sections, and in fresh tissue, we saw a large variation in FcRL4 numbers. In paraffin sections, this variation could be explained by the small size of tissue obtained. Intriguingly in PBC, not every small bile duct is affected, which means that it is possible to miss all damaged epithelium in the small area of tissue used for IHC staining. Conversely, one section could also contain epithelium at different stages of destruction, making it possible to visualise the whole course of disease. With fresh tissue digestion, we used mechanical methods to extract infiltrating lymphocytes. We cannot with any certainty declare that all lymphocytes are removed from the tissue. End-stage PBC livers are cirrhotic, which could impact on the efficiency of the tissue digestion protocol.

During this project we were unable to obtain matched samples from patients. pSS and RA are both common comorbidities observed in PBC patients. $FcRL4^+$ B cells have been identified and demonstrated to be pathogenic in both diseases. Matched salivary gland and joint biopsies from PBC patients prior to clinical onset of pSS and RA could determine the role FcRL4 expressing B cells in disease onset. Additionally, matched blood samples from patients could help show the migration of $FcRL4^+$ B cells between inflammatory sites.

One theory for the development of PBC suggests that molecular mimicry leads to the breakdown to tolerance at mucosal sites. FcRL4 expressing B cells in the PBC liver preferentially express IgA indicating that they may originate from mucosal sites, and they are found in tonsils and other mucosal sites such as the gut. Although more work is required to determine their chemokine receptor profile, allowing important clues about the migration between the mucosa and the liver. Additionally, it will be important to test these cells can for cross-reactivity with bacterial derived antigen, which would indicate if these cells were part of the initial breakdown in tolerance.

The autoantigen in PBC is well characterised, and the presence of AMAs is seen in almost all patients. Although we were able to stimulate PBC derived FcRL4^{+} B cells to produce antibodies, further work is required to determine if those antibodies are AMAs. For example, immunoglobulin variable regions can be cloned from single cell sorted PBC derived FcRL4^{+} B cells to generate recombinant antibodies. These can then be tested for specificity against mitochondrial antigen. This method was first used to generate monoclonal antibodies against influenza virus[384] and has subsequently been used to demonstrate that FcRL4^{+} B cells in the RA joint participate in the autoantibody response[129].

7 REFERENCES

1. Cobaleda, C., Schebesta, A., Delogu, A. & Busslinger, M. Pax5: The guardian of B cell identity and function. *Nature Immunology* **8**, 463–470 (2007).
2. Cambier, J. C., Gauld, S. B., Merrell, K. T. & Vilen, B. J. B-cell anergy: From transgenic models to naturally occurring anergic B cells? *Nature Reviews Immunology* **7**, 633–643 (2007).
3. Thomas, M. D., Srivastava, B. & Allman, D. Regulation of peripheral B cell maturation. *Cellular Immunology* **239**, 92–102 (2006).
4. Wardemann, H. *et al.* Predominant autoantibody production by early human B cell precursors. *Science (80-.).* **301**, 1374–1377 (2003).
5. Enders, A. *et al.* Loss of the pro-apoptotic BH3-only Bcl-2 family member Bim inhibits BCR stimulation-induced apoptosis and deletion of autoreactive B cells. *J. Exp. Med.* **198**, 1119–1126 (2003).
6. Melamed, D., Benschop, R. J., Cambier, J. C. & Nemazee, D. Developmental regulation of B lymphocyte immune tolerance compartmentalizes clonal selection from receptor selection. *Cell* **92**, 173–182 (1998).
7. Giltiay, N. V., Chappell, C. P. & Clark, E. A. B-cell selection and the development of autoantibodies. *Arthritis Res. Ther.* **14**, 1–13 (2012).
8. Rathmell, J. C., Townsend, S. E., Xu, J. C., Flavell, R. A. & Goodnow, C. C. Expansion or elimination of B cells in vivo: Dual roles for CD40- and Fas (CD95)-ligands modulated by the B cell antigen receptor. *Cell* **87**, 319–329 (1996).
9. Hervé, M. *et al.* CD40 ligand and MHC class II expression are essential for human peripheral B cell tolerance. *J. Exp. Med.* **204**, 1583–1593 (2007).
10. Cyster, J. G. Chemokines, sphingosine-1-phosphate, and cell migration in secondary lymphoid organs. *Annu. Rev. Immunol.* **23**, 127–159 (2005).
11. Kerfoot, S. M. *et al.* Germinal center B cell and T follicular helper cell development initiates in the interfollicular zone. *Immunity* **34**, 947–960 (2011).
12. Shlomchik, M. J. & Weisel, F. Germinal center selection and the development of

memory B and plasma cells. *Immunol. Rev.* **247**, 52–63 (2012).

13. Zan, H. & Casali, P. Regulation of Aicda expression and AID activity. *Autoimmunity* **46**, 83–101 (2013).

14. Conticello, S. G. The AID/APOBEC family of nucleic acid mutators. *Genome Biol.* **9**, (2008).

15. Muramatsu, M. *et al.* Class switch recombination and hypermutation require activation-induced cytidine deaminase (AID), a potential RNA editing enzyme. *Cell* **102**, 553–563 (2000).

16. Honjo, T., Nagaoka, H., Shinkura, R. & Muramatsu, M. AID to overcome the limitations of genomic information. *Nat. Immunol.* **6**, 655–661 (2005).

17. Peled, J. U. *et al.* The biochemistry of somatic hypermutation. *Annu. Rev. Immunol.* **26**, 481–511 (2008).

18. Storb, U. & Stavnezer, J. Immunoglobulin genes: Generating diversity with AID and UNG. *Curr. Biol.* **12**, (2002).

19. Teng, G. & Papavasiliou, F. N. Immunoglobulin somatic hypermutation. *Annu. Rev. Genet.* **41**, 107–120 (2007).

20. Klein, U. & Dalla-Favera, R. Germinal centres: role in B-cell physiology and malignancy. *Nat. Rev. Immunol. 2008 81* **8**, 22–33 (2008).

21. Nutt, S. L. & Tarlinton, D. M. Germinal center B and follicular helper T cells: Siblings, cousins or just good friends? *Nature Immunology* **12**, 472–477 (2011).

22. Verbeke, C. S., Wenthe, U. & Zentgraf, H. Fas ligand expression in the germinal centre. *J. Pathol.* **189**, 155–160 (1999).

23. Takahashi, Y., Ohta, H. & Takemori, T. Fas is required for clonal selection in germinal centers and the subsequent establishment of the memory B cell repertoire. *Immunity* **14**, 181–192 (2001).

24. Xu, Z., Zan, H., Pone, E. J., Mai, T. & Casali, P. Immunoglobulin class-switch DNA recombination: Induction, targeting and beyond. *Nat. Rev. Immunol.* **12**, 517–531 (2012).

25. Stavnezer, J., Guikema, J. E. J. & Schrader, C. E. Mechanism and regulation of class

switch recombination. *Annu. Rev. Immunol.* **26**, 261–292 (2008).

26. Chaudhuri, J. & Alt, F. W. Class-switch recombination: Interplay of transcription, DNA deamination and DNA repair. *Nature Reviews Immunology* **4**, 541–552 (2004).

27. Bannard, O. *et al.* Germinal Center Centroblasts Transition to a Centrocyte Phenotype According to a Timed Program and Depend on the Dark Zone for Effective Selection. *Immunity* **39**, 1182 (2013).

28. Phan, T. G. *et al.* High affinity germinal center B cells are actively selected into the plasma cell compartment. *J. Exp. Med.* **203**, 2419–2424 (2006).

29. Allen, C. D. C. *et al.* Germinal center dark and light zone organization is mediated by CXCR4 and CXCR5. *Nat. Immunol.* **5**, 943–952 (2004).

30. Wang, Y. & Carter, R. H. CD19 regulates B cell maturation, proliferation, and positive selection in the FDC zone of murine splenic germinal centers. *Immunity* **22**, 749–761 (2005).

31. Camacho, S. A., Kosco-Vilbois, M. H. & Berek, C. The dynamic structure of the germinal center. *Immunol. Today* **19**, 511–514 (1998).

32. Schwickert, T. A. *et al.* In vivo imaging of germinal centres reveals a dynamic open structure. *Nature* **446**, 83–87 (2007).

33. Bemark, M. Translating transitions - how to decipher peripheral human B cell development. *J. Biomed. Res.* **29**, 264–284 (2015).

34. Simon, Q. *et al.* In-depth characterization of CD24highCD38high transitional human B cells reveals different regulatory profiles. *J. Allergy Clin. Immunol.* **137**, 1577-1584.e10 (2016).

35. Sims, G. P. *et al.* Identification and characterization of circulating human transitional B cells. *Blood* **105**, 4390–4398 (2005).

36. Teague, B. N. *et al.* Cutting Edge: Transitional T3 B Cells Do Not Give Rise to Mature B Cells, Have Undergone Selection, and Are Reduced in Murine Lupus. *J. Immunol.* **178**, 7511–7515 (2007).

37. Wirths, S. & Lanzavecchia, A. ABCB1 transporter discriminates human resting naive B cells from cycling transitional and memory B cells. *Eur. J. Immunol.* **35**, 3433–3441

(2005).

38. Palanichamy, A. *et al.* Novel human transitional B cell populations revealed by B cell depletion therapy. *J. Immunol.* **182**, 5982–5993 (2009).

39. Koethe, S. *et al.* Pivotal Advance: CD45RB glycosylation is specifically regulated during human peripheral B cell differentiation. *J. Leukoc. Biol.* **90**, 5–19 (2011).

40. Bemark, M. *et al.* A glycosylation-dependent CD45RB epitope defines previously unacknowledged CD27-IgMhigh B cell subpopulations enriched in young children and after hematopoietic stem cell transplantation. *Clin. Immunol.* **149**, 421–431 (2013).

41. Macallan, D. C. *et al.* B-cell kinetics in humans: Rapid turnover of peripheral blood memory cells. *Blood* **105**, 3633–3640 (2005).

42. Deenen, G. J. & Kroese, F. G. M. Kinetics of peritoneal B-1a cells (CD5 B cells) in young adult mice. *Eur. J. Immunol.* **23**, 12–16 (1993).

43. Kantor, A. B., Stall, A. M., Adams, S., Herzenberg, L. A. & Herzenberg, L. A. Differential development of progenitor activity for three B-cell lineages. *Proc. Natl. Acad. Sci. U. S. A.* **89**, 3320–3324 (1992).

44. KANTOR, A. B., STALL, A. M., ADAMS, S., HERZENBERG, L. A. & HERZENBERG, L. A. Adoptive Transfer of Murine B-Cell Lineages. *Ann. N. Y. Acad. Sci.* **651**, 168–169 (1992).

45. Haas, K. M., Poe, J. C., Steeber, D. A. & Tedder, T. F. B-1a and B-1b cells exhibit distinct developmental requirements and have unique functional roles in innate and adaptive immunity to S. pneumoniae. *Immunity* **23**, 7–18 (2005).

46. Eva Szomolanyi-Tsuda, L., Woodland, R. T., Kishore R Alugupalli, J. M., Gerstein, R. M. & Chen, J. The resolution of relapsing fever borreliosis requires IgM and is concurrent with expansion of B1b lymphocytes. *Am Assoc Immnol* **170**, 3819–3827 (2022).

47. Baumgarth, N. *et al.* B-1 and b-2 cell-derived immunoglobulin m antibodies are nonredundant components of the protective response to influenza virus infection. *J. Exp. Med.* **192**, 271–280 (2000).

48. Rothstein, T. L., Griffin, D. O., Holodick, N. E., Quach, T. D. & Kaku, H. Human B-1 cells take the stage. *Ann. N. Y. Acad. Sci.* **1285**, 97 (2013).

49. Tornberg, U. C. & Holmberg, D. B-1a, B-1b and B-2 B cells display unique V(H)DJ(H) repertoires formed at different stages of ontogeny and under different selection pressures. *EMBO J.* **14**, 1680–1689 (1995).

50. Kantor, A. B., Merrill, C. E., Herzenberg, L. A. & Hillson, J. L. An unbiased analysis of V(H)-D-J(H) sequences from B-1a, B-1b, and conventional B cells. *J. Immunol.* **158**, 1175–86 (1997).

51. Duan, B. & Morel, L. Role of B-1a cells in autoimmunity. *Autoimmun. Rev.* **5**, 403–408 (2006).

52. Kubo, T. *et al.* Augmented TLR9-induced Btk activation in PIR-B-deficient B-1 cells provokes excessive autoantibody production and autoimmunity. *J. Exp. Med.* **206**, 1971–1982 (2009).

53. Duan, B., Croker, B. P. & Morel, L. Lupus resistance is associated with marginal zone abnormalities in an NZM murine model. *Lab. Invest.* **87**, 14–28 (2007).

54. Tumang, J. R., Hastings, W. D., Bai, C. & Rothstein, T. L. Peritoneal and splenic B-1 cells are separable by phenotypic, functional, and transcriptomic characteristics. *Eur. J. Immunol.* **34**, 2158–2167 (2004).

55. Zhong, X. *et al.* A novel subpopulation of B-1 cells is enriched with autoreactivity in normal and lupus-prone mice. *Wiley Online Libr.* **60**, 3734–3743 (2009).

56. Kantor, A. B. & Herzenberg, L. A. Origin of murine B cell lineages. *Annual Review of Immunology* **11**, 501–538 (1993).

57. Lee, J., Kuchen, S., Fischer, R., Chang, S. & Lipsky, P. E. Identification and Characterization of a Human CD5+ Pre-Naive B Cell Population. *J. Immunol.* **182**, 4116–4126 (2009).

58. Casali, P. & Notkins, A. L. Probing the Human B-Cell Repertoire with EBV: Polyreactive Antibodies and CD5+ B Lymphocytes. *http://dx.doi.org/10.1146/annurev.iy.07.040189.002501* **7**, 513–535 (2003).

59. Griffin, D. O., Holodick, N. E. & Rothstein, T. L. Human B1 cells in umbilical cord and adult peripheral blood express the novel phenotype CD20+CD27+CD43+CD70−. *J. Exp. Med.* **208**, 67–80 (2011).

60. Suo, C. *et al.* Mapping the developing human immune system across organs. *Science* **376**, (2022).

61. Rodriguez-Zhurbenko, N., Quach, T. D., Hopkins, T. J., Rothstein, T. L. & Hernandez, A. M. Human B-1 cells and B-1 cell antibodies change with advancing age. *Front. Immunol.* **10**, 483 (2019).

62. Villarreal, L. *et al.* Cutting edge: long-term B cell memory in humans after smallpox vaccination. *Am Assoc Immnol* **171**, 4969–4973 (2003).

63. Yu, X. *et al.* Neutralizing antibodies derived from the B cells of 1918 influenza pandemic survivors. *Nature* **455**, 532–536 (2008).

64. Good, K. L., Avery, D. T. & Tangye, S. G. Resting Human Memory B Cells Are Intrinsically Programmed for Enhanced Survival and Responsiveness to Diverse Stimuli Compared to Naive B Cells. *J. Immunol.* **182**, 890–901 (2009).

65. Bernasconi, N. L., Traggiai, E. & Lanzavecchia, A. Maintenance of serological memory by polyclonal activation of human memory B cells. *Science (80-.).* **298**, 2199–2202 (2002).

66. Seifert, M. *et al.* Functional capacities of human igm memory b cells in early inflammatory responses and secondary germinal center reactions. *Proc. Natl. Acad. Sci. U. S. A.* **112**, E546–E555 (2015).

67. Luo, Y., Yoshihara, A., Oda, K., Ishido, Y. & Suzuki, K. Excessive cytosolic DNA fragments as a potential trigger of graves' disease: An encrypted message sent by animal models. *Front. Endocrinol. (Lausanne).* **7**, (2016).

68. Wienands, J. & Engels, N. Control of memory B cell responses by extrinsic and intrinsic mechanisms. *Immunol. Lett.* **178**, 27–30 (2016).

69. Good, K. L. & Tangye, S. G. Decreased expression of Krüppel-like factors in memory B cells induces the rapid response typical of secondary antibody responses. *Proc. Natl. Acad. Sci. U. S. A.* **104**, 13420–13425 (2007).

70. Bernasconi, N. L., Onai, N. & Lanzavecchia, A. A role for toll-like receptors in acquired immunity: Up-regulation of TLR9 by BCR triggering in naive B cells and constitutive expression in memory B cells. *Blood* **101**, 4500–4504 (2003).

71. Avery, D. T. *et al.* B cell-intrinsic signaling through IL-21 receptor and STAT3 is required for establishing long-lived antibody responses in humans. *J. Exp. Med.* **207**, 155–171 (2010).

72. Yoshida, T. *et al.* Memory B and memory plasma cells. *Immunol. Rev.* **237**, 117–139 (2010).

73. Mcheyzer-Williams, L. J., Milpied, P. J., Okitsu, S. L. & Mcheyzer-Williams, M. G. Class-switched memory B cells remodel BCRs within secondary germinal centers. *Nat. Immunol.* **16**, 296–305 (2015).

74. Dogan, I. *et al.* Multiple layers of B cell memory with different effector functions. *Nat. Immunol.* **10**, 1292–1299 (2009).

75. Sacquin, A., Gador, M. & Fazilleau, N. The strength of BCR signaling shapes terminal development of follicular helper T cells in mice. *Eur. J. Immunol.* **47**, 1295–1304 (2017).

76. Nowosad, C. R., Spillane, K. M. & Tolar, P. Germinal center B cells recognize antigen through a specialized immune synapse architecture. *Nat. Immunol.* **17**, 870–877 (2016).

77. Reddy, V. *et al.* Obinutuzumab induces superior B-cell cytotoxicity to rituximab in rheumatoid arthritis and systemic lupus erythematosus patient samples. *Rheumatology (Oxford).* **56**, 1227 (2017).

78. Leandro, M. J. B-cell subpopulations in humans and their differential susceptibility to depletion with anti-CD20 monoclonal antibodies. *Arthritis Res. Ther.* **15 Suppl 1**, (2013).

79. Cho, A. *et al.* Robust memory responses against influenza vaccination in pemphigus patients previously treated with rituximab. *JCI insight* **2**, (2017).

80. Muto, K. *et al.* Memory B cell resurgence requires repeated rituximab in myasthenia gravis. *Neuromuscul. Disord.* **27**, 918–922 (2017).

81. Odendahl, M. *et al.* Generation of migratory antigen-specific plasma blasts and mobilization of resident plasma cells in a secondary immune response. *Blood* **105**, 1614–1621 (2005).

82. Muehlinghaus, G. *et al.* Regulation of CXCR3 and CXCR4 expression during terminal differentiation of memory B cells into plasma cells. *Blood* **105**, 3965–3971 (2005).

83. Pillai, S., Cariappa, A. & Moran, S. T. Marginal zone B cells. *Annu. Rev. Immunol.* **23**, 161–196 (2005).

84. Garraud, O. *et al.* Revisiting the B-cell compartment in mouse and humans: More than one B-cell subset exists in the marginal zone and beyond. *BMC Immunol.* **13**, (2012).

85. Weill, J. C., Weller, S. & Reynaud, C. A. Human marginal zone B cells. *Annual Review of Immunology* **27**, 267–285 (2009).

86. Descatoire, M. *et al.* Identification of a human splenic marginal zone B cell precursor with NOTCH2-dependent differentiation properties. *J. Exp. Med.* **211**, 987–1000 (2014).

87. Klein, U., Rajewsky, K. & Küppers, R. Human immunoglobulin (Ig)M+IgD+ peripheral blood B cells expressing the CD27 cell surface antigen carry somatically mutated variable region genes: CD27 as a general marker for somatically mutated (memory) B cells. *J. Exp. Med.* **188**, 1679–1689 (1998).

88. Fecteau, J. F., Côté, G. & Néron, S. A New Memory CD27 − IgG + B Cell Population in Peripheral Blood Expressing V H Genes with Low Frequency of Somatic Mutation. *J. Immunol.* **177**, 3728–3736 (2006).

89. Wei, C. *et al.* A New Population of Cells Lacking Expression of CD27 Represents a Notable Component of the B Cell Memory Compartment in Systemic Lupus Erythematosus. *J. Immunol.* **178**, 6624–6633 (2007).

90. Bagnara, D. *et al.* A Reassessment of IgM Memory Subsets in Humans. *J. Immunol.* **195**, 3716–3724 (2015).

91. Moir, S. *et al.* Evidence for HIV-associated B cell exhaustion in a dysfunctional memory B cell compartment in HIV-infected viremic individuals. *J. Exp. Med.* **205**, 1797–1805 (2008).

92. Wu, Y. C. B., Kipling, D. & Dunn-Walters, D. K. The relationship between CD27 negative and positive B cell populations in human peripheral blood. *Front. Immunol.*

2, 81 (2011).

93. Sanz, I. *et al.* Challenges and opportunities for consistent classification of human b cell and plasma cell populations. *Front. Immunol.* **10**, 2458 (2019).

94. Jenks, S. A. *et al.* Distinct Effector B Cells Induced by Unregulated Toll-like Receptor 7 Contribute to Pathogenic Responses in Systemic Lupus Erythematosus. *Immunity* **49**, 725-739.e6 (2018).

95. Ehrhardt, G. R. A. *et al.* Expression of the immunoregulatory molecule FcRH4 defines a distinctive tissue-based population of memory B cells. **202**, 783 (2005).

96. Jenks, S. A. *et al.* Distinct effector B-cells induced by unregulated Toll-like receptor 7 contribute to pathogenic responses in Systemic Lupus Erythematosus. *Immunity* **49**, 725 (2018).

97. Fraussen, J. *et al.* Phenotypic and Ig Repertoire Analyses Indicate a Common Origin of IgD − CD27 − Double Negative B Cells in Healthy Individuals and Multiple Sclerosis Patients . *J. Immunol.* **203**, 1650–1664 (2019).

98. Mahmood, Z. *et al.* CD27-IgD- memory B cells are modulated by in vivo interleukin-6 receptor (IL-6R) blockade in rheumatoid arthritis. *Arthritis Res. Ther.* **17**, 1–11 (2015).

99. Schrezenmeier, E., Jayne, D. & Dörner, T. Targeting B cells and plasma cells in glomerular diseases: Translational perspectives. *Journal of the American Society of Nephrology* **29**, 741–758 (2018).

100. Wang, S. *et al.* IL-21 drives expansion and plasma cell differentiation of autoreactive CD11c hi T-bet + B cells in SLE. *Nat. Commun.* **9**, (2018).

101. Rubtsov, A. V. *et al.* Toll-like receptor 7 (TLR7)–driven accumulation of a novel CD11c+ B-cell population is important for the development of autoimmunity. *Blood* **118**, 1305–1315 (2011).

102. Cancro, M. P. Age-Associated B Cells. *Annu. Rev. Immunol.* **38**, 315–340 (2020).

103. Karnell, J. L. *et al.* Role of CD11c+ T-bet+ B cells in human health and disease. *Cell. Immunol.* **321**, 40–45 (2017).

104. Rubtsov, A. V., Marrack, P. & Rubtsova, K. T-bet expressing B cells - Novel target for autoimmune therapies? *Cell. Immunol.* **321**, 35–39 (2017).

105. Du, S. W., Arkatkar, T., Jacobs, H. M., Rawlings, D. J. & Jackson, S. W. Generation of functional murine CD11c + age-associated B cells in the absence of B cell T-bet expression. *Eur. J. Immunol.* **49**, 170–178 (2019).

106. Johnson, J. L. *et al.* The Transcription Factor T-bet Resolves Memory B Cell Subsets with Distinct Tissue Distributions and Antibody Specificities in Mice and Humans. *Immunity* **52**, 842-855.e6 (2020).

107. Kenderes, K. J. *et al.* T-Bet + IgM Memory Cells Generate Multi-lineage Effector B Cells. *Cell Rep.* **24**, 824-837.e3 (2018).

108. Hao, Y., O'Neill, P., Naradikian, M. S., Scholz, J. L. & Cancro, M. P. A B-cell subset uniquely responsive to innate stimuli accumulates in aged mice. *Blood* **118**, 1294–1304 (2011).

109. Riley, R. L., Khomtchouk, K. & Blomberg, B. B. Age-associated B cells (ABC) inhibit B lymphopoiesis and alter antibody repertoires in old age. *Cell. Immunol.* **321**, 61–67 (2017).

110. Ratliff, M., Alter, S., Frasca, D., Blomberg, B. B. & Riley, R. L. In senescence, age-associated B cells secrete TNFα and inhibit survival of B-cell precursors. *Aging Cell* **12**, 303–311 (2013).

111. Wang, Z. *et al.* T-bet-Expressing B Cells Are Positively Associated with Crohn's Disease Activity and Support Th1 Inflammation. *DNA Cell Biol.* **35**, 628–635 (2016).

112. Claes, N. *et al.* Age-Associated B Cells with Proinflammatory Characteristics Are Expanded in a Proportion of Multiple Sclerosis Patients. *J. Immunol.* **197**, 4576–4583 (2016).

113. Saadoun, D. *et al.* Expansion of autoreactive unresponsive CD21-/low B cells in sjögren's syndrome-associated lymphoproliferation. *Arthritis Rheum.* **65**, 1085–1096 (2013).

114. Weiss, G. E. *et al.* Atypical Memory B Cells Are Greatly Expanded in Individuals Living in a Malaria-Endemic Area. *J. Immunol.* **183**, (2009).

115. Domeier, P. P. *et al.* IFN-γ receptor and STAT1 signaling in B cells are central to spontaneous germinal center formation and autoimmunity. *J. Exp. Med.* **213**, 715–

732 (2016).

116. Li, F. J. *et al.* Emerging roles for the FCRL family members in lymphocyte biology and disease. *Curr. Top. Microbiol. Immunol.* **382**, 29–50 (2014).

117. Hatzivassiliou, G. *et al.* IRTA1 and IRTA2, novel immunoglobulin superfamily receptors expressed in B cells and involved in chromosome 1q21 abnormalities in B cell malignancy. *Immunity* **14**, 277–289 (2001).

118. Miller, I., Hatzivassiliou, G., Cattoretti, G., Mendelsohn, C. & Dalla-Favera, R. IRTAs: A new family of immunoglobulinlike receptors differentially expressed in B cells. *Blood* **99**, 2662–2669 (2002).

119. Falini, B. *et al.* Expression of the IRTA1 receptor identifies intraepithelial and subepithelial marginal zone B cells of the mucosa-associated lymphoid tissue (MALT). *Blood* **102**, 3684–3692 (2003).

120. Ehrhardt, G. R. A. *et al.* The inhibitory potential of Fc receptor homolog 4 on memory B cells. *Proc. Natl. Acad. Sci. U. S. A.* **100**, 13489–94 (2003).

121. Siewe, B., Nipper, A. J., Sohn, H., Stapleton, J. T. & Landay, A. FcRL4 expression identifies a pro-inflammatory B cell subset in viremic HIV-infected subjects. *Front. Immunol.* **8**, 1339 (2017).

122. Wilson, T. J., Fuchs, A. & Colonna, M. Human FcRL4 and FcRL5 are receptors for IgA and IgG. *J. Immunol.* **188**, 4741 (2012).

123. Liu, Y. *et al.* FCRL4 Is an Fc Receptor for Systemic IgA, but Not Mucosal Secretory IgA. *J. Immunol.* **205**, 533–538 (2020).

124. Liu, Y. *et al.* Antibodies encoded by FCRL4-bearing memory B cells preferentially recognize commensal microbial antigens. *J. Immunol.* **200**, 3962 (2018).

125. Ehrhardt, G. R. A. & Cooper, M. D. Immunoregulatory roles for fc receptor-like molecules. *Curr. Top. Microbiol. Immunol.* **350**, 89–104 (2011).

126. Tolnay, M. Lymphocytes sense antibodies through human FCRL proteins: Emerging roles in mucosal immunity. *J. Leukoc. Biol.* **111**, 477–487 (2022).

127. Yeo, L. *et al.* Cytokine mRNA profiling identifies B cells as a major source of RANKL in rheumatoid arthritis. *Ann. Rheum. Dis.* **70**, 2022–2028 (2011).

128. Yeo, L. *et al.* Expression of FcRL4 defines a pro-inflammatory, RANKL-producing B cell subset in rheumatoid arthritis. *Ann. Rheum. Dis.* **74**, 928–935 (2015).

129. Amara, K. *et al.* B cells expressing the IgA receptor FcRL4 participate in the autoimmune response in patients with rheumatoid arthritis. *J. Autoimmun.* **81**, 34–43 (2017).

130. Haacke, E. A. *et al.* FcRL4 + B-cells in salivary glands of primary Sjögren's syndrome patients. *J. Autoimmun.* **81**, 90–98 (2017).

131. Penninger, J. M. *et al.* OPGL is a key regulator of osteoclastogenesis, lymphocyte development and lymph-node organogenesis. *Nature* **397**, 315–323 (1999).

132. Chervonsky, A. V. Microbiota and autoimmunity. *Cold Spring Harb. Perspect. Biol.* **5**, a007294 (2013).

133. Rosenstein, E. D., Greenwald, R. A., Kushner, L. J. & Weissmann, G. Hypothesis: The Humoral Immune Response to Oral Bacteria Provides a Stimulus for the Development of Rheumatoid Arthritis. *Inflammation* **28**, 311–318 (2004).

134. Catrina, A. I., Ytterberg, A. J., Reynisdottir, G., Malmström, V. & Klareskog, L. Lungs, joints and immunity against citrullinated proteins in rheumatoid arthritis. *Nat. Rev. Rheumatol.* **10**, 645–653 (2014).

135. Verstappen, G. M. *et al.* Gene expression profiling of epithelium-associated FcRL4+ B cells in primary Sjögren's syndrome reveals a pathogenic signature. *J. Autoimmun.* 102439 (2020). doi:10.1016/j.jaut.2020.102439

136. Cuello, C. *et al.* Chemokine expression and leucocyte infiltration in Sjögren's syndrome. *Br. J. Rheumatol.* **37**, 779–783 (1998).

137. Verstappen, G. M. *et al.* B Cell Depletion Therapy Normalizes Circulating Follicular Th Cells in Primary Sjögren Syndrome. *J. Rheumatol.* **44**, 49–58 (2017).

138. Cesta, M. F. Normal Structure, Function, and Histology of Mucosa-Associated Lymphoid Tissue. *Toxicol. Pathol.* **34**, 599–608 (2006).

139. Kogame, T., Kabashima, K. & Egawa, G. Putative Immunological Functions of Inducible Skin-Associated Lymphoid Tissue in the Context of Mucosa-Associated Lymphoid Tissue. *Frontiers in Immunology* **12**, 3387 (2021).

140. Pabst, R. The anatomical basis for the immune function of the gut. *Anat. Embryol. 1987 1762* **176**, 135–144 (1987).

141. Strober, W., Murray, P. J., Kitani, A. & Watanabe, T. Signalling pathways and molecular interactions of NOD1 and NOD2. *Nature Reviews Immunology* **6**, 9–20 (2006).

142. Akira, S., Takeda, K. & Kaisho, T. Toll-like receptors: Critical proteins linking innate and acquired immunity. *Nature Immunology* **2**, 675–680 (2001).

143. Swamy, M., Jamora, C., Havran, W. & Hayday, A. Epithelial decision makers: In search of the 'epimmunome'. *Nature Immunology* **11**, 656–665 (2010).

144. Owyang, A. M. *et al.* Interleukin 25 regulates type 2 cytokine-dependent immunity and limits chronic inflammation in the gastrointestinal tract. *J. Exp. Med.* **203**, 843–849 (2006).

145. Schottelius, A. J. G. & Baldwin, A. S. A role for transcription factor NF-kB in intestinal inflammation. *Int. J. Color. Dis. 1999 141* **14**, 18–28 (1999).

146. Byrne, B. *et al.* Human duodenal epithelial cells constitutively express molecular components of antigen presentation but not costimulatory molecules. *Hum. Immunol.* **63**, 977–986 (2002).

147. Cruickshank, S. M., McVay, L. D., Baumgart, D. C., Felsburg, P. J. & Carding, S. R. Colonic epithelial cell mediated suppression of CD4 T cell activation. *Gut* **53**, 678–684 (2004).

148. Niess, J. H. *et al.* CX3CR1-mediated dendritic cell access to the intestinal lumen and bacterial clearance. *Science (80-.).* **307**, 254–258 (2005).

149. Johansson-Lindbom, B. *et al.* Functional specialization of gut CD103+ dendritic cells in the regulation of tissue-selective T cell homing. *J. Exp. Med.* **202**, 1063–1073 (2005).

150. Makita, S. *et al.* Intestinal Lamina Propria Retaining CD4+CD25+ Regulatory T Cells Is A Suppressive Site of Intestinal Inflammation. *J. Immunol.* **178**, 4937–4946 (2007).

151. Reboldi, A. & Cyster, J. G. Peyer's patches: organizing B-cell responses at the intestinal frontier. *Immunol. Rev.* **271**, 230–245 (2016).

152. Bemark, M., Boysen, P. & Lycke, N. Y. Induction of gut IgA production through T cell-

dependent and T cell-independent pathways. *Ann. N. Y. Acad. Sci.* **1247**, 97–116 (2012).

153. Kuhn, K. A., Pedraza, I. & Demoruelle, M. K. Mucosal immune responses to microbiota in the development of autoimmune disease. *Rheum. Dis. Clin. North Am.* **40**, 711–725 (2014).

154. Brandtzaeg, P. *et al.* The B-cell system of human mucosae and exocrine glands. *Immunol. Rev.* **171**, 45–87 (1999).

155. Brandtzaeg, P., Kiyono, H., Pabst, R. & Russell, M. W. Terminology: nomenclature of mucosa-associated lymphoid tissue. *Mucosal Immunol.* **1**, 31–37 (2008).

156. Farache, J. *et al.* Luminal bacteria recruit CD103+ dendritic cells into the intestinal epithelium to sample bacterial antigens for presentation. *Immunity* **38**, 581–595 (2013).

157. Reboldi, A. *et al.* IgA production requires B cell interaction with subepithelial dendritic cells in Peyer's patches. *Science* **352**, (2016).

158. Pabst, O. New concepts in the generation and functions of IgA. *Nat. Rev. Immunol.* **12**, 821–832 (2012).

159. Cao, A. T. *et al.* Interleukin (IL)-21 promotes intestinal IgA response to microbiota. *Mucosal Immunol.* **8**, 1072 (2015).

160. Ferrari, S. *et al.* Mutations of CD40 gene cause an autosomal recessive form of immunodeficiency with hyper IgM. *Proc. Natl. Acad. Sci. U. S. A.* **98**, 12614–12619 (2001).

161. Bergqvist, P., Gärdby, E., Stensson, A., Bemark, M. & Lycke, N. Y. Gut IgA class switch recombination in the absence of CD40 does not occur in the lamina propria and is independent of germinal centers. *J. Immunol.* **177**, 7772–7783 (2006).

162. Sakurai, D. *et al.* TACI regulates IgA production by APRIL in collaboration with HSPG. *Blood* **109**, 2961–2967 (2007).

163. Mestecky, J., Russell, M. W., Jackson, S. & Brown, T. A. The human IgA system: a reassessment. *Clin. Immunol. Immunopathol.* **40**, 105–114 (1986).

164. Steffen, U. *et al.* IgA subclasses have different effector functions associated with

distinct glycosylation profiles. *Nat. Commun.* **11**, 1–12 (2020).

165. Mantis, N. J., Rol, N. & Corthésy, B. Secretory IgA's complex roles in immunity and mucosal homeostasis in the gut. *Mucosal Immunol.* **4**, 603–611 (2011).

166. Wright, A., Lamm, M. E. & Huang, Y. T. Excretion of human immunodeficiency virus type 1 through polarized epithelium by immunoglobulin A. *J. Virol.* **82**, 11526–11535 (2008).

167. Robinson, J. K., Blanchard, T. G., Levine, A. D., Emancipator, S. N. & Lamm, M. E. A mucosal IgA-mediated excretory immune system in vivo. *J. Immunol.* **166**, 3688–3692 (2001).

168. Aleyd, E., Heineke, M. H. & van Egmond, M. The era of the immunoglobulin A Fc receptor FcαRI; its function and potential as target in disease. *Immunol. Rev.* **268**, 123–138 (2015).

169. Smith, P. D. *et al.* Intestinal macrophages lack CD14 and CD89 and consequently are down-regulated for LPS- and IgA-mediated activities. *J. Immunol.* **167**, 2651–2656 (2001).

170. Blank, U., Launay, P., Benhamou, M. & Monteiro, R. C. Inhibitory ITAMs as novel regulators of immunity. *Immunol. Rev.* **232**, 59–71 (2009).

171. Van Egmond, M. *et al.* FcalphaRI-positive liver Kupffer cells: reappraisal of the function of immunoglobulin A in immunity. *Nat. Med.* **6**, 680–685 (2000).

172. Weisbart, R. H., Kacena, A., Schuh, A. & Golde, D. W. GM-CSF induces human neutrophil IgA-mediated phagocytosis by an IgA Fc receptor activation mechanism. *Nature* **332**, 647–648 (1988).

173. Sheth, K. & Bankey, P. The liver as an immune organ. *Curr. Opin. Crit. Care* **7**, 99–104 (2001).

174. Trefts, E., Gannon, M. & Wasserman, D. H. The liver. *Curr. Biol.* **27**, R1147 (2017).

175. Reshetnyak, V. I. Physiological and molecular biochemical mechanisms of bile formation. *World J. Gastroenterol.* **19**, 7341 (2013).

176. Michalopoulos, G. K. Liver Regeneration. *J. Cell. Physiol.* **213**, 286 (2007).

177. Fox, E. S., Thomas, P. & Broitman, S. A. Comparative studies of endotoxin uptake by

isolated rat Kupffer and peritoneal cells. *Infect. Immun.* **55**, 2962 (1987).

178. Rappaport, A. M., Borowy, Z. J., Lougheed, W. M. & Lotto, W. N. Subdivision of hexagonal liver lobules into a structural and functional unit. Role in hepatic physiology and pathology. *Anat. Rec.* **119**, 11–33 (1954).

179. Fraser, R., Dobbs, B. R. & Rogers, G. W. T. Lipoproteins and the liver sieve: The role of the fenestrated sinusoidal endothelium in lipoprotein metabolism, atherosclerosis, and cirrhosis. *Hepatology* **21**, 863–874 (1995).

180. Braet, F. *et al.* Comparative atomic force and scanning electron microscopy: an investigation on fenestrated endothelial cells in vitro. *J. Microsc.* **181**, 10–17 (1996).

181. Crawford, J. M. *et al.* Imaging biliary lipid secretion in the rat: ultrastructural evidence for vesiculation of the hepatocyte canalicular membrane. (1995). doi:10.1016/S0022-2275(20)39199-9

182. Boyer, J. L. Bile Formation and Secretion. *Compr. Physiol.* **3**, 1035–1078 (2013).

183. Hundt, M., Basit, H. & John, S. Physiology, Bile Secretion. *StatPearls* (2021).

184. Wang, L. & Boyer, J. L. The maintenance and generation of membrane polarity in hepatocytes. *Hepatology* **39**, 892–899 (2004).

185. Roskams, T. A. *et al.* Nomenclature of the finer branches of the biliary tree: Canals, ductules, and ductular reactions in human livers. *Hepatology* **39**, 1739–1745 (2004).

186. Banales, J. M. *et al.* Cholangiocyte pathobiology. *Nat. Rev. Gastroenterol. Hepatol. 2019 165* **16**, 269–281 (2019).

187. Chuang, Y. H., Lan, R. Y. & Eric Gershwin, M. The immunopathology of human biliary cell epithelium. *Semin. Immunopathol.* **31**, 323–331 (2009).

188. Russell, M. W., Kilian, M., Mantis, N. J. & Corthésy, B. Biological Activities of IgA. *Mucosal Immunol. Fourth Ed.* **1**–**2**, 429–454 (2015).

189. Stadtmueller, B. M. *et al.* The structure and dynamics of secretory component and its interactions with polymeric immunoglobulins. *Elife* **5**, (2016).

190. Ishibashi, H., Nakamura, M., Komori, A., Migita, K. & Shimoda, S. Liver architecture, cell function, and disease. *Semin. Immunopathol.* **31**, 399–409 (2009).

191. Valdivia, L. A. *et al.* DENDRITIC CELL REPLACEMENT IN LONG-SURVIVING LIVER AND CARDIAC XENOGRAFTS. *Transplantation* **56**, 482 (1993).

192. Prickett, T. C., McKenzie, J. L. & Hart, D. N. J. Characterization of interstitial dendritic cells in human liver. *Transplantation* **46**, 754–761 (1988).

193. Norris, S. *et al.* Resident human hepatic lymphocytes are phenotypically different from circulating lymphocytes. *J. Hepatol.* **28**, 84–90 (1998).

194. Exley, M. A. & Koziel, M. J. To be or not to be NKT: natural killer T cells in the liver. *Hepatology* **40**, 1033–1040 (2004).

195. Emoto, M. *et al.* Participation of leukocyte function-associated antigen-1 and NK cells in the homing of thymic CD8 + NKT cells to the liver. doi:10.1002/1521-4141

196. Knolle, P. A. *et al.* Induction of cytokine production in naive CD4(+) T cells by antigen-presenting murine liver sinusoidal endothelial cells but failure to induce differentiation toward Th1 cells. *Gastroenterology* **116**, 1428–1440 (1999).

197. Lohse, A. W. *et al.* Antigen-presenting function and B7 expression of murine sinusoidal endothelial cells and Kupffer cells. *Gastroenterology* **110**, 1175–1181 (1996).

198. Steffan, A. -M, Gendrault, J. -L, McCuskey, R. S., McCuskey, P. A. & Kirn, A. Phagocytosis, an unrecognized property of murine endothelial liver cells. *Hepatology* **6**, 830–836 (1986).

199. Racanelli, V. & Rehermann, B. The liver as an immunological organ. *Hepatology* **43**, S54–S62 (2006).

200. Holz, L. E., Warren, A., Le Couteur, D. G., Bowen, D. G. & Bertolino, P. CD8+ T cell tolerance following antigen recognition on hepatocytes. *J. Autoimmun.* **34**, 15–22 (2010).

201. Kita, H., Mackay, I. R., Van de Water, J. & Gershwin, M. E. The lymphoid liver: Considerations on pathways to autoimmune injury. *Gastroenterology* **120**, 1485–1501 (2001).

202. Calne, R. Y. *et al.* Induction of immunological tolerance by porcine liver allografts. *Nature* **223**, 472–476 (1969).

203. Horst, A. K., Neumann, K., Diehl, L. & Tiegs, G. Modulation of liver tolerance by conventional and nonconventional antigen-presenting cells and regulatory immune cells. *Cell. Mol. Immunol. 2016 133* **13**, 277–292 (2016).

204. Xia, S. *et al.* Hepatic microenvironment programs hematopoietic progenitor differentiation into regulatory dendritic cells, maintaining liver tolerance. *Blood* **112**, 3175–3185 (2008).

205. Cederbom, L., Hall, H. & Ivars, F. CD4 + CD25 + regulatory T cells down-regulate co-stimulatory molecules on antigen-presenting cells. doi:10.1002/1521-4141

206. Morelli, A. E. & Thomson, A. W. Tolerogenic dendritic cells and the quest for transplant tolerance. *Nat. Rev. Immunol. 2007 78* **7**, 610–621 (2007).

207. Crispe, I. N. Hepatic T cells and liver tolerance. *Nat. Rev. Immunol. 2003 31* **3**, 51–62 (2003).

208. Zhang, M., Xu, S., Han, Y. & Cao, X. Apoptotic cells attenuate fulminant hepatitis by priming Kupffer cells to produce interleukin-10 through membrane-bound TGF-β. *Hepatology* **53**, 306–316 (2011).

209. Crispe, I. N. Immune Tolerance in Liver Disease. *Hepatology* **60**, 2109 (2014).

210. Ke, W., Kryczek, I., Chen, L., Zou, W. & Welling, T. H. Kupffer cell suppression of CD8+ T cells in human hepatocellular carcinoma is mediated by B7-H1/programmed death-1 interactions. *Cancer Res.* **69**, 8067–8075 (2009).

211. Dillon, P. W., Belchis, D., Minnick, K. & Tracy, T. Differential Expression of the Major Histocompatibility Antigens and ICAM-1 on Bile Duct Epithelial Cells in Biliary Atresia. *Tohoku J. Exp. Med.* **181**, 33–40 (1997).

212. Leon, M. P. *et al.* Immunogenicity of biliary epithelium: investigation of antigen presentation to CD4+ T cells. *Hepatology* **24**, 561–567 (1996).

213. Ronca, V. *et al.* Immune system and cholangiocytes: A puzzling affair in primary biliary cholangitis. *Journal of Leukocyte Biology* **108**, 659–671 (2020).

214. Takeda, K. *et al.* Death receptor 5 mediated-apoptosis contributes to cholestatic liver disease. *Proc. Natl. Acad. Sci. U. S. A.* **105**, 10895–10900 (2008).

215. Mataki, N. *et al.* Expression of PD-1, PD-L1, and PD-L2 in the liver in autoimmune liver

diseases. *Am. J. Gastroenterol.* **102**, 302–312 (2007).

216. Ahn, S. *et al.* Programmed cell death ligand-1 (PD-L1) expression in extrahepatic biliary tract cancers: a comparative study using 22C3, SP263 and E1L3N anti-PD-L1 antibodies. *Histopathology* **75**, 526–536 (2019).

217. Angulo, P. *et al.* Liver Fibrosis, but no Other Histologic Features, Associates with Long-term Outcomes of Patients With Nonalcoholic Fatty Liver Disease. *Gastroenterology* **149**, 389 (2015).

218. Liu, K. & McCaughan, G. W. Epidemiology and Etiologic Associations of Non-alcoholic Fatty Liver Disease and Associated HCC. *Adv. Exp. Med. Biol.* **1061**, 3–18 (2018).

219. Thomas, L. V., Ockhuizen, T. & Suzuki, K. Exploring the influence of the gut microbiota and probiotics on health: a symposium report. *Br. J. Nutr.* **112 Suppl 1**, (2014).

220. Miele, L. *et al.* Increased intestinal permeability and tight junction alterations in nonalcoholic fatty liver disease. *Hepatology* **49**, 1877–1887 (2009).

221. Walenbergh, S. M. A., Koek, G. H., Bieghs, V. & Shiri-Sverdlov, R. Non-alcoholic steatohepatitis: The role of oxidized low-density lipoproteins. *J. Hepatol.* **58**, 801–810 (2013).

222. Cnossen, W. R. & Drenth, J. P. H. Polycystic liver disease: an overview of pathogenesis, clinical manifestations and management. *Orphanet J. Rare Dis.* **9**, 69 (2014).

223. Abu-Wasel, B., Walsh, C., Keough, V. & Molinari, M. Pathophysiology, epidemiology, classification and treatment options for polycystic liver diseases. *World J. Gastroenterol.* **19**, 5775–5786 (2013).

224. van Keimpema, L. *et al.* Lanreotide reduces the volume of polycystic liver: a randomized, double-blind, placebo-controlled trial. *Gastroenterology* **137**, (2009).

225. Hogan, M. C. *et al.* Randomized clinical trial of long-acting somatostatin for autosomal dominant polycystic kidney and liver disease. *J. Am. Soc. Nephrol.* **21**, 1052–1061 (2010).

226. Neijenhuis, M. K. *et al.* Impact of liver volume on polycystic liver disease-related symptoms and quality of life. *United Eur. Gastroenterol. J.* **6**, 81–88 (2018).

227. Bernts, L. H. P., Drenth, J. P. H. & Tjwa, E. T. T. L. Management of portal hypertension and ascites in polycystic liver disease. *Liver Int.* **39**, 2024–2033 (2019).

228. Zhang, Z. Y., Wang, Z. M. & Huang, Y. Polycystic liver disease: Classification, diagnosis, treatment process, and clinical management. *World J. Hepatol.* **12**, 72 (2020).

229. Chapman, M. H. *et al.* British Society of Gastroenterology and UK-PSC guidelines for the diagnosis and management of primary sclerosing cholangitis. *Gut* **68**, 1356 (2019).

230. Kummen, M. *et al.* The gut microbial profile in patients with primary sclerosing cholangitis is distinct from patients with ulcerative colitis without biliary disease and healthy controls. *Gut* **66**, 611–619 (2017).

231. Lindor, K. D. *et al.* Primary biliary cirrhosis. *Hepatology* **50**, 291–308 (2009).

232. Poupon, R. E. *et al.* Combined analysis of randomized controlled trials of ursodeoxycholic acid in primary biliary cirrhosis. *Gastroenterology* **113**, 884–890 (1997).

233. Tanaka, A. Current understanding of primary biliary cholangitis. *Clin. Mol. Hepatol.* **27**, 1 (2021).

234. Hirschfield, G. M. *et al.* The British Society of Gastroenterology/UK-PBC primary biliary cholangitis treatment and management guidelines. *Gut* **67**, 1568–1594 (2018).

235. Tanaka, A., Leung, P. S. C. & Gershwin, M. E. Evolution of our understanding of PBC. *Best Pract. Res. Clin. Gastroenterol.* **34**–**35**, 3–9 (2018).

236. Hirschfield, G. M. *et al.* EASL Clinical Practice Guidelines: The diagnosis and management of patients with primary biliary cholangitis. *J. Hepatol.* **67**, 145–172 (2017).

237. Ter Borg, P. C. J., Schalm, S. W., Hansen, B. E. & Van Buuren, H. R. Prognosis of ursodeoxycholic acid-treated patients with primary biliary cirrhosis. Results of a 10-yr cohort study involving 297 patients. *Am. J. Gastroenterol.* **101**, 2044–2050 (2006).

238. Kamihira, T. *et al.* Distinct costimulation dependent and independent autoreactive T-cell clones in primary biliary cirrhosis. *Gastroenterology* **125**, 1379–1387 (2003).

239. Kamihira, T. *et al.* Biliary epithelial cells regulate autoreactive T cells: Implications for biliary-specific diseases. *Hepatology* **41**, 151–159 (2005).

240. Shigematsu, H. *et al.* Fine specificity of T cells reactive to human PDC-E2 163-176 peptide, the immunodominant autoantigen in primary biliary cirrhosis: implications for molecular mimicry and cross-recognition among mitochondrial autoantigens. *Hepatology* **32**, 901–909 (2000).

241. Shimoda, S. *et al.* Autoreactive T-cell responses in primary biliary cirrhosis are proinflammatory whereas those of controls are regulatory. *Gastroenterology* **131**, 606–618 (2006).

242. Shimoda, S. *et al.* Mimicry peptides of human PDC-E2 163-176 peptide, the immunodominant T-cell epitope of primary biliary cirrhosis. *Hepatology* **31**, 1212–1216 (2000).

243. Van De Water, J., Gershwin, M. E., Leung, P., Ansari, A. & Coppel, R. L. The autoepitope of the 74-kD mitochondrial autoantigen of primary biliary cirrhosis corresponds to the functional site of dihydrolipoamide acetyltransferase. *J. Exp. Med.* **167**, 1791–1799 (1988).

244. Klatskin, G. & Kantor, F. S. Mitochondrial antibody in primary biliary cirrhosis and other diseases. *Ann. Intern. Med.* **77**, 533–541 (1972).

245. Tsuneyama, K. *et al.* Abnormal expression of the E2 component of the pyruvate dehydrogenase complex on the luminal surface of biliary epithelium occurs before major histocompatibility complex class II and BB1/B7 expression. *Hepatology* **21**, 1031–1037 (1995).

246. Dubel, L. *et al.* Autoepitope mapping and reactivity of autoantibodies to the dihydrolipoamide dehydrogenase-binding protein (E3BP) and the glycine cleavage proteins in primary biliary cirrhosis. *Hepatology* **29**, 1013–1018 (1999).

247. Palmer, J. M., Jones, D. E. J., Quinn, J., McHugh, A. & Yeaman, S. J. Characterization of the autoantibody responses to recombinant E3 binding protein (protein X) of pyruvate dehydrogenase in primary biliary cirrhosis. *Hepatology* **30**, 21–26 (1999).

248. Quinn, J., Diamond, A. & Palmer, J. Lipoylated and unlipoylated domains of human PDC-E2 as autoantigens in primary biliary cirrhosis: significance of lipoate attachment. *Hepatology* **18**, 1384–1391 (1993).

249. Bruggraber, S. F. A. *et al.* Autoreactivity to lipoate and a conjugated form of lipoate in

primary biliary cirrhosis. *Gastroenterology* **125**, 1705–1713 (2003).

250. Leung, P. S. C. *et al.* Autoantibodies to BCOADC-E2 in patients with primary biliary cirrhosis recognize a conformational epitope. *Hepatology* **22**, 505–513 (1995).

251. Moteki, S. *et al.* Epitope mapping and reactivity of autoantibodies to the E2 component of 2-oxoglutarate dehydrogenase complex in primary biliary cirrhosis using recombinant 2-oxoglutarate dehydrogenase complex. *Hepatology* **23**, 436–444 (1996).

252. Surh, C. D., Coppel, R. & Gershwin, M. E. Structural requirement for autoreactivity on human pyruvate dehydrogenase-E2, the major autoantigen of primary biliary cirrhosis. Implication for a conformational autoepitope. *J. Immunol.* **144**, (1990).

253. Metcalf, J. V. *et al.* Natural history of early primary biliary cirrhosis. *Lancet (London, England)* **348**, 1399–1402 (1996).

254. Nakamura, M. *et al.* Peripheral B lymphocyte repertoire to mitochondrial antigen in primary biliary cirrhosis--positive correlation between the disease activity and the frequency of circulating B lymphocytes specific for pyruvate dehydrogenase complex. *Autoimmunity* **21**, 253–262 (1995).

255. Takahashi, T. *et al.* Plasma cells and the chronic nonsuppurative destructive cholangitis of primary biliary cirrhosis. *Hepatology* **55**, 846–855 (2012).

256. Chung, B. K. *et al.* Phenotyping and auto-antibody production by liver-infiltrating B cells in primary sclerosing cholangitis and primary biliary cholangitis. *J. Autoimmun.* **77**, 45–54 (2017).

257. Klein, R., Wiebel, M., Engelhart, S. & Berg, P. A. Sera from patients with tuberculosis recognize the M2a-epitope (E2-subunit of pyruvate dehydrogenase) specific for primary biliary cirrhosis. *Clin. Exp. Immunol.* **92**, 308–316 (1993).

258. Epstein, O., Thomas, H. C. & Sherlock, S. Primary biliary cirrhosis is a dry gland syndrome with features of chronic graft-versus-host disease. *Lancet (London, England)* **1**, 1166–1168 (1980).

259. Tsuneyama, K. *et al.* Primary biliary cirrhosis an epithelitis: evidence of abnormal salivary gland immunohistochemistry. *Autoimmunity* **26**, 23–31 (1997).

260. Tsuneyama, K. *et al.* Human combinatorial autoantibodies and mouse monoclonal antibodies to PDC-E2 produce abnormal apical staining of salivary glands in patients with coexistent primary biliary cirrhosis and Sjögren's syndrome. *Hepatology* **20**, 893–898 (1994).

261. Reynoso-Paz, S. *et al.* Evidence for a locally driven mucosal response and the presence of mitochondrial antigens in saliva in primary biliary cirrhosis. *Hepatology* **31**, 24–29 (2000).

262. Nishio, A. *et al.* Comparative studies of antimitochondrial autoantibodies in sera and bile in primary biliary cirrhosis. *Hepatology* **25**, 1085–1089 (1997).

263. HANSEN, B. U. *et al.* Clinical and immunological features of Sjögren's syndrome in patients with primary biliary cirrhosis with emphasis on focal sialadenitis. *Acta Med. Scand.* **224**, 611–619 (1988).

264. Mazanec, M. B., Kaetzel, C. S., Lamm, M. E., Fletcher, D. & Nedrud, J. G. Intracellular neutralization of virus by immunoglobulin A antibodies. *Proc. Natl. Acad. Sci. U. S. A.* **89**, 6901 (1992).

265. Malmborg, A. C. *et al.* Penetration and co-localization in MDCK cell mitochondria of IgA derived from patients with primary biliary cirrhosis. *J. Autoimmun.* **11**, 573–580 (1998).

266. Matsumura, S. *et al.* Caspase induction by IgA antimitochondrial antibody: IgA-mediated biliary injury in primary biliary cirrhosis. *Hepatology* **39**, 1415–1422 (2004).

267. Teoh, K. -L *et al.* Enzyme inhibitory autoantibodies to pyruvate dehydrogenase complex in primary biliary cirrhosis: Applications of a semiautomated assay. *Hepatology* **20**, 1220–1224 (1994).

268. Hollingsworth, K. G. *et al.* Pilot Study of Peripheral Muscle Function in Primary Biliary Cirrhosis: Potential Implications for Fatigue Pathogenesis. *Clin. Gastroenterol. Hepatol.* **6**, 1041–1048 (2008).

269. Jopson, L. & Jones, D. E. J. Fatigue in Primary Biliary Cirrhosis: Prevalence, Pathogenesis and Management. *Dig. Dis.* **33 Suppl 2**, 109–114 (2015).

270. Kingham, J. G. C., Goldblatt, J. & Jones, D. E. J. Discussion on the true impact of

fatigue in primary biliary cirrhosis: A population study [1] (multiple letters). *Gastroenterology* **124**, 582 (2003).

271. Devauchelle-Pensec, V. *et al.* Effects of rituximab therapy on quality of life in patients with primary Sjögren's syndrome. *Clin. Exp. Rheumatol.* **29**, 6–12 (2011).

272. Meijer, J. M. *et al.* Effectiveness of rituximab treatment in primary sjögren's syndrome: A randomized, double-blind, placebo-controlled trial. *Arthritis Rheum.* **62**, 960–968 (2010).

273. Rigby, W. *et al.* Effect of rituximab on physical function and quality of life in patients with rheumatoid arthritis previously untreated with methotrexate. *Arthritis Care Res. (Hoboken).* **63**, 711–720 (2011).

274. Fluge, Ø. *et al.* Benefit from B-Lymphocyte Depletion Using the Anti-CD20 Antibody Rituximab in Chronic Fatigue Syndrome. A Double-Blind and Placebo-Controlled Study. *PLoS One* **6**, e26358 (2011).

275. Myers, R. P., Swain, M. G., Lee, S. S., Shaheen, A. A. M. & Burak, K. W. B-Cell Depletion With Rituximab in Patients With Primary Biliary Cirrhosis Refractory to Ursodeoxycholic Acid. *Am. J. Gastroenterol.* **108**, 933–941 (2013).

276. Tsuda, M. *et al.* Biochemical and immunologic effects of rituximab in patients with primary biliary cirrhosis and an incomplete response to ursodeoxycholic acid. *Hepatology* **55**, 512–521 (2012).

277. Khanna, A. *et al.* Rituximab Is Ineffective for Treatment of Fatigue in Primary Biliary Cholangitis: A Phase 2 Randomized Controlled Trial. *Hepatology* **70**, 1646–1657 (2019).

278. Jopson, L. *et al.* RITPBC: B-cell depleting therapy (rituximab) as a treatment for fatigue in primary biliary cirrhosis: study protocol for a randomised controlled trial. *BMJ Open* **5**, e007985 (2015).

279. Nakamura, M. *et al.* Anti-gp210 and anti-centromere antibodies are different risk factors for the progression of primary biliary cirrhosis. *Hepatology* **45**, 118–127 (2007).

280. Wesierska-Gadek, J. *et al.* Correlation of initial autoantibody profile and clinical

outcome in primary biliary cirrhosis. *Hepatology* **43**, 1135–1144 (2006).

281. Tan, Y. *et al.* Clonal Characteristics of Circulating B Lymphocyte Repertoire in Primary Biliary Cholangitis. *J. Immunol.* **197**, 1609–1620 (2016).

282. Jiang, N. *et al.* Lineage structure of the human antibody repertoire in response to influenza vaccination. *Sci. Transl. Med.* **5**, (2013).

283. European Association for the Study of the Liver. EASL Clinical Practice Guidelines: management of cholestatic liver diseases. *J. Hepatol.* **51**, 237–267 (2009).

284. Lammers, W. J. *et al.* Levels of alkaline phosphatase and bilirubin are surrogate end points of outcomes of patients with primary biliary cirrhosis: an international follow-up study. *Gastroenterology* **147**, 1338-1349.e5 (2014).

285. Li, Y. *et al.* Chemokine (C-X-C motif) ligand 13 promotes intrahepatic chemokine (C-X-C motif) receptor 5+ lymphocyte homing and aberrant B-cell immune responses in primary biliary cirrhosis. *Hepatology* **61**, 1998–2007 (2015).

286. Cichoż-Lach, H. *et al.* Deviations in Peripheral Blood Cell Populations are Associated with the Stage of Primary Biliary Cholangitis and Presence of Itching. *Arch. Immunol. Ther. Exp. (Warsz).* **66**, 443–452 (2018).

287. Jang, J. S. *et al.* Single-cell mass cytometry on peripheral blood identifies immune cell subsets associated with primary biliary cholangitis. *Sci. Rep.* **10**, (2020).

288. O'Neill, S. K. *et al.* Antigen-Specific B Cells Are Required as APCs and Autoantibody-Producing Cells for Induction of Severe Autoimmune Arthritis. *J. Immunol.* **174**, 3781–3788 (2005).

289. Kikuchi, K. *et al.* Bacterial CpG induces hyper-IgM production in CD27+ memory B cells in primary biliary cirrhosis. *Gastroenterology* **128**, 304–312 (2005).

290. Myers, R. P., Swain, M. G., Lee, S. S., Shaheen, A. A. M. & Burak, K. W. B-Cell Depletion With Rituximab in Patients With Primary Biliary Cirrhosis Refractory to Ursodeoxycholic Acid. *Am. J. Gastroenterol.* **108**, 933–941 (2013).

291. Shimoda, S. *et al.* CD4 T-cell autoreactivity to the mitochondrial autoantigen PDC-E2 in AMA-negative primary biliary cirrhosis. *J. Autoimmun.* **31**, 110–115 (2008).

292. Kita, H. *et al.* Quantitative and functional analysis of PDC-E2–specific autoreactive

cytotoxic T lymphocytes in primary biliary cirrhosis. *J. Clin. Invest.* **109**, 1231–1240 (2002).

293. Yang, G. X. *et al.* Adoptive transfer of CD8+ T cells from transforming growth factor beta receptor type II (dominant negative form) induces autoimmune cholangitis in mice. *Hepatology* **47**, 1974–1982 (2008).

294. Lan, R. Y. *et al.* Liver-targeted and peripheral blood alterations of regulatory T cells in primary biliary cirrhosis. *Hepatology* **43**, 729–737 (2006).

295. Fehérvari, Z. & Sakaguchi, S. CD4+ Tregs and immune control. *J. Clin. Invest.* **114**, 1209–1217 (2004).

296. Wang, L. *et al.* CXCR5+ CD4+ T follicular helper cells participate in the pathogenesis of primary biliary cirrhosis. *Hepatology* **61**, 627–638 (2015).

297. Yong, L. *et al.* Expanded circulating peripheral helper T cells in primary biliary cholangitis: Tph cells in PBC. *Mol. Immunol.* **131**, 44–50 (2021).

298. Rao, D. A. *et al.* Pathologically expanded peripheral T helper cell subset drives B cells in rheumatoid arthritis. *Nat. 2017 5427639* **542**, 110–114 (2017).

299. Makiyama, A. *et al.* Expanded circulating peripheral helper T cells in systemic lupus erythematosus: association with disease activity and B cell differentiation. *Rheumatology* **58**, 1861–1869 (2019).

300. Van De Water, J. *et al.* Immunohistochemical evidence of disease recurrence after liver transplantation for primary biliary cirrhosis. *Hepatology* **24**, 1079–1084 (1996).

301. Lleo, A. *et al.* Apotopes and the biliary specificity of primary biliary cirrhosis. *Hepatology* **49**, 871–879 (2009).

302. Odin, J. A., Huebert, R. C., Casciola-Rosen, L., LaRusso, N. F. & Rosen, A. Bcl-2-dependent oxidation of pyruvate dehydrogenase-E2, a primary biliary cirrhosis autoantigen, during apoptosis. *J. Clin. Invest.* **108**, 223–232 (2001).

303. Charlotte, F. *et al.* Immunohistochemical detection of bcl-2 protein in normal and pathological human liver. *Am. J. Pathol.* **144**, 460 (1994).

304. Rong, G. *et al.* Epithelial Cell Specificity and Apotope Recognition by Serum Autoantibodies in Primary Biliary Cirrhosis. *Hepatology* **54**, 196 (2011).

305. Lleo, A. *et al.* Biliary apotopes and anti-mitochondrial antibodies activate innate immune responses in primary biliary cirrhosis. *Hepatology* **52**, 987–998 (2010).

306. Koga, H., Sakisaka, S., Ohishi, M., Sata, M. & Tanikawa, K. Nuclear DNA fragmentation and expression of Bcl-2 in primary biliary cirrhosis. *Hepatology* **25**, 1077–1084 (1997).

307. Mells, G. F. *et al.* Genome-wide association study identifies 12 new susceptibility loci for primary biliary cirrhosis. *Nat. Genet.* **43**, 329–332 (2011).

308. Liu, X. *et al.* Genome-wide meta-analyses identify three loci associated with primary biliary cirrhosis. *nature.com*

309. Liu, J. Z. *et al.* Dense fine-mapping study identifies new susceptibility loci for primary biliary cirrhosis. *Nat. Genet.* **44**, 1137–1141 (2012).

310. Kawashima, M., Hitomi, Y., … Y. A.-H. molecular & 2017, U. Genome-wide association studies identify PRKCB as a novel genetic susceptibility locus for primary biliary cholangitis in the Japanese population. *academic.oup.com*

311. Juran, B. D. *et al.* Immunochip analyses identify a novel risk locus for primary biliary cirrhosis at 13q14, multiple independent associations at four established risk loci and epistasis between 1p31 and 7q32 risk Variants. *Hum. Mol. Genet.* **21**, 5209–5221 (2012).

312. Hirschfield, G. M. *et al.* Association of primary biliary cirrhosis with variants in the CLEC16A, SOCS1, SPIB and SIAE immunomodulatory genes. *Genes Immun.* **13**, 328–335 (2012).

313. Hirschfield, G. M. *et al.* Primary Biliary Cirrhosis Associated with HLA, IL12A, and IL12RB2 Variants . *N. Engl. J. Med.* **360**, 2544–2555 (2009).

314. Libert, C., Dejager, L. & Pinheiro, I. The X chromosome in immune functions: when a chromosome makes the difference. *Nat. Rev. Immunol. 2010 108* **10**, 594–604 (2010).

315. Invernizzi, P. *et al.* Frequency of monosomy X in women with primary biliary cirrhosis. *Lancet* **363**, 533–535 (2004).

316. Selmi, C. *et al.* Genome-wide analysis of DNA methylation, copy number variation, and gene expression in monozygotic twins discordant for primary biliary cirrhosis. *Front. Immunol.* **5**, 128 (2014).

317. Lleo, A. *et al.* DNA methylation profiling of the X chromosome reveals an aberrant demethylation on CXCR3 promoter in primary biliary cirrhosis. *Clin. Epigenetics* **7**, (2015).

318. Lacotte, S., Brun, S., Muller, S. & Dumortier, H. CXCR3, Inflammation, and Autoimmune Diseases. *Ann. N. Y. Acad. Sci.* **1173**, 310–317 (2009).

319. Groom, J. R. & Luster, A. D. CXCR3 in T cell function. *Exp. Cell Res.* **317**, 620 (2011).

320. Chuang, Y. H. *et al.* Increased levels of chemokine receptor CXCR3 and chemokines IP-10 and MIG in patients with primary biliary cirrhosis and their first degree relatives. *J. Autoimmun.* **25**, 126–132 (2005).

321. Elgueta, R. *et al.* Molecular mechanism and function of CD40/CD40L engagement in the immune system. *Immunol. Rev.* **229**, 152–172 (2009).

322. Pessach, I. M. & Notarangelo, L. D. X-linked primary immunodeficiencies as a bridge to better understandingX-chromosome related autoimmunity. *J. Autoimmun.* **33**, 17–24 (2009).

323. Conley, M. E. *et al.* Hyper IgM syndrome associated with defective CD40-mediated B cell activation. *J. Clin. Invest.* **94**, 1404 (1994).

324. Lleo, A. *et al.* Immunoglobulin M levels inversely correlate with CD40 ligand promoter methylation in patients with primary biliary cirrhosis. *Hepatology* **55**, 153–160 (2012).

325. Hu, Z. *et al.* β-Arrestin 1 modulates functions of autoimmune T cells from primary biliary cirrhosis patients. *J. Clin. Immunol.* **31**, 346–355 (2011).

326. Sparks, J. A. *et al.* Associations of smoking and age with inflammatory joint signs among first-degree relatives without rheumatoid arthritis: Results from the Studies of the Etiology of RA. *Arthritis Rheumatol. (Hoboken, N.J.)* **68**, 1828 (2016).

327. Burroughs, A. K., Butler, P., Sternberg, M. J. E. & Baum, H. Molecular mimicry in liver disease [13]. *Nature* **358**, 377–378 (1992).

328. Shimoda, S. *et al.* Identification and precursor frequency analysis of a common T cell epitope motif in mitochondrial autoantigens in primary biliary cirrhosis. *J. Clin. Invest.* **102**, 1831–1840 (1998).

329. Yang, Y. *et al.* E. coli and the etiology of human PBC: Antimitochondrial antibodies

and spreading determinants. *Hepatology* **75**, 266–279 (2022).

330. Selmi, C. *et al.* Patients with primary biliary cirrhosis react against a ubiquitous xenobiotic-metabolizing bacterium. *Hepatology* **38**, 1250–1257 (2003).

331. Mattner, J. *et al.* Liver Autoimmunity Triggered by Microbial Activation of Natural Killer T Cells. *Cell Host Microbe* **3**, 304–315 (2008).

332. Gershwin, M. E. *et al.* Risk factors and comorbidities in primary biliary cirrhosis: A controlled interview-based study of 1032 patients. *Hepatology* **42**, 1194–1202 (2005).

333. Prince, M. I. *et al.* The geographical distribution of primary biliary cirrhosis in a well-defined cohort. *Elsevier* **34**, 1083–1088 (2001).

334. McNally, R. J. Q., James, P. W., Ducker, S., Norman, P. D. & James, O. F. W. No Rise in Incidence but Geographical Heterogeneity in the Occurrence of Primary Biliary Cirrhosis in North East England. *Am. J. Epidemiol.* **179**, 492–498 (2014).

335. Ala, A. *et al.* Increased prevalence of primary biliary cirrhosis near Superfund toxic waste sites. *Wiley Online Libr.* **43**, 525–531 (2006).

336. Rieger, R. *et al.* Identification of 2-nonynoic acid, a cosmetic component, as a potential trigger of primary biliary cirrhosis. *J. Autoimmun.* **27**, 7–16 (2006).

337. Mikio Zeniya, G. *et al.* Additive, 2-Octynoic Acid Food Common Environmental, Cosmetic, and Identification of Antibodies against a Autoantigens in Primary Biliary Cirrhosis: Chemical Xenobiotics and Mitochondrial. *J Immunol Ref.* **174**, 5874–5883 (2022).

338. Prieto, J., Banales, J. M. & Medina, J. F. Primary biliary cholangitis: pathogenic mechanisms. *Curr. Opin. Gastroenterol.* **37**, 91 (2021).

339. Warren, K. W., Athanassiades, S. & Monge, J. I. Primary sclerosing cholangitis. A study of forty-two cases. *Am. J. Surg.* **111**, 23–38 (1966).

340. Thorpe, M. E., Scheuer, P. J. & Sherlock, S. Primary sclerosing cholangitis, the biliary tree, and ulcerative colitis. *Gut* **8**, 435–448 (1967).

341. Whiteside, T. L., Lasky, S., Si, L. & van Thiel, D. H. Immunologic analysis of mononuclear cells in liver tissues and blood of patients with primary sclerosing cholangitis. *Hepatology* **5**, 468–474 (1985).

342. Ponsioen, C. Y. *et al.* Immunohistochemical analysis of inflammation in primary sclerosing cholangitis. *Eur. J. Gastroenterol. Hepatol.* **11**, 769–774 (1999).

343. Everson, G. T. *et al.* Polycystic liver disease: quantitation of parenchymal and cyst volumes from computed tomography images and clinical correlates of hepatic cysts. *Hepatology* **8**, 1627–1634 (1988).

344. Parés, A. *et al.* Long-term effects of ursodeoxycholic acid in primary biliary cirrhosis: results of a double-blind controlled multicentric trial. UDCA-Cooperative Group from the Spanish Association for the Study of the Liver. *J. Hepatol.* **32**, 561–566 (2000).

345. Kikuchi, K. *et al.* Ursodeoxycholic acid reduces CpG-induced IgM production in patients with primary biliary cirrhosis. *Hepatol. Res.* **39**, 448–454 (2009).

346. Zhao, Y. *et al.* Spatiotemporal segregation of human marginal zone and memory B cell populations in lymphoid tissue. *Nat. Commun. 2018 91* **9**, 1–15 (2018).

347. Sabino, J. *et al.* Primary sclerosing cholangitis is characterised by intestinal dysbiosis independent from IBD. *Gut* **65**, 1681–1689 (2016).

348. Leung, C., Rivera, L., Furness, J. B. & Angus, P. W. The role of the gut microbiota in NAFLD. *Nat. Rev. Gastroenterol. Hepatol.* **13**, 412–425 (2016).

349. Qin, N. *et al.* Alterations of the human gut microbiome in liver cirrhosis. *Nat. 2014 5137516* **513**, 59–64 (2014).

350. Leung, P. S. C. *et al.* A contemporary perspective on the molecular characteristics of mitochondrial autoantigens and diagnosis in primary biliary cholangitis. *Expert Rev. Mol. Diagn.* **16**, 697–705 (2016).

351. Fussey, S. P. M. *et al.* Reactivity of primary biliary cirrhosis sera with Escherichia coli dihydrolipoamide acetyltransferase (E2p): characterization of the main immunogenic region. *Proc. Natl. Acad. Sci. U. S. A.* **87**, 3987–3991 (1990).

352. Bogdanos, D. P. & Vergani, D. Origin of cross-reactive autoimmunity in primary biliary cirrhosis. *Liver Int.* **26**, 633–635 (2006).

353. Varyani, F. K., West, J. & Card, T. R. An increased risk of urinary tract infection precedes development of primary biliary cirrhosis. *BMC Gastroenterol.* **11**, 1–6 (2011).

354. Daniels, J. A., Torbenson, M., Anders, R. A. & Boitnott, J. K. Immunostaining of Plasma Cells in Primary Biliary Cirrhosis. *Am. J. Clin. Pathol.* **131**, 243–249 (2009).

355. Moreira, R. K., Revetta, F., Koehler, E. & Washington, M. K. Diagnostic utility of IgG and IgM immunohistochemistry in autoimmune liver disease. *World J. Gastroenterol.* **16**, 453 (2010).

356. Chen, W. *et al.* Comprehensive Analysis of Serum and Fecal Bile Acid Profiles and Interaction with Gut Microbiota in Primary Biliary Cholangitis. *Clin. Rev. Allergy Immunol.* **58**, 25–38 (2020).

357. Chen, Q. *et al.* CD19 + CD24 hi CD38 hi B Cell Dysfunction in Primary Biliary Cholangitis. *Mediators Inflamm.* **2020**, (2020).

358. Flores-Borja, F. *et al.* CD19+CD24hiCD38hi B cells maintain regulatory T cells while limiting TH1 and TH17 differentiation. *Sci. Transl. Med.* **5**, (2013).

359. Blair, P. A. *et al.* CD19(+)CD24(hi)CD38(hi) B cells exhibit regulatory capacity in healthy individuals but are functionally impaired in systemic Lupus Erythematosus patients. *Immunity* **32**, 129–140 (2010).

360. Wang, X. *et al.* Ulcerative Colitis Is Characterized by a Decrease in Regulatory B Cells. *J. Crohns. Colitis* **10**, 1212–1223 (2016).

361. Haynes, D. R. *et al.* Osteoprotegerin and receptor activator of nuclear factor kappaB ligand (RANKL) regulate osteoclast formation by cells in the human rheumatoid arthritis joint. *Rheumatology* **40**, 623–630 (2001).

362. Wright, H. L., McCarthy, H. S., Middleton, J. & Marshall, M. J. RANK, RANKL and osteoprotegerin in bone biology and disease. *Curr. Rev. Musculoskelet. Med.* **2**, 56–64 (2009).

363. Boyce, B. F. & Xing, L. Functions of RANKL/RANK/OPG in bone modeling and remodeling. *Arch. Biochem. Biophys.* **473**, 139 (2008).

364. Svärd, A., Kastbom, A., Reckner-Olsson, Å. & Skogh, T. Presence and utility of IgA-class antibodies to cyclic citrullinated peptides in early rheumatoid arthritis: the Swedish TIRA project. *Arthritis Res. Ther.* **10**, R75 (2008).

365. Lindqvist, E., Eberhardt, K., Bendtzen, K., Heinegård, D. & Saxne, T. Prognostic

laboratory markers of joint damage in rheumatoid arthritis. *Ann. Rheum. Dis.* **64**, 196–201 (2005).

366. Takano, K. *et al.* IgM response is a prognostic biomarker of primary biliary cholangitis treated with ursodeoxycholic acid and bezafibrate. *J. Gastroenterol. Hepatol.* **35**, 663–672 (2020).

367. Mackay, F. & Browning, J. L. BAFF: A fundamental survival factor for B cells. *Nat. Rev. Immunol. 2002 27* **2**, 465–475 (2002).

368. McIlwain, D. R., Berger, T. & Mak, T. W. Caspase functions in cell death and disease. *Cold Spring Harb. Perspect. Biol.* **5**, 1–28 (2013).

369. Lleo, A. *et al.* Quantitation of the Rank-Rankl Axis in Primary Biliary Cholangitis. *PLoS One* **11**, (2016).

370. Mounach, A. *et al.* Primary biliary cirrhosis and osteoporosis: a case-control study. *J. Bone Miner. Metab.* **26**, 379–384 (2008).

371. Vondenhoff, M. F. *et al.* LTbetaR signaling induces cytokine expression and up-regulates lymphangiogenic factors in lymph node anlagen. *J. Immunol.* **182**, 5439–5445 (2009).

372. Manzo, A., Bombardieri, M., Humby, F. & Pitzalis, C. Secondary and ectopic lymphoid tissue responses in rheumatoid arthritis: from inflammation to autoimmunity and tissue damage/remodeling. *Immunol. Rev.* **233**, 267–285 (2010).

373. Totsuka, T. *et al.* RANK-RANKL Signaling Pathway Is Critically Involved in the Function of CD4+CD25+ Regulatory T Cells in Chronic Colitis. *J. Immunol.* **182**, 6079–6087 (2009).

374. Akiyama, T., Shinzawa, M. & Akiyama, N. RANKL-RANK interaction in immune regulatory systems. *World J. Orthop.* **3**, 142 (2012).

375. Lan, R. Y. *et al.* Liver-targeted and peripheral blood alterations of regulatory T cells in primary biliary cirrhosis. *Hepatology* **43**, 729–737 (2006).

376. Ashcroft, A. J. *et al.* Colonic Dendritic Cells, Intestinal Inflammation, and T Cell-Mediated Bone Destruction Are Modulated by Recombinant Osteoprotegerin. *Immunity* **19**, 849–861 (2003).

377. Nagura, H., Smith, P. D., Nakane, P. K. & Brown, W. R. IGA in human bile and liver. *J. Immunol.* **126**, (1981).

378. Shipa, M. *et al.* Effectiveness of Belimumab After Rituximab in Systemic Lupus Erythematosus : A Randomized Controlled Trial. *Ann. Intern. Med.* **174**, 1647–1657 (2021).

379. Chuang, Y. H., Ridgway, W. M., Ueno, Y. & Gershwin, M. E. Animal models of primary biliary cirrhosis. *Clin. Liver Dis.* **12**, 333 (2008).

380. Mergental, H. *et al.* Transplantation of discarded livers following viability testing with normothermic machine perfusion. *Nat. Commun. 2020 111* **11**, 1–12 (2020).

381. Dutkowski, P. *et al.* Are there better guidelines for allocation in liver transplantation?: A novel score targeting justice and utility in the model for end-stage liver disease era. *Ann. Surg.* **254**, 745–753 (2011).

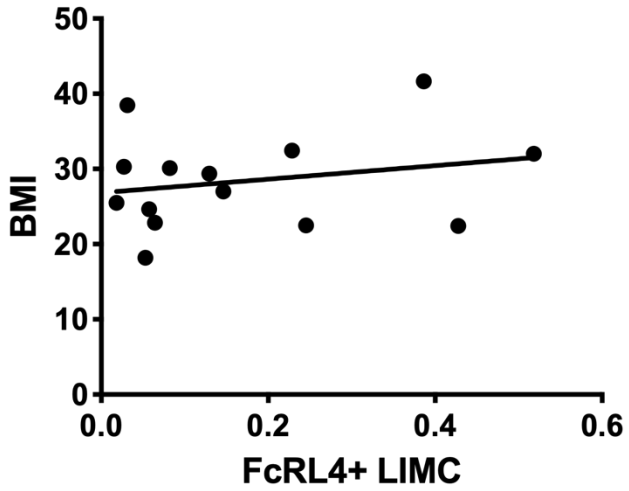
382. Avramović, V., Petrović, V., Jović, M. & Vlahović, P. Quantification of cells expressing markersof proliferation and apoptosis in chronic tonsilitis. *Acta Otorhinolaryngol. Ital.* **35**, 277 (2015).

383. Jin, Q. *et al.* Comparative analysis of portal cell infiltrates in antimitochondrial autoantibody-positive versus antimitochondrial autoantibody-negative primary biliary cirrhosis. *Hepatology* **55**, 1495–1506 (2012).

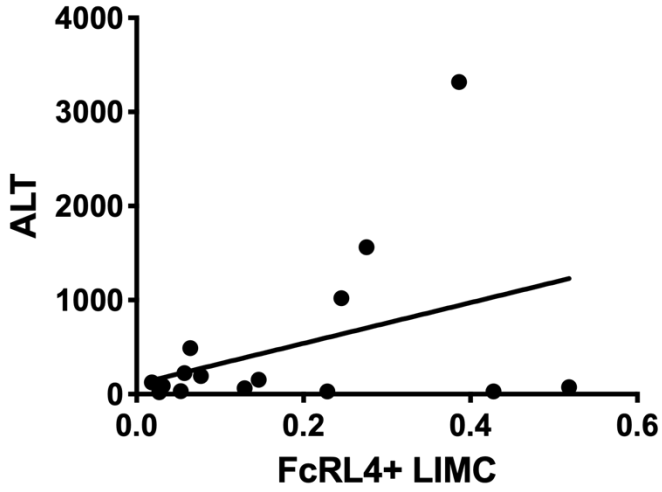
384. Wrammert, J. *et al.* Rapid cloning of high-affinity human monoclonal antibodies against influenza virus. *Nat. 2008 4537195* **453**, 667–671 (2008).

8 APPENDIX

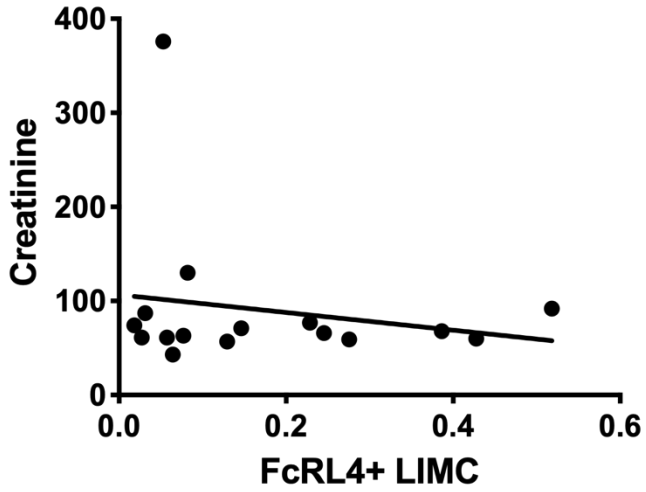
A

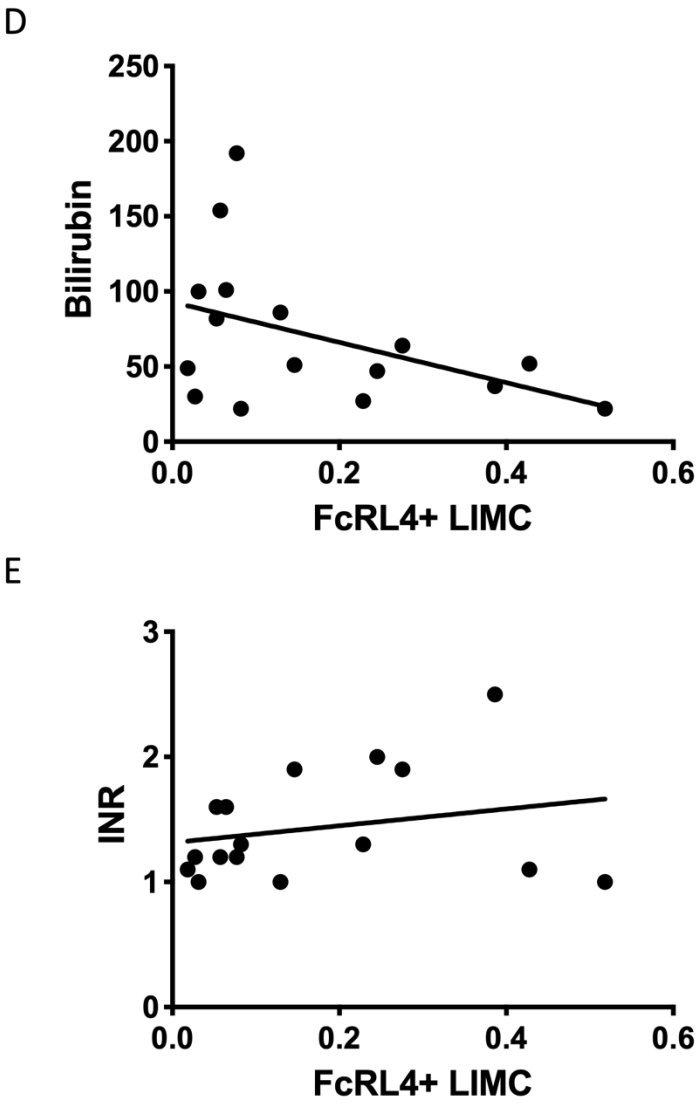


B

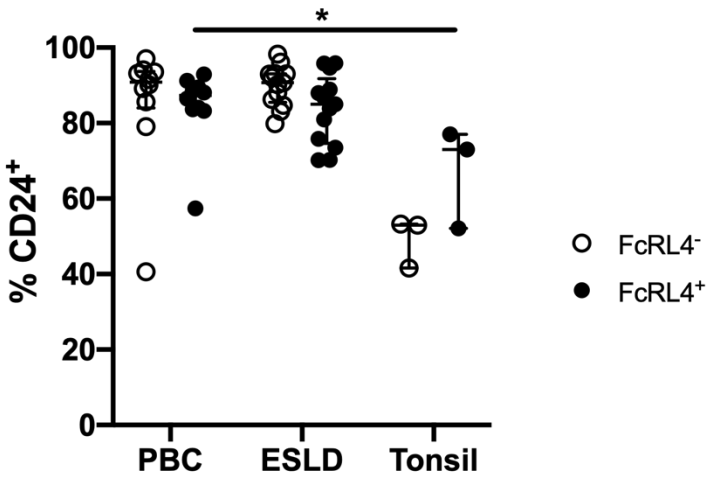


C





Supplementary Figure 7.1 Clinical significance of FcRL4$^+$ B cells. *FcRL4$^+$ B cell population within the total LIMCs population in end-stage PBC livers compared to patient clinical data.* ***(A)*** *Body mass index (BMI). Spearman rank correlation coefficient = 0.09451, p = 0.75.* ***(B)*** *Alanine aminotransferase (ALT) is used to assess liver damage. Spearman rank correlation coefficient = 0.2250, p = 0.419.* ***(C)*** *Creatinine is used to assess liver function; poor liver function interferes with creatinine production. Spearman rank correlation coefficient = -0.0986, p = 0.7151.* ***(D)*** *Bilirubin levels indicate damage to liver bile ducts. Spearman rank correlation coefficient = -0.362, p = 0.1677.* ***(E)*** *International normalised ratio (INR) is a blood clotting test. Liver cirrhosis reduces the production of clotting factor in the liver. Spearman rank correlation coefficient = 0.2374, p = 0.373.*



Supplementary Figure 7.2. CD24 expression on FcRL4$^+$ B cells. *CD24 expression of FcRL4$^+$ FcRL4$^-$ B cells in PBC, other end-stage liver diseases and inflamed tonsil. Statistics – Mann-Whitney test. PBC (n=10), ESLD (n=13), tonsil (n=3).*

Disease	Gender	BMI	Cholestasis	UCDA Treatment	ALP	Bilirubin	ALT	Creatinine	INR
PBC	F	32.44	Y	Y	159	27	29	77	1.3
PBC	F	32.01	Y	Y	393	22	75	92	1
PBC	F		Y	Y	149	64	1562	59	1.9
PBC	F	22.51	Y	Y	80	47	1020	66	2
PBC	F	25.51	N	Y	85	49	126	74	1.1
PBC	F	30.13		Y	655	22		130	1.3
PBC	F	41.64		Y	531	37	3317	68	2.5
PBC	F	29.39		Y	161	86	63	57	1
PBC	F	22.41	Y	Y	533	52	31	60	1.1
PBC	F	27.01		N	713	51	155	71	1.9
PBC	F	30.28	Y	Y	203	30	22	61	1.2
PBC	F		Y	Y	528	192	193	63	1.2
PBC	M	18.18	Y	Y	476	82	33	376	1.6
PBC	M	38.47	N	Y	88	100	88	87	1
PBC	M	22.86		Y	47	101	489	43	1.6
PBC	M	24.66	Y	N	712	154	224	61	1.2
NASH	M	27.77	Y		83	60	610	118	1.4
NASH	M	46.79	N		42	50	45		
NASH	M	32.52	N		235	48	27		
NASH	F	26.84	N		406	16	52		
NASH	M	34.37	N		152	10	43		
NASH	F	26.61	N		166	35	33	47	1.7
NASH	F	33.04	N		75	25	37	87	1.6
NASH	M	33.61	N		82	20	55		
NASH HCC	M	27.36	N		80	29	1437		
NASH HCC	F	26.02	N		59	70	298	46	1.8

Disease	Gender	BMI	Cholestasis	UCDA Treatment	ALP	Bilirubin	ALT	Creatinine	INR
Polycystic	F	34.65	N		32	18	883		
Polycystic	F	37.08			84	6	14		
Polycystic	F	24.79	N		98	17	373		
Polycystic	M	25.06	Y		259	10	29	146	1
Polycystic	F	31.2	N		56	7	11		
Polycystic	M	35.51	N		82	8	28		
Polycystic	M	27.17	Y		42	52	964		
Polycystic	F	34.18			276	26	29	96	1.3
Polycystic	F	26.75			197	12	13	81	1.1
PSC	F	20.93	N	N	225	60	413		
PSC	M	23.65	N	N	359	19	40		
PSC	M	21.97	Y	N	1658	150	424		
PSC	M	27.12	N	N	140	26	829	74	1.4
PSC	F	32.1	Y	N	645	424	94		
PSC	F	24.77	N	N	283	31	35	51	1
PSC	M		Y	N	603	11	172		
PSC	M	19.02	Y	N	401	42	1729		
PSC	F	20.91	Y	N	724	261	106	68	
PSC	F		Y	N	551	88	43		
PSC	F	32.89		Y	980	20	199	47	1
PSC	M	22.77	Y	Y	237	37	41	74	1.1
PSC	M	33.37	Y	N	121	64	260	64	1.1
PSC	M	20.28	N	N	1123	70	485	68	1
PSC	M	25.01	Y	N	970	189	108	65	1

Supplementary Table 7.1. Clinical data from end-stage liver disease patients.